UNIVERSITY OF OKLAHOMA

GRADUATE COLLEGE

SINGLE CELL MASS SPECTROMETRY METABOLOMICS STUDY OF DRUG-RESISTANT CELLS

A DISSERTATION

SUBMITTED TO THE GRADUATE FACULTY

in partial fulfillment of the requirement for the

Degree of

DOCTOR OF PHILOSOPHY

By

Xingxiu Chen

Norman, Oklahoma

2022

Downloaded from SHAREOK. Persistent Handle URL: https://hdl.handle.net/11244/335634

SINGLE CELL MASS SPECTROMETRY METABOLOMICS STUDY OF DRUG-RESISTANT CELLS

A DISSERTATION APPROVED FOR THE DEPARTMENT OF CHEMISTRY AND BIOCHEMISTRY

By THE COMMITTEE CONSISTING OF

Dr. Zhibo Yang

Dr. Bin Wang

Dr. Si Wu

Dr. Yihan Shao

© Copyright by XINGXIU CHEN 2022
All Rights Reserved.

I dedicate this dissertation to a journey.

Two roads diverged in a wood, and I—

I took the one less traveled by,

And that has made all the difference.

------Robert Frost

Acknowledgments

First of all, I would like to acknowledge my advisor, Dr. Yang, for taking me into the fascinating mass spectrometry research field, passing numerous knowledge of advanced analytical technologies to me and helping me carry out all of my research projects. Dr. Yang is a truly respectable and knowledgeable scholar, who devotes countless of his time to single cell analysis research and advanced study. Without the influence of him being a diligent role model, and without his patience and guidance, I cannot finish any of my projects successfully in the past five years. Besides research, he also shares with me a lot of valuable life lessons and encourages me to improve my communication skills and presentation skills.

Secondly, I would like to thank my committee members, including Dr. Bin Wang, Dr. Si Wu, Dr. Yihan Shao, and the former committee member, Dr. Chuanbin Mao, for providing advice for my preliminary, General Exam and helping keep track of my research progress.

I also want to thank all my collaborators for lending instruments/parts and offering critical suggestions for my research. The portable fluorescence microscope cannot be constructed without Dr. Tingting Gu's guidance, the cell viability measurement cannot be performed without Dr. Sims Paul's absorbance plate reader, the co-culture system cannot be studied without Dr. Chuanbin Mao's Nikon Ti-S microscope, and the nicotine and cotinine concentration from maggots' sample cannot be analyzed without Dr. Steven Foster's GC MS.

Last but not least, I want to thank all the lab members, Zou Zhu, Zongkai Peng, Yunpeng Lan, Tra Ngyuen, Dan Chen and Amit Singh, and previous lab members, Dr. Ning Pan, Dr. Renmeng Liu, Dr. Mei Sun, Dr. Xiang Tian, Dr. Yanlin Zhu, Dr. Shawna Standke, and Jonathan Pope. It's my honor to work with them all. Particularly, the training and help Dr. Mei Sun, Dr. Xiang Tian, Dr. Renmeng Liu and Dr. Yanlin Zhu gave me is immeasurable.

Table of Contents

Abstract xiii

Chapter 1. Introduction 1

1.1 Single cell analysis 1

1.2 Mass spectrometry 1

1.2.1 Vacuum-based SCMS methods 2

1.2.1.1 SIMS 3

1.2.1.2 MALDI 4

1.2.2 Ambient SCMS methods 7

1.2.2.1 Probe-based techniques 8

1.2.2.1.1 Solid probes 8

1.2.2.1.2 Mono-channel probes 10

1.2.2.1.3 Multi-channel probes 15

1.2.2.2 Laser-based techniques 18

1.2.3 Multimodal methods 19

1.2.3.1 Separation-assisted techniques 20

1.2.3.2 Microfluidics-based techniques 22

1.2.3.3 Spectroscopy-assisted techniques 24

References 27

Chapter 2. Research Overview 33

Chapter 3. Single Cell Mass Spectrometry Analysis of Drug-resistant Cancer Cells: Metabolomics Studies of Synergetic Effect of Combinational Treatment 36

3.1 Abstract 36
3.2 Introduction 37
3.3 Experimental section 40
3.3.1 Cell culture 40
3.3.2 The Single-probe SCMS analysis 41
3.3.3 Cell viability analysis 42
3.3.4 Enzymatic activity analysis 42
3.3.5 HPLC-MS 43
3.3.6 Data analysis 44
3.4 Results and Discussion 45
3.4.1 Co-treatment of metformin and IRI exhibited synergistic effect in IRI-resistant cells. 45
3.4.2 Metformin treatment resulted in downregulated fatty acids and lipids. 46
3.4.3 Metformin and IRI co-treatment resulted in downregulated lipids, fatty acids, and ceramide phosphoethanolamine. 48
3.4.4 Co-treatment of metformin and IRI more efficiently reduced FASN enzymatic activity compared with the mono-treatment. 51
3.5 Conclusion 54
Chapter 4. Metabolomics Studies of Cell-Cell Interactions using Single Cell Mass Spectrometry Combined with Fluorescence Microscopy 36
4.1 Abstract 62
4.2 Introduction 63

4.3 Methods 67
4.3.1 Materials and chemicals 67
4.3.2 Mono-culture systems 67
4.3.3 Indirect and direct co-culture systems 68
4.3.4 MTT assay 70
4.3.5 LC-MS/MS Identification 70
4.3.6 The single-probe SCMS setup 71
4.3.7 SCMS analyses of cells in direct co-culture 72
4.3.8 SCMS data analysis 72
4.4 Results and discussions 74
4.4.1 Changes of drug-resistance levels by IRI-resistant cells in drug-free medium. 74
4.4.2 Changes of drug-resistance levels of drug-sensitive cells in co-culture conditions. 74
4.4.3 Metabolomics profile change of cells in co-culture systems 77
4.4.4 Potential metabolic mechanisms of spreading drug resistance by drug-resistant cells 79
4.5 Conclusion 83
Appendix I: Support Information of Chapter 3 91
S1. Instrumental setup of the Single-probe SCMS studies 91
S2. Cell viability measurement 92
S3. Online MS^2 identification of metabolites in single IRI-resistant cells 97

S4. MS^2 identification of ions of interest from cell lysate using HPLC-MS/MS 100

S5. Chromatogram of cell lysate in HPLC-MS analysis 101

Reference 101

Appendix II: Support Information of Chapter 4 102

Fig. S1. Cell viability measurements 102

Fig. S2. Quantification of fluorescence intensity 103

Fig. S3. PCA, PLS-DA, and 3D PCA results of SCMS 104

Fig. S4. Typical background-subtracted SCMS spectra 105

Fig. S5. Typical background-subtracted SCMS spectra. 106

Fig. S6A. MS^2 identification of ions of interest at the single-cell level 109

Fig. S7A. MS^2 identification of ions of interest from cell lysate 112

Fig. S7B. MS^2 identification of ions of interest from cell lysate 113

Fig. S8A. MS^2 identification of ions of interest with CID from cell lysate using HPLC-MS/MS 115

Fig. S8B. MS^2 identification of ions of interest with CID from cell lysate using HPLC-MS/MS 116

Appendix III: Copyrights 117

List of Figures

Chapter 1. Introduction

Fig. 1 ..... **6**

Fig. 2 ..... **9**

Fig. 3 ..... **14**

Fig. 4 ..... **17**

Fig. 5 ..... **20**

Fig. 6 ..... **25**

Chapter 3. Single cell mass spectrometry analysis of drug-resistant cancer cells: metabolomics studies of synergetic effect of combinational treatment

Fig. 1 ..... **46**

Fig. 2 ..... **47**

Fig. 3 ..... **50**

Fig. 4 ..... **53**

Chapter 4. Metabolomics studies of cell-cell interactions using single cell mass spectrometry combined with fluorescence microscopy

Fig. 1 ..... **66**

Fig. 2 ..... **74**

Fig. 3 ..... **76**

Fig. 4 ..... **78**

Fig. 5 ..... **80**

Appendix I. Support information of Chapter 3

Fig. S1 ..... **91**

Fig. S2 ..... **92**

Fig. S3 ..... **93**

Fig. S4 ..... **98**

Fig. S5 ..... **101**

Appendix II. Support information of Chapter 4

Fig. S1 ..... **102**

Fig. S2 ..... **103**

Fig. S3 ..... **104**

Fig. S4 ..... **105**

Fig. S5 ..... **106**

Fig. S6 ..... **107**

Fig. S7 ..... **108**

Fig. S8 ..... **112**

Fig. S9 ..... **114**

Fig. S10 ..... **117**

Abstract

Single cell analysis is an emerging area to reveal the heterogeneity of individual cells among all populations. Understanding the cell-to-cell variation can greatly promote the development of drug discovery, disease diagnostics and prognostics. Metabolites, the end products of cellular metabolism, directly reflect the phenotype, status, and microenvironment of cells. Single-cell metabolomics is the study of complete metabolites' profiles in individual cells under certain conditions, illustrating the biological heterogeneity among different cells. Numerous studies of single cell metabolomics have been achieved, and the pioneering work is benefited from technology development in this field. The analytical techniques utilized for single cell metabolomics primarily include fluorescence, electrochemical analysis, and mass spectrometry, whereas the integration of different analytical tools can provide additional molecular information of single cells. My PhD studies mainly focus on single cell mass spectrometry (SCMS) metabolomics studies of drug-resistant cancer cells. This thesis consists of four chapters. Chapter 1 introduces the background information covering the current MS-based techniques for SCMS studies to date. In Chapter 2, I summarized the major projects that I accomplished. Studies in Chapter 3 are focused on elucidating the influence of combinational drug treatment. The Single-probe SCMS technique was utilized to study the metabolomic changes of Irinotecan-resistant cells upon metformin treatment and metformin-Irinotecan co-treatment. Combinational index values calculated by Chow-Talalay method verified the synergistic effect between metformin and irinotecan in our cell models, enzymatic activity assay of fatty-acid synthase was further performed to the possible mechanism of synergistic interaction. In Chapter 4, a workflow was designed to combine the Single-

probe SCMS technique with fluorescence microscopy to study cell-cell interactions in co-culture systems involving cells with different levels of anticancer drug resistance.

Chapter 1. Introduction

1.1 Single cell analysis

Cell is the most fundamental unit of all living organisms. Heterogeneous cells with distinct morphology features and phenotypic profiles coexist in biological systems, implying the collective study of a population of cells cannot represent the behavior of individual cells. The importance of cell heterogeneity has been appreciated in many studies of diseases, such as cancers, infectious diseases, and brain disorders, as human body is composed of various cell types with unique functions and in different microenvironments.[3] Studies of cellular heterogeneity have been performed in different areas, including genomics, transcriptomics, proteomics, and metabolomics. Metabolites, the downstream products cell metabolism, are small biomolecules (molecular weight < 2 kDa) directly involved in numerous cellular functions such as metabolism, growth, and reproduction of cells. Biological heterogeneity of cells can be revealed by studying their metabolites at the single-cell level. The major challenges in single cell metabolomics studies include rapid turnover rate, low concentrations, limited volume of sample, and high structural diversity.[4-5] Fortunately, recent development of highly sensitive analytical techniques enables us to perform single cell metabolomics analyses. A variety of analytical techniques, including florescence, NMR (nuclear magnetic resonance), electrochemical detection, microfluidic device, and mass spectrometry (MS), have been used for the research of single cell metabolomics. This chapter focuses on reviewing recent development of techniques, with an emphasis on MS-based methods, for single cell metabolites studies.

1.2 Mass spectrometry

Mass spectrometry (MS), owing to its high sensitivity, multiplexing capabilities, high analyte coverages, and excellent versatility, has become the major analytical platform for both targeted and untargeted metabolomics studies, including at the single-cell level. The development of instrumentation, such as sampling device, ionization method, and mass analyzer, plays a key role in single cell metabolomics study.

Recent advancement in sampling and ionization methods enables MS to study a wide range of cell types, ranging from small bacterial cells (e.g., E. coli, cell length <2.0 μm) to large embryonic cells (e.g., *Xenopus Laevis* embryo, cell diameter ~1 mm) under different conditions.[6-8] Based on the sampling and ionization environment, single cell MS (SCMS) metabolomics experiments can be performed under vacuum condition, in which cells needs to be dehydrated prior to the measurement, or in ambient environment, in which live cells can be directly analyzed in their native or near-native environment. Although many types of mass analyzers can be utilized in single cell MS platforms, their selection is generally determined by the purposes of studies. The commonly used mass analyzers in the reported studies include the TOF (time of flight), ion mobility spectrometer, Fourier-transform ion cyclotron resonance (FT-ICR), and Orbitrap. These mass analyzers provide different advantages: the TOF offers fast scan rate and broad mass range, ion mobility spectrometer enables the separation of metabolites (e.g., isomers) in the gas-phase, and the FT-ICR as well as Orbitrap have high mass accuracy and high mass resolution.

1.2.1 Vacuum-based SCMS methods

Secondary ion MS (SIMS) and matrix-assisted laser desorption ionization (MALDI) are common approaches to conduct single cell metabolomics study under vacuum

sampling and ionization conditions. These methods have been commercialized, and they provide high spatial resolution and excellent sensitivities for single cell measurement.

1.2.1.1 SIMS

The operation of SIMS relies on the detection of secondary ions sputtered by bombarding the sample surface with a focused, highly energetic primary ion beam. The major advantages of SIMS include low detection limit, high spatial resolution, and capability of depth analysis. This technique has been utilized for metabolomics analysis at cellular and subcellular levels, allowing for single cell imaging.[9-11] However, the major disadvantage of SIMS is that highly fragmented ions are produced, and data analysis of large numbers of biomolecules is challenging. To reduce ion fragmentation while increasing the sensitivity, devices producing ion clusters and polyatomic primary ion beams, including argon gas cluster ion gun, bismuth cluster ion gun, and C_{60}^+ primary ion source, have been widely used in single cell metabolomics studies. In addition, sample preparation methods (e.g., surface modification) have been developed to minimize ion fragmentation. Previous studies indicate that ionic liquid matrix-enhanced SIMS can enhance the signals of certain intact lipids (Fig. 1A),[12] and metal-assisted SIMS can enhance the signal intensities of intact cholesterol and lipid molecules in single cell studies.[13]

There are a variety of different applications of using TOF-SIMS to qualitatively and quantitatively study metabolites, lipids, and drugs in single cells. This method has been utilized to classify bacterial phenotypes[14] and to distinguish different breast cancer cell lines based on their differences of chemical profiles.[15] Due to its high spatial resolution (e.g., below 100 nm[15]), SIMS is well-suited for MS imaging studies of single cells. In

particular, the state of art systems of nanoscale secondary ion mass spectrometry (Nano-SIMS) has achieved a spatial resolution down to 50 nm. Combined with its capability of depth analysis, SIMS enables mapping the 3D distribution of metabolites, small molecules, lipids, and drug compounds in single cells. For example, *Ostrowski* et al. used SIMS imaging to determine cholesterol concentration in plasma membranes of single macrophage cells, and the obtained SIMS images were correlated with fluorescence images to confirm chemical differences between drug treated and control J774 cells (Fig. 1B).[16] In another study, 3D SIMS imaging experiment was combined with multivariate data analysis to discriminate different cell compartments, including cell nucleus, intracellular space, and cell membrane, inside single HeLa cells.[17] Quantitative studies of different cell compartments can be achieved using cells labeled by stable isotopes. *Jiang* et al. combined Nano SIMS imaging with backscattered electron imaging to quantify ^{15}N-labelled glutamine in subcellular structures such as nucleus, endoplasmic reticulum, and Golgi apparatus.[18]

1.2.1.2 MALDI

MALDI uses intense laser pulses to ablate the sample incorporated with matrix molecules for desorption and ionization of analytes. This technique has been widely used in MS imaging studies of proteins, owing to its wide mass range coverage, and metabolites. Recent developments in the application of MALDI MS in single cell metabolomics study include applying novel sampling devices to increase the analytical throughput of profiling metabolites in cells and optimizing sample preparation condition to decrease the influence of matrix. Combined with other techniques, MALDI allows for high-throughput analyses of single cell. *Ong et al.* used an optical microscopy to record cell

coordinates of single cells, followed by automated MALDI-TOF analysis. This method significantly reduced data acquisition time when analyzing a large number of cells (e.g., 3000 cells were analyzed within one hour) compared with typical MALDI MS (e.g., several hundred hours).[19] In addition, microarray substrates, which are composed of hydrophilic reservoirs on an omniphobic surface, have been designed to automatedly aliquot cell suspension by trapping uniform droplets (contains single cells) into the hydrophilic reservoirs (Fig. 1C), facilitating high-throughput MALDI-MS analysis (i.e., more than 2 samples per second).[20 21]

Although matrixes are needed for MALDI experiments, they generally produce significant background noises at low-mass range, complicating the spectrum interpretation of metabolites. To circumvent this limitation, several techniques have been developed to conduct matrix-free desorption ionization MS studies. Desorption ionization on silicon (DIOS) uses porous silicon as the substrate to absorb UV laser for the desorption and ionization of analytes. Kruse et al. reported protocols to directly culture invertebrate neurons on the surface of porous silicon, and they detected peptides from individual neurons using DIOS-MS analysis.[22] Although the development of nanostructure-initiator MS (NIMS) was based on DIOS-MS, initiator compounds were used to promote desorption and ionization of analytes.[23] Specifically, NIMS substrate contains nano porous silicon, in which initiators are trapped. Upon being irradiated by a UV laser, rapid heating of porous silicon surface causes vaporization of the initiator, which

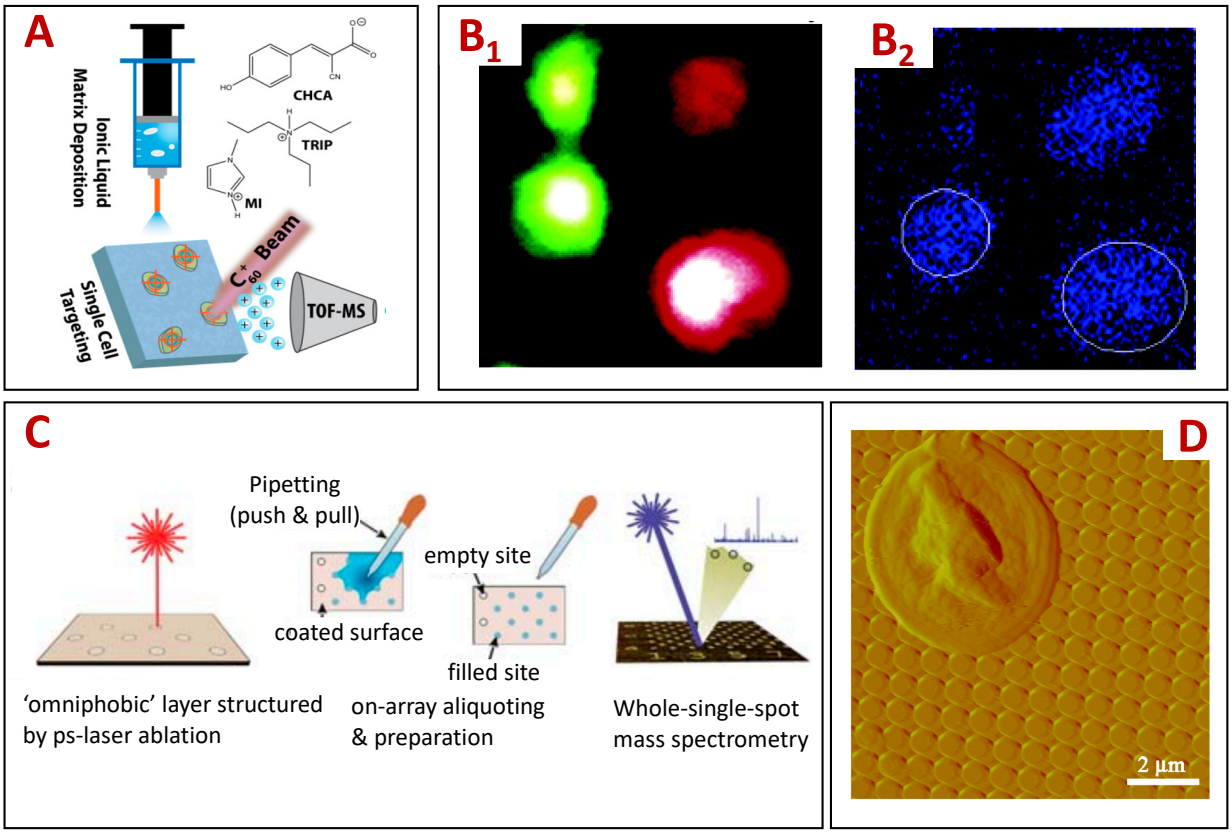


Fig. 1. Examples of vacuum-based MS techniques for single cell metabolomics studies. (A) Using ionic liquid for matrix-enhanced SIMS analysis of lipids. Reproduced from Ref. 10, with permission from American Chemical Society. (B) SIMS studies. (B_1) Control (green) and cholesterol-treated (red) J774 cells, which are illustrated by two-color fluorescence images, were analyzed by SIMS showing the images of $C_5H_9^+$ from single cells. Reproduced from Ref. 14, with permission from American Chemical Society. (C) Experimental workflow of using microarrays for high-throughput single cell MALDI-MS analysis. Reproduced from Ref. 19, with permission from Royal Society of Chemistry. (D) Atomic force microscope (AFM) image of a single yeast cell on the NAPA prepared for matrix-free desorption ionization MS analysis. Reproduced from Ref. 23, permission from American Chemical Society.

further improves the desorption/ionization of analytes. Because of the absence of traditional matrix, NIMS facilitates the analysis of metabolites in low-mass range. For example, O'Brien et al. successfully applied NIMS to detect chemotherapy drugs and endogenous metabolites in single cells.[24] Nanopost array structure (NAPA) is another example of matrix-free substrate in MS studies. NAPA has a structure of columnar silicon nanopost array with precisely produced height, diameter, and periodicity. In particular, the optimized aspect ratio (height/diameter) and subwavelength post diameters of NAPA increased ion yields of small molecules via the resonance-like enhancement (Fig. 1D).[25] For example, 24 biologically significant metabolites, accounting for 4% of the yeast metabolome, were detected in a single yeast cell using NAPA laser desorption ionization MS method.[25]

1.2.2 Ambient SCMS methods

Metabolomics studies at the single-cell level can be carried out in ambient conditions (i.e., room temperature and atmospheric pressure) with no or minimum sample preparation, allowing for cells to be studied in their native or near-native environment. Recent development of ambient sampling and ionization techniques greatly fostered direct, real-time analysis of living single cells, and improved our understanding of the functions and regulations of cellular metabolism.[26-27] Numerous ambient sampling and ionization techniques have been developed for single cell metabolomics studies. Here, we will summarize these methods into three major categories: probe-based, laser-based, and microfluidics-based techniques. In addition, separation methods (either before or after ionization) and spectroscopy techniques can be coupled to ambient SCMS

techniques to acquire additional advantages (e.g., increased sensitivity and additional structure information).

1.2.2.1 Probe-based techniques

The structures of the sampling and ionization probes are the cores of probe-based techniques. Depending the channel numbers inside these probes, we tentatively classify them into three major categories: solid probes (without channel), mono-channel probes (with one channel), and multi-channel probes (with two or more channels). The general working mechanisms of probes in these three categories are similar: cellular contents are extracted by a probe followed by nanoESI-based ionization and MS detection.

1.2.2.1.1 Solid probes

These probes are designed as solid metal needles without inner channel, and experiments are generally performed in two consecutive steps: cellular contents sampling and MS analysis. Direct micro-sampling is generally achieved by extracting cellular contents onto the surface of a solid metal needle with the tip size smaller than a cell. Hiraoka and coworkers developed probe electrospray ionization (PESI), which employs a solid needle as both the microsampling probe and the electrospray emitter.[28] Surface modification of PESI probes have been carried out to improve their performance. Solid phase microextraction (SPME) has been used a separation method to extract analytes by a modified solid support, and the absorbed analytes can be desorbed (e.g., using thermal heating and solvent) for analysis.[29] PESI probes prepared using metal needles with modified surface have been utilized to enrich metabolites in single cells. Gong et al. produced tungsten probes to conduct qualitative and quantitative metabolites in subcellular compartment of *Allium cepa* cells(Fig. 2A).[30] To decease the solvent volume

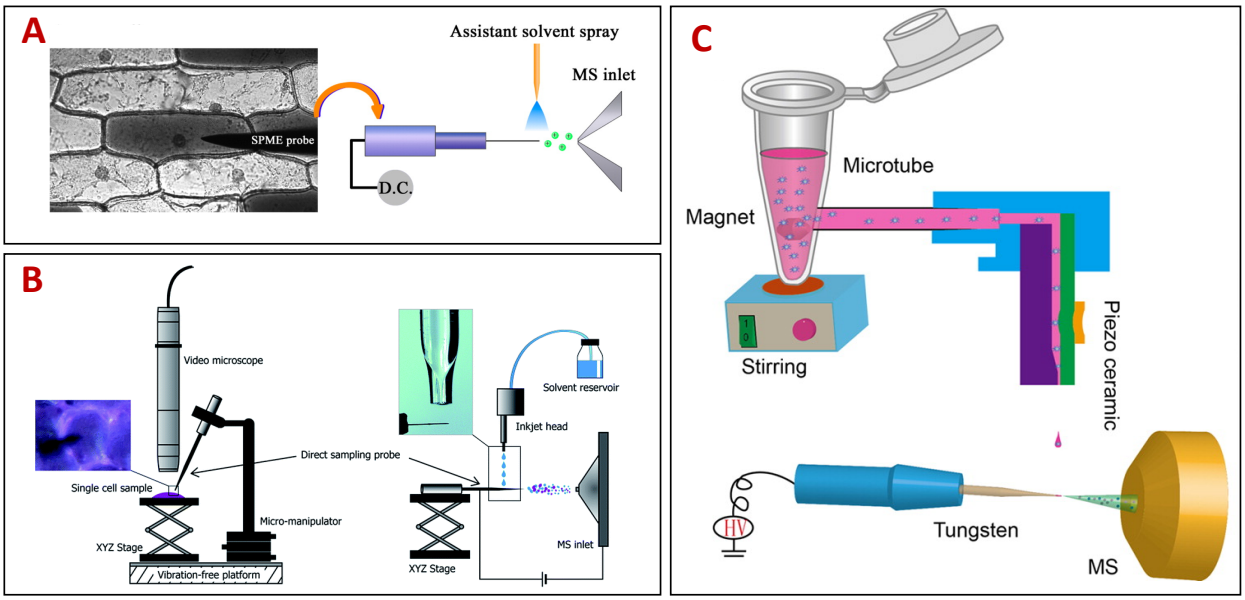


Fig. 2. Examples of solid probes used in the probe-based SCMS metabolomics techniques. (A) Using PESI-MS to analyze a single A. cepa cells. The tungsten-made probe was used as sampling probe and ESI emitter. Reproduced from Ref. 28, with permission from American Chemical Society. (B) The instrumental setup for direct sampling probe MS. A stainless steel with hydrophilic surface was used for sampling, and ionization of metabolites extracted on needle surface was assisted by solvent ejected from a piezoelectric inkjet system. Reproduced from Ref. 29, with permission from Royal Society of Chemistry. (C) Integrated inkjet cell printing and PESI-MS setup. Droplets containing single cells were generated from the inkjet nozzle cell manipulator and dripped on the tungsten probe for ionization and MS analysis. Reproduced from Ref. 30, with permission from American Chemical Society.

on the probe tip and subsequently increase the sensitivity, Yu et al. prepared hydrophilic surface (via oxidative treatment) on stainless-steel sampling probes, and they used a piezoelectric inkjet system to provide auxiliary solvent and assist ESI process (Fig.

2B).[31] Chen et al. developed a single-cell MS screening platform by combing drop-on-demand inkjet cell printing with PESI MS (Fig. 2C).[32] By aligning the inkjet nozzle with the tungsten tip, droplets containing single cells are sprayed onto the needle and subsequently ionized. Recently, Zheng et al. functionalized copper probes using reduced graphene oxide to increase their surface area for improved enrichment of analytes. In addition, a nitrogen aggregation/gas heating system was introduced to promote desorption of absorbed metabolites and facilitate ion transport for improved detection sensitivity.[33]

1.2.2.1.2 Mono-channel probes

A mono-channel probe contains an inner channel, and this type of device is used as both sampling needle and nanoESI emitter to directly analyze extracted cellular contents from selected single cells. Accordingly, experiments are generally performed in two consecutive steps: cellular contents sampling and MS analysis. Direct micro-sampling is generally achieved by drawing cellular contents through micropipettes with sharp tips smaller than cell size. Collected cellular contents will then be ionized though nanoESI for MS analysis. These probes are generally produced using quartz/fused silica and borosilicate glass. Typical examples of these techniques include PESI MS[30, 34], Live single-cell MS[35], capillary micropipette with induced ESI MS[36-37], and micropipette needle[38]. Although the PESI probes were originally produced as solid metal needles, probes containing an inner channel have been fabricated using nonmetal materials such as quartz and glass.[34, 39] In fact, these types of PESI probes are essentially nanoESI emitters.

Live single-cell MS utilizes a metal-coated glass nanospray emitter, which is used as both the micro-sampling device and nanoESI source (Fig. 3A).[40-41] Cellular contents are sucked into the nanospray emitter using a micromanipulator, and then a small amount of organic solvent is added and mixed with cellular content. The nanoESI emitter is then connected to an ionization source for MS analysis. Applications of Live single-cell MS include detecting endogenous metabolites, extracellular compounds, and drug and drug metabolites from single cells and subcellular compartments.[42] To analyze nonadherent cells, sonication can be used to improve lysis efficiency and assist mixing of lysate and organic solvent, resulting in increased detection of metabolites.[43] Live single-cell MS technique has been combined with other imaging tools, such as fluorescence imaging, holographic, and tomographic laser microscopy, to target organelles for metabolomics analysis and to perform quantitative studies of single cells.[44-45] Nakashima et al. used quartz capillaries to produce PESI probes, which have similar designs as the nanoESI emitters. They added an ionic liquid and placed a titanium wire electrode inside the probe to improve electric conductivity and increase MS detection sensitivity.[39] Zhao et al. coupled a glass pressure-assisted microsampling probe with hydrogen flame desorption ionization (HFDI) to achieve direct quantitation of metabolites in single cells.[46]

Induced nano-electrospray ionization (induced nESI), developed by Cooks and coworkers, is an efficient ionization technique with a high tolerance to matrix effect. In this design, electrospray of analytes is induced by placing an electrode, which carries pulsed potential, close to the emitter (e.g., <2 mm).[47] The induced nESI ionization method has been modified to improve its performance in single cell analysis. To enhance the detection sensitivity of cysteine, Zhuang et al. conjugated a charge tag (quaternary ammonium

group) to cysteine through the click reaction, and then they used induced nESI MS to measure cysteine concentration in single living Hela and HepG2 cells.[36] Under the inspiration of bipolar spray process in induced nESI, Hu et al. developed a synchronized polarization induced electrospray ionization (SPI-ESI) method to acquire both positive-ion and negative-ion mass spectra in one measurement. [37]

Verbeck and coworkers developed an approach to coupling a nanomanipulator workstation with nanoESI MS.[48] A solid quartz probe (tip size: ~8 μm) was used for cell puncture. Next, a Pd/Au-coated nanospray emitter (tip size: ~1 μm) was inserted into the cell through the puncture site to inject (using a precisely controlled four-channel pressure injector) a solvent mixture to extract metabolites and then draw the mixture for MS analysis. They observed a distinct difference of triacylglcerol abundance between the healthy and tumorous adipocytes, and then determined the heterogeneity of lipid droplets in living adipocyte cells.

A great effort has been put for quantitative single cell MS analysis using techniques based on mono-channel probes. Gholipour et al. used quartz capillary to fabricate the cell pressure probe, which was prefilled with oil mixture, to draw single-cell sap from tulip bulb (Fig. 3B).[34] Using a motorized micrometer, the sampling volume inside transparent probe can be precisely determined under a digital microscope. In addition, relative quantitation of metabolites in single cells can be measured by mixing internal reference solution (100 pl mannitol) with cell sap solution inside the capillary. In addition to syringe pump, electroosmotic extraction, which is induced by applying a voltage across the liquid/liquid interface, has been used to draw and inject small volumes (e.g., attoliter to picoliter) of solutions (Fig. 3C).[49] In the studies performed by Laskin and coworkers, one Pt electrode

was inserted into a nanopipette (filled with a hydrophobic electrolyte solution), and the other was placed on the top of the cell.[50] A voltage was then applied on both electrodes to extract the cytoplasmic content into the nanopipette, which was later transferred to a mass spectrometer for analysis. Interestingly, the partition of metabolites between the aqueous and hydrophobic electrolyte solution can provide a separation of hydrophobic and hydrophilic analytes. In addition, glucose extracted from individual A. *cepa* epidermal cells was quantified by adding the internal standard compounds (glucose-d_2) into nanopipette using a second electroosmotic extraction.

To acquire richer structural information from metabolites in single cells, reactive SCMS studies have been carried out. The Yang group developed the micropipette needle, which was prepared by combing a pulled glass capillary needle with a fused silica capillary, to characterize carbon-carbon double (C=C) bonds in unsaturated lipids via Paternó-Büchi (PB) reactions (Fig. 3D).[38] Briefly, an organic solution (e.g., acetone or benzophenone dissolved in acetonitrile) was added into the micropipette needle and used as cell lysis solution and PB reagent. A whole suspension cell was drawn into the micropipette to produce lysate for MS analysis, and then PB reactions were initiated by UV irradiation for the same single cell lysate. Finally, assisted by Python scripts, C=C bond locations were determined from mass spectra obtained before and after PB reactions.

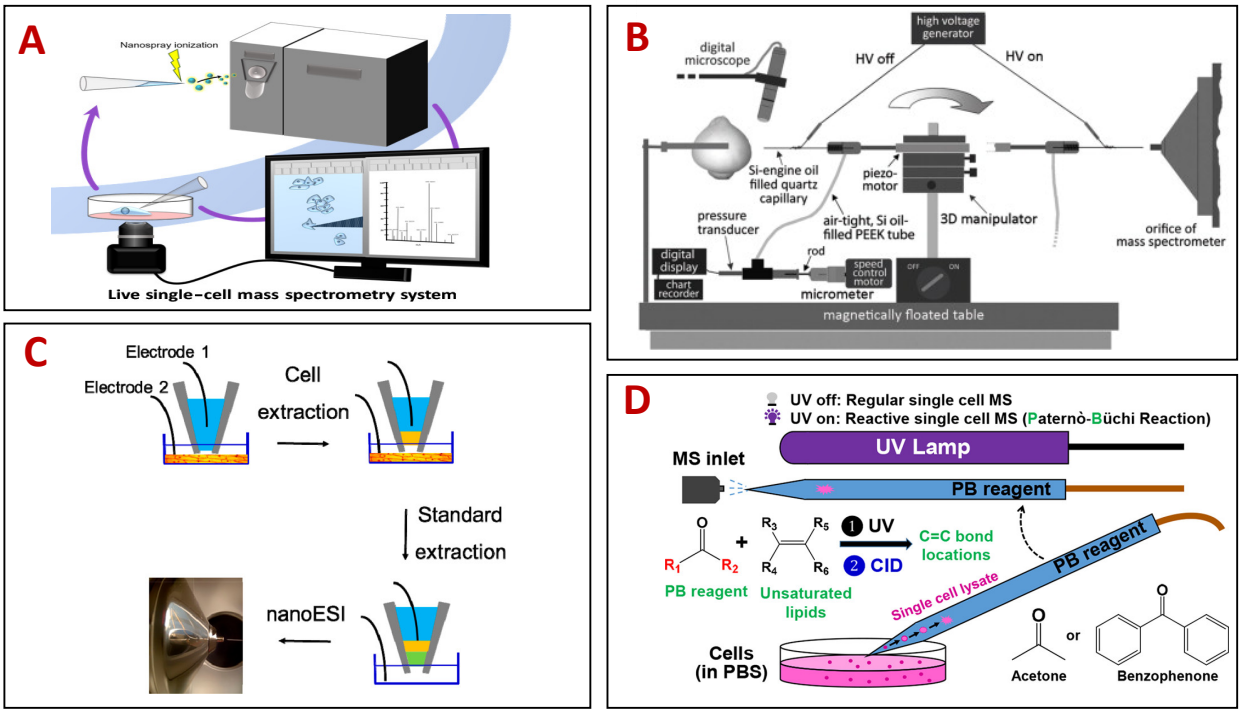


Fig. 3. Examples of mono-channel probes used in the probe-based SCMS metabolomics techniques. (A) The experiment design of Live single-cell MS. A metal-coated nanoESI emitter was used to suck cellular contents controlled by micromanipulator, and the emitter was then transferred to a mass spectrometer for analysis. Reproduced from Ref. 38, with permission from John Wiley and Sons. (B) The instrumental design of the cell pressure probe. Single cell sampling was achieved by inserting a quartz probe into single cell prior to MS detection. Reproduced from Ref. 32, with permission from Elsevier. (C) Combining electroosmotic extraction with MS for single cell metabolomics study. Electrode 1 was inserted into a nanopipette containing electrolyte solution, and electrode 2 was placed onto the sample. By applying voltage between these two electrodes, cell contents were extracted into the nanopipette for subsequent MS analysis. Reproduced from Ref. 48, with permission from American Chemical Society. (D) Using micropipette needles to determine C=C bond positions in unsaturated lipids in single cells. The glass micropipette

needle was utilized as the single cell sampling probe, PB reaction container, and nanoESI emitter. Reproduced from Ref. 54, with permission from American Chemical Society.

1.2.2.1.3 Multi-channel probes

Although a variety of different mono-channel probes have been successfully used for SCMS metabolomics studies, experiments generally need to be conducted via two consecutive steps: single cell sampling and MS analysis. To improve the experimental throughput, probes with multiple inner channels have been developed. The major techniques in this category include the nanospray DESI (Nano-DESI)[51], Single-probe[52-54], and T-probe[55-56]. The nano-DESI probe was assembled with a primary capillary and a secondary capillary, positioned at an optimum angle to each other. The analytes on the sample surface are desorbed into a flowing liquid bridge formed by the two capillaries. Although this method was originally designed for MS imaging studies[57-58], it has been used for SCMS experiments, in which the targets are individual human cheek cells placed on microscope glass.[51, 57-58] In addition, by adding internal standard into the nano-DESI solvent, Bergman et al. demonstrated nano-DESI MS the ability to carry out online quantification analysis of endogenous metabolites in single cell.[51]

The Single-probe, developed by the Yang group, is a miniaturized, multifunctional sampling and ionization device for real-time, in situ SCMS metabolomics studies (Fig. 4A).[52] A Single-probe is produced by embedding a solvent-providing silica capillary and a nano-ESI emitter into a dual-bore quartz needle (tip size <10 μm). The solvent-providing capillary, which is connected to a syringe pump, provides solvent to the dual-bore quartz needle tip, where solvent forms a liquid junction. By inserting the tip of dual-bore quartz needle into a target cell, metabolites can be extracted by solvent and then automatically

delivered to the nano-ESI emitter for ionization. To maximize the amount of information in positive ionization mode of single cells analysis by increasing the detection of the negatively charged species, Pan et al. utilized dicationic ion-pairing reagents in the sampling solvent to convert the negatively charged metabolites into positively charged adducts.[59] In addition, quantitative SCMS studies have been performed using this technique. To quantify drug uptake in single cells, Pan et al. added the internal standard into the sampling solvent, and used the Single-probe to analyze single cells cultured in microwells on glass chips.[53] To expand its capability of analyzing suspended cells, Standke et al. integrated the Single-probe with a cell manipulating platform.[54, 60] A single suspension cell can be captured a cell selection probe and transferred to the tip of the Single-probe for solvent induced lysis, followed by immediate MS analysis. By adding internal standard (^{15}N-gemcitabine) into the sampling solvent, this approach was used to measure intracellular drug (gemcitabine) concentration using cultured single cancer cells. Particularly, this technique allowed for quantifying amounts of gemcitabine in single cells isolated from patients undergoing gemcitabine treatment.[61] In addition to SCMS studies, the Single-probe device has been used to analyze extracellular metabolites inside live multicellular spheroids (Fig. 4B)[62] and high spatial resolution ambient MS imaging.[63-65]

The T-probe, another multi-channel probe developed by the Yang group, has been used for adherence single cell studies. Three pieces produced from the fused silica capillary (i.e., the solvent-providing capillary, sampling probe, and nanoESI emitter) are connected at a T-junction and sandwiched by two polycarbonate substrates via thermo binding (Fig. 4C).[55] Once the sampling probe (tip size: ~5-8 μm) is inserted

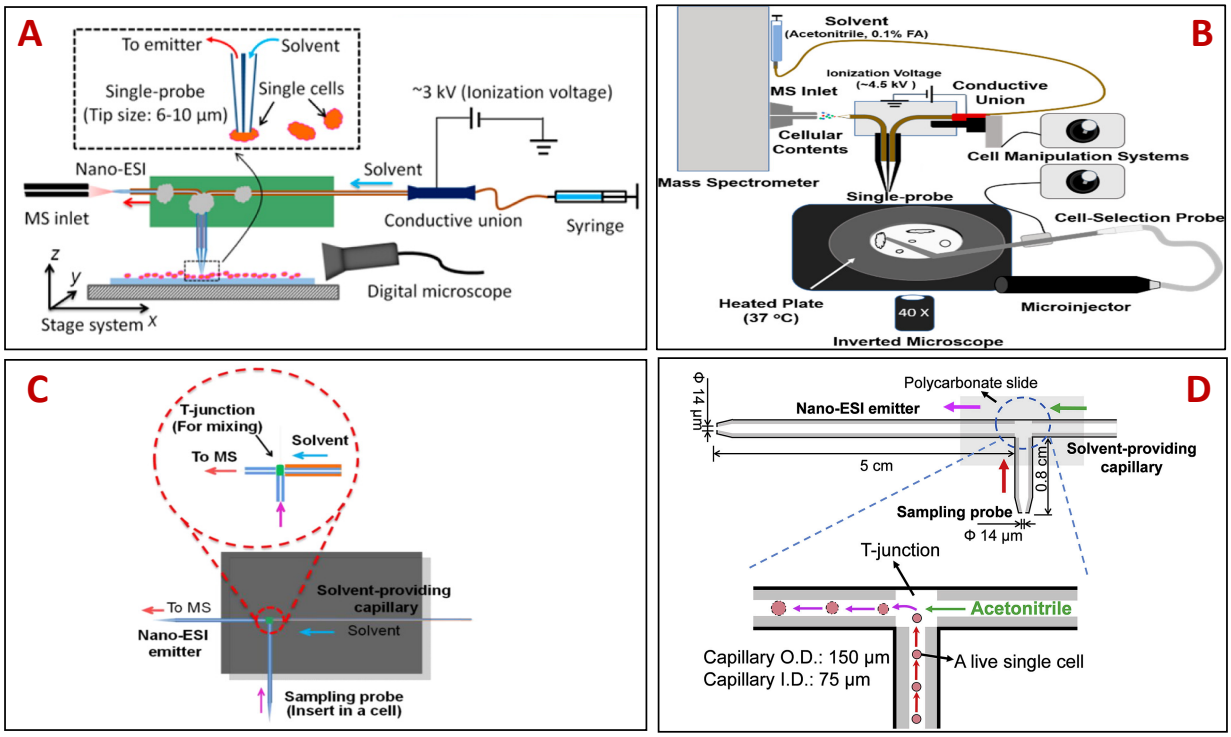


Fig. 4. Examples of multi-channel probes used in the probe-based SCMS metabolomics techniques. (A) Schematic of the Single-probe SCMS setup. A Single-probe was fabricated by embedding a solvent-providing capillary and a nano-ESI emitter in a laser-pulled dual-bore quartz. Reproduced from Ref. 50, with permission from American Chemical Society. (B) Coupling the Single-probe MS to cell manipulation platform to quantify anticancer drug in single cancer cells isolated from patients. Reproduced from Ref. 59, with permission from American Chemical Society. (C) Working mechanism of the T-probe. Three components (sampling probe, solvent-providing capillary, and nano-ESI emitter) were sandwiched by two polycarbonate slides. The suction force at the sampling probe tip was induced by nanoESI and solvent flow. Reproduced from Ref. 53, with permission from American Chemical Society. (D) The redesigned T-probe for the analysis of nonadherent single cells. A suspended single cell was captured by the sampling probe

and drawn into the long nano-ESI emitter for rapid cell lysis and MS analysis. Reproduced from Ref. 54, with permission from Elsevier.

into a target single cell, the suction force, which is induced by nanoESI and solvent flow, draws cellular contents towards the nano-ESI emitter for ionization. To analyze whole suspension cells, the redesigned T-probe has been developed. This new design has with two major changes: a sampling probe with larger orifice (~14 μm) and a longer nano-ESI emitter (5.5 cm). These two features allow for drawing a whole cell into the nanoESI emitter for complete lysis prior to MS detection (Fig. 4D).[56]

1.2.2.2 Laser-based techniques

Laser-based techniques utilize laser for ablation sampling, whereas ionization of analytes occurs either simultaneously along with ablation (e.g., laser desorption/ionization droplet delivery (LDIDD))[66] or assisted by ESI (e.g., laser ablation electrospray ionization (LAESI)[67-68]). LDIDD uses pulsed UV laser beam to desorb and ionize analytes. Liquid droplets are sprayed onto the laser-irradiated region to minimize analyte loss and to assist the delivery of ions to a mass spectrometer inlet (Fig. 5A).[66] LDIDD MS achieved high sensitivity (e.g., the limit of detection of lysine is ~2 attomole) and spatial resolution (3 μm on mouse brain tissue). Using this method, different metabolomic profiles were observed between healthy and apoptotic HEK cells. LAESI, developed by Vertes and coworkers, utilizes a focused mid-infrared (IR) laser beam to ablate water-containing samples, and the ejected neutral species are then picked up and ionized by the charged droplets from ESI (Fig. 5B).[69] Its capability of single cell studies was first demonstrated by analyzing metabolomic profiles of plant cells. To ablate single cells, the mid-IR laser pulses were delivered using an optical fiber with a sharp tip (radius

of curvature ~15 μm).[67] More detailed studies were performed in later studies to improve the performance of this technique. For example, the effectiveness of IR laser delivery was evaluated using both the conventional and etched optical fibers.[68] Although the physical sizes of optical fiber tips are large compared with typical mammalian cells (e.g., diameter ~10μm), this technique can be combined with microdissection (e.g., using a tungsten needle to expose the organelles and cytoplasm in plant cells) to study metabolites in subcellular compartment.[70] Because the microablation by focused laser beam has no significant influence on metabolites in neighboring cells, Shrestha et al. used this technique for MS imaging studies of cells in plant tissues.[71] The success of these studies lead to the development of automated single cell analysis for targeted morphologies.[72] Briefly, after the cell with particular morphology was recognized in the microscopy image, this cell was set as a target with centroid coordinates. A home-developed stage-control program was then utilized to control the translation stage, which moves the cell to the optical fiber for ablation and MS measurement.

1.2.3 Multimodal methods

As summarized in the above contexts, advancements in sampling and ionization methods play vital roles in promoting MS to be the primary tool for single cell metabolomics studies. In fact, other analytical techniques, including separation, microfluidics, and spectroscopy, have been integrated with MS for multidimensional analysis. These hybrid technologies provide additional structure information that can enhance molecular identification and promote experiment throughput.

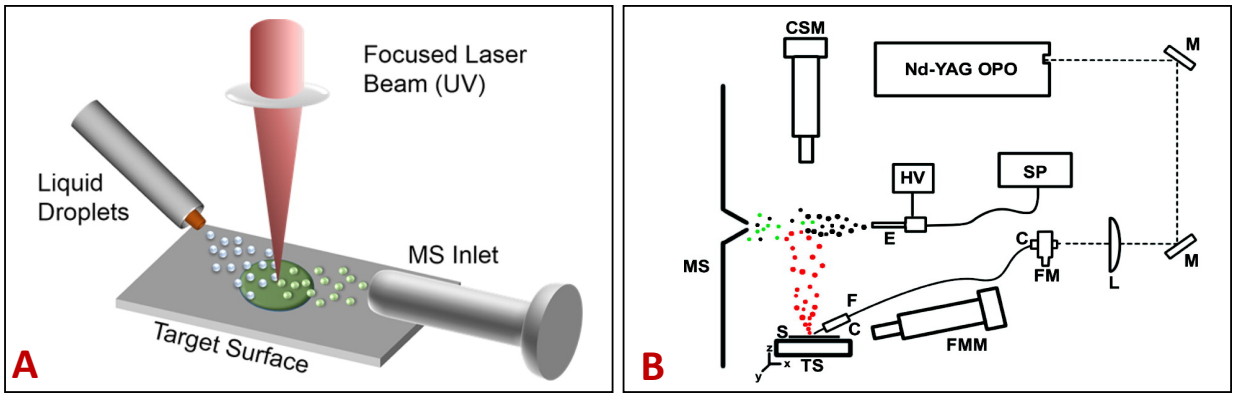


Fig. 5. Examples of laser-based SCMS metabolomics techniques. (A) Experimental setup of LDIDD-MS. Metabolite ions generated by UV laser desorption and ionization were captured liquid droplets and directed into MS. Reproduced from Ref. 64, with permission from American Chemical Society. (B) Instrumental setup for LAESI-MS. Mid-IR laser was delivered to single cell through an etched optical fiber tip for ablating neutral species, which were picked and ionized by charged droplet from ESI. Reproduced from Ref. 65, with permission from American Chemical Society.

1.2.3.1 Separation-assisted techniques

Most SCMS metabolomics experiments are carried out without separation, primarily due to two reasons: extremely limited amounts of analytes in individual cells and potential sample loss and dilution induced by separation. However, separation can greatly reduce the interference from matrix (i.e., increase detection sensitivity) and provide orthogonal structural information for molecular identification. According to the sequence to perform separation and ionization, there are major two types of separation methods, i.e., pre-ionization and post-ionization, used in ambient SCMS metabolomics studies.

As a typical pre-ionization separation technique, capillary electrophoresis (CE), which utilizes electric field to separate analytes based on their charge to size ratio, can be used to provide a rapid separation of analytes with very small sample consumption. The combination of CE and MS, in which ESI is generally used as the ionization method, has been utilized in proteomics and metabolomics studies at the single-cell level. Sweedler and coworkers developed a CE-ESI setup, in which the ESI nebulizer was replaced by a coaxial sheath-flow interface, that can be coupled to MS (Fig. 6A).[73] During the experiment, a single cell (preserved in a home-built stainless steel nanovial) was injected from one end of the CE capillary. This capillary end was then placed into a stainless-steel containing background electrolyte, and CE separation was achieved by applying a voltage gradually increased from 0 V to 20 kV. This setup provided stable ion signal and high sensitivity (limit of detection was in the nanomolar range), allowing for the metabolic profiles to be obtained from single neuron cells and their subcellular regions. Nemes et al. improved the CE-ESI-MS design by using programed device to acquire a time-dependent output voltage.[74] They used this new method for qualitative and quantitative measurements of endogenous metabolites in neutrons.[75] They further modified the design to produce a CE-μESI interface, which was then used to compare and track metabolites in frog embryos during their development.[7, 76]

Separation can be also achieved in the gas phase after the ionization processes. Ion mobility spectrometry (IMS) separates ions based on their difference of mobilities, which are originated from differences in charge, mass, and cross section, in a buffer gas with the presence of an electric field. Vertes and coworker utilized the capillary microsampling for ESI-IMS-MS experiments (Fig. 6B).[77] The microcapillary, pulled from

a glass capillary by a micropipette puller, was used to extract cellular content via a motorized micromanipulator. After adding electrospray solution into the microcapillary, a platinum wire was inserted for applying voltage between the microcapillary and MS inlet. The generated ions were separated the IMS to eliminate the isobaric interferences and improve molecular coverage in MS analysis. This group further utilized this technique to study the influence of xenobiotic treatment on cellular metabolism (e.g., adenylate energy charge levels and lipid turnover rates) in single human hepatocellular carcinoma cells.[78]

1.2.3.2 Microfluidics-based techniques

The integration of SCMS with microfluidics added additional benefits for versatile studies. Particularly, microfluidics can be designed to achieve a variety of different functions, such as cell identification, sorting, and separation, in high-throughput analysis. So far, different types of microfluidic devices (e.g., microwells and droplet-based microfluidics) have been developed to isolate and capture single cells in suspension for analysis.[79] An integrated microfluidic device combining electrophoresis channel, in which rapid single cell lysis and metabolites separation occur, and electrospray emitter has been developed, leading to a great throughput (12 cells per minute).[80] The combination of microfluidic chip and MALDI-MS achieved automatic, high-throughput analysis. In this design, a microwell-based microfluidic device was utilized to capture single cells for the formation of cell array, and MALDI-MS imaging was then used to analyze the metabolites in single cells automatically.[81] Jiaxin et al. further coupled the microwell-based microfluidic device with ESI-MS for metabolites quantitation analysis in single cells (Fig. 6C).[82] After single cells were captured in the microwells, a pulled capillary containing extraction solvent and internal standard was dip into microwells. The cellular content along with

internal standard were then aspirated back to the capillary for MS detection. Using this method, author quantified concentrations of glucose phosphate in single K562 cells. The integration of microfluidic device eliminates matrix effect when analyzing live cells present in culture medium or buffer that contains high concentrations of salts. Zhang et al developed a three-phase droplet-based single-cell printing analysis system to separate and print single cells suspended in PBS (phosphate buffered saline).[83] In this design, the organic extraction phase, octyl alcohol/acetonitrile, was used to extract cellular metabolites from the aqueous saline matrices. The separation of organic and aqueous phases occurred due to hydrophilic and hydrophobic interactions at the interface. The extract containing cellular metabolites was then printed to a microarray chip for MALDI-MS analysis. A high throughput (three to four single cells per second) has been achieved using this system. In another study, the Lin group integrated droplet-based inkjet printing, dielectrophoretic manipulation, and de-emulsification interface with a microfluidic system to reduce the matrix interference for SCMS analysis.[84] Single cells were separated from the culture medium by splitting the droplet using a Y-shaped bifurcate structure in the dielectrophoretic channel. Using this system, they studied the heterogeneity of the healthy and cancer cells, and measured lipids' alterations due to drug treatment. In addition to suspension cells, microfluidic devices can be coupled with MS techniques for the analysis of adherent cells. The Lin group recently introduced a microfluidic-based in situ single-cell recognition system to achieve this purpose (Fig. 6D).[85] A single-cell probe fabricated from polydimethylsiloxane (PDMS) was used to capture and isolate single cells cultured in Petri dish with the assistance of a microscope. Methanol was then introduced to the compartment formed by the single-cell probe to extract lipids in a single cell, and the

extraction solution was analyzed by MS. Authors conducted analyses of lipids (e.g., phosphatidylcholine) in single cells of different human cell lines.

1.2.3.3 Spectroscopy-assisted techniques

Spectroscopy techniques, including fluorescence and Raman, can be integrated for multidimensional analysis. In one of the early studies[86], fluorescence microscopy was used to locate fluorescently labeled cells in TOF-SIMS measurements of single cell metabolomics analysis. To analyze changes in relative abundances of metabolites and lipids of cells in different mitotic stages (e.g., prometaphase, metaphase, anaphase, cytokinesis), fluorescence microscopy (to determine mitotic stages) was combined with capillary microsampling ESI-IMS-MS to analyze single hepatocellular carcinoma cells.[87] Immunocytochemical assay is another analytical tool for classifying cell types, and this method has been combined with MALDI-MS to explore heterogeneous lipid compositions in single neurons and astrocytes.[88] Briefly, MALDI-MS was used to analyze rat brain cells present in mixed populations. After MS measurements, MALDI matrix was removed, cells were fixed, and immunocytochemical assay was subsequently performed to identify the neurons and astrocytes by labeling them with the corresponding antibodies.

Raman spectroscopy, as a non-destructive analysis tool, has been commonly used to acquire complementary chemical information (e.g., determination of functional groups in molecules). For single cell dynamic studies, measurements using Raman spectroscopy and fluorescence imaging techniques were consecutively applied prior to MAIDI MS experiments.[89] In another study, these two spectroscopy techniques integrated with matrix-free laser desorption/ionization MS for multidimensional chemical analysis of single algae cells,[90] which contain autofluorescent cellular contents.

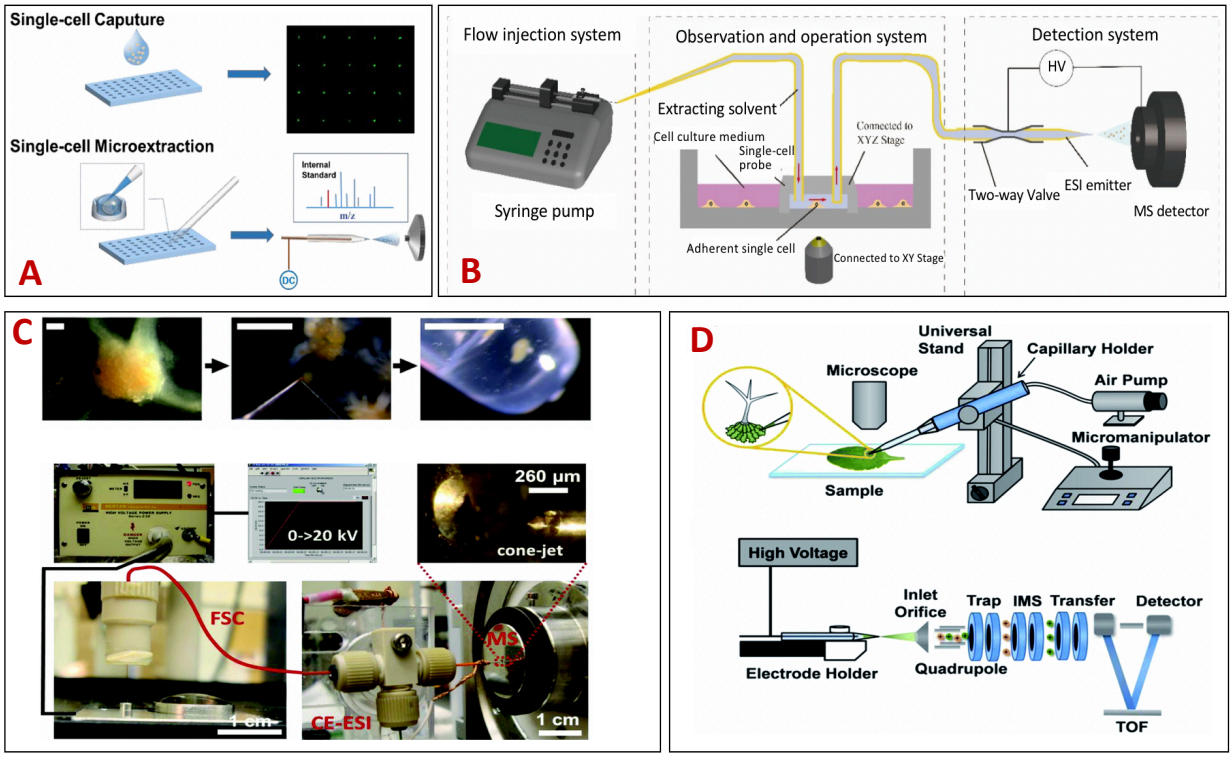


Fig. 6. Examples of multimodal methods, including (A-B) microfluidic-based and (C-D) separation-assisted SCMS metabolomics techniques. (A) Workflow of microwell-based nanoliter droplet microextraction and MS analysis of single cells. A microfluidic cell array was used to confine single cells, extraction solvent, and internal standard, allowing for quantitative measurement of glucose-phosphate concentration in single cells. Reproduced from Ref. 80, with permission from American Chemical Society. (B) Working mechanism of microfluidic-based, in situ single-cell recognition system. Single-cell probe (fabricated from PDMS) was used for single cell capture and cellular contents extraction from cells cultured in Petri dish. Reproduced from Ref. 83, with permission from the author. (C) CE-ESI-MS platform for single cell analysis. Single neutron cell lysate was introduced and separated by CE, and then cellular contents were sprayed into MS using a coaxial sheath-flow ESI source. Reproduced from Ref. 72, with permission from American

Chemical Society. (D) Experimental design of capillary microsampling ESI-IMS-MS. Separation of metabolite ions was achieved by ion mobility in studies of single plant and human cells. Reproduced from Ref. 75, with permission from Royal Society of Chemistry.

References

1. Strzelecka, P. M.; Ranzoni, A. M.; Cvejic, A., Dissecting human disease with single-cell omics: application in model systems and in the clinic. *Dis Model Mech* **2018,** *11* (11).
2. Zenobi, R., Single-Cell Metabolomics: Analytical and Biological Perspectives. *Science* **2013,** *342* (6163), 1201.
3. Zhang, L. W.; Vertes, A., Single-Cell Mass Spectrometry Approaches to Explore Cellular Heterogeneity. *Angew Chem Int Edit* **2018,** *57* (17), 4466-4477.
4. Arnold, R. J.; Reilly, J. P., Fingerprint matching of E-coli strains with matrix-assisted laser desorption ionization time-of-flight mass spectrometry of whole cells using a modified correlation approach. *Rapid Commun Mass Sp* **1998,** *12* (10), 630-636.
5. Onjiko, R. M.; Morris, S. E.; Moody, S. A.; Nemes, P., Single-cell mass spectrometry with multi-solvent extraction identifies metabolic differences between left and right blastomeres in the 8-cell frog (Xenopus) embryo. *Analyst* **2016,** *141* (12), 3648-3656.
6. Onjiko, R. M.; Moody, S. A.; Nemes, P., Single-cell mass spectrometry reveals small molecules that affect cell fates in the 16-cell embryo. *P Natl Acad Sci USA* **2015,** *112* (21), 6545-6550.
7. Colliver, T. L.; Brummel, C. L.; Pacholski, M. L.; Swanek, F. D.; Ewing, A. G.; Winograd, N., Atomic and molecular imaging at the single-cell level with TOF-SIMS. *Analytical Chemistry* **1997,** *69* (13), 2225-2231.
8. Mai, F. D.; Chen, B. J.; Wu, L. C.; Li, F. Y.; Chen, W. K., Imaging of single liver tumor cells intoxicated by heavy metals using ToF-SIMS. *Appl Surf Sci* **2006,** *252* (19), 6809-6812.
9. Li, H. W.; Hua, X.; Long, Y. T., Graphene quantum dots enhanced ToF-SIMS for single-cell imaging. *Analytical and Bioanalytical Chemistry* **2019,** *411* (18), 4025-4030.
10. Do, T. D.; Comi, T. J.; Dunham, S. J. B.; Rubakhin, S. S.; Sweedler, J. V., Single Cell Profiling Using Ionic Liquid Matrix-Enhanced Secondary Ion Mass Spectrometry for Neuronal Cell Type Differentiation. *Analytical Chemistry* **2017,** *89* (5), 3078-3086.
11. Altelaar, A. F. M.; Klinkert, I.; Jalink, K.; de Lange, R. P. J.; Adan, R. A. H.; Heeren, R. M. A.; Piersma, S. R., Gold-enhanced biomolecular surface imaging of cells and tissue by SIMS and MALDI mass spectrometry. *Analytical Chemistry* **2006,** *78* (3), 734-742.
12. Wehrli, P. M.; Lindberg, E.; Angerer, T. B.; Wold, A. E.; Gottfries, J.; Fletcher, J. S., Maximising the potential for bacterial phenotyping using time-of-flight secondary ion mass spectrometry with multivariate analysis and Tandem Mass Spectrometry. *Surf Interface Anal* **2014,** *46*, 173-176.
13. Robinson, M. A.; Graham, D. J.; Morrish, F.; Hockenbery, D.; Gamble, L. J., Lipid analysis of eight human breast cancer cell lines with ToF-SIMS. *Biointerphases* **2016,** *11* (2).
14. Ostrowski, S. G.; Kurczy, M. E.; Roddy, T. P.; Winograd, N.; Ewing, A. G., Secondary ion MS imaging to relatively quantify cholesterol in the membranes of individual cells from differentially treated populations. *Analytical Chemistry* **2007,** *79* (10), 3554-3560.
15. Rabbani, S.; Fletcher, J. S.; Lockyer, N. P.; Vickerman, J. C., Exploring subcellular imaging on the buncher-ToF J105 3D chemical imager. *Surf Interface Anal* **2011,** *43* (1-2), 380-384.
16. Jiang, H.; Favaro, E.; Goulbourne, C. N.; Rakowska, P. D.; Hughes, G. M.; Ryadnov, M. G.; Fong, L. G.; Young, S. G.; Ferguson, D. J.; Harris, A. L.; Grovenor, C. R., Stable isotope imaging of

biological samples with high resolution secondary ion mass spectrometry and complementary techniques. *Methods* **2014,** *68* (2), 317-24.
17. Ong, T. H.; Kissick, D. J.; Jansson, E. T.; Comi, T. J.; Romanova, E. V.; Rubakhin, S. S.; Sweedler, J. V., Classification of Large Cellular Populations and Discovery of Rare Cells Using Single Cell Matrix-Assisted Laser Desorption/Ionization Time-of-Flight Mass Spectrometry. *Analytical Chemistry* **2015,** *87* (14), 7036-7042.
18. Ibanez, A. J.; Fagerer, S. R.; Schmidt, A. M.; Urban, P. L.; Jefimovs, K.; Geiger, P.; Dechant, R.; Heinemann, M.; Zenobi, R., Mass spectrometry-based metabolomics of single yeast cells. *P Natl Acad Sci USA* **2013,** *110* (22), 8790-8794.
19. Urban, P. L.; Jefimovs, K.; Amantonico, A.; Fagerer, S. R.; Schmid, T.; Madler, S.; Puigmarti-Luis, J.; Goedecke, N.; Zenobi, R., High-density micro-arrays for mass spectrometry. *Lab Chip* **2010,** *10* (23), 3206-3209.
20. Kruse, R. A.; Rubakhin, S. S.; Romanova, E. V.; Bohn, P. W.; Sweedler, J. V., Direct assay of Aplysia tissues and cells with laser desorption/ionization mass spectrometry on porous silicon. *J Mass Spectrom* **2001,** *36* (12), 1317-1322.
21. Greving, M. P.; Patti, G. J.; Siuzdak, G., Nanostructure-Initiator Mass Spectrometry Metabolite Analysis and Imaging. *Analytical Chemistry* **2011,** *83* (1), 2-7.
22. O'Brien, P. J.; Lee, M.; Spilker, M. E.; Zhang, C. C.; Yan, Z.; Nichols, T. C.; Li, W.; Johnson, C. H.; Patti, G. J.; Siuzdak, G., Monitoring metabolic responses to chemotherapy in single cells and tumors using nanostructure-initiator mass spectrometry (NIMS) imaging. *Cancer & Metabolism* **2013,** *1* (1), 4.
23. Walker, B. N.; Stolee, J. A.; Vertes, A., Nanophotonic Ionization for Ultratrace and Single-Cell Analysis by Mass Spectrometry. *Analytical Chemistry* **2012,** *84* (18), 7756-7762.
24. Chen, Y. T.; Li, G. Y.; Yuan, S. M.; Pan, Y.; Liu, Y. Z.; Huang, G. M., Ultrafast Microelectrophoresis: Behind Direct Mass Spectrometry Measurements of Proteins and Metabolites in Living Cell/Cells. *Analytical Chemistry* **2019,** *91* (16), 10441-10447.
25. Cooks, R. G.; Ouyang, Z.; Takats, Z.; Wiseman, J. M., Ambient mass spectrometry. *Science* **2006,** *311* (5767), 1566-1570.
26. Hiraoka, K.; Nishidate, K.; Mori, K.; Asakawa, D.; Suzuki, S., Development of probe electrospray using a solid needle. *Rapid Commun Mass Sp* **2007,** *21* (18), 3139-3144.
27. Arthur, C. L.; Pawliszyn, J., Solid-Phase Microextraction with Thermal-Desorption Using Fused-Silica Optical Fibers. *Analytical Chemistry* **1990,** *62* (19), 2145-2148.
28. Gong, X. Y.; Zhao, Y. Y.; Cai, S. Q.; Fu, S. J.; Yang, C. D.; Zhang, S. C.; Zhang, X. R., Single Cell Analysis with Probe ESI-Mass Spectrometry: Detection of Metabolites at Cellular and Subcellular Levels. *Analytical Chemistry* **2014,** *86* (8), 3809-3816.
29. Yu, Z.; Chen, L. C.; Ninomiya, S.; Mandal, M. K.; Hiraoka, K.; Nonami, H., Piezoelectric inkjet assisted rapid electrospray ionization mass spectrometric analysis of metabolites in plant single cells via a direct sampling probe. *Analyst* **2014,** *139* (22), 5734-5739.
30. Chen, F. M.; Lin, L. Y.; Zhang, J.; He, Z. Y.; Uchiyama, K.; Lin, J. M., Single-Cell Analysis Using Drop-on-Demand Inkjet Printing and Probe Electrospray Ionization Mass Spectrometry. *Analytical Chemistry* **2016,** *88* (8), 4354-4360.
31. Zheng, Y.; Liu, Z. Q.; Xing, J. P.; Zheng, Z.; Pi, Z. F.; Song, F. R.; Liu, S., In situ analysis of single cell and biological samples with rGO-Cu functional probe ESI-MS spectrometry. *Talanta* **2020,** *211*.

32. Gholipour, Y.; Erra-Balsells, R.; Hiraoka, K.; Nonami, H., Living cell manipulation, manageable sampling, and shotgun picoliter electrospray mass spectrometry for profiling metabolites. *Anal Biochem* **2013,** *433* (1), 70-78.
33. Tsuyama, N.; Mizuno, H.; Tokunaga, E.; Masujima, T., Live single-cell molecular analysis by video-mass spectrometry. *Analytical Sciences* **2008,** *24* (5), 559-561.
34. Zhuang, M. H.; Hou, Z. H.; Chen, P. Y.; Liang, G. L.; Huang, G. M., Introducing charge tag via click reaction in living cells for single cell mass spectrometry. *Chem Sci* **2020,** *11* (28), 7308-7312.
35. Hu, J.; Jiang, X.-X.; Wang, J.; Guan, Q.-Y.; Zhang, P.-K.; Xu, J.-J.; Chen, H.-Y., Synchronized Polarization Induced Electrospray: Comprehensively Profiling Biomolecules in Single Cells by Combining both Positive-Ion and Negative-Ion Mass Spectra. *Analytical Chemistry* **2016,** *88* (14), 7245-7251.
36. Zhu, Y. L.; Wang, W. H.; Yang, Z. B., Combining Mass Spectrometry with Paterno-Buchi Reaction to Determine Double-Bond Positions in Lipids at the Single-Cell Level. *Analytical Chemistry* **2020,** *92* (16), 11380-11387.
37. Nakashima, T.; Wada, H.; Morita, S.; Erra-Balsells, R.; Hiraoka, K.; Nonami, H., Single-Cell Metabolite Profiling of Stalk and Glandular Cells of Intact Trichomes with Internal Electrode Capillary Pressure Probe Electrospray Ionization Mass Spectrometry. *Analytical Chemistry* **2016,** *88* (6), 3049-3057.
38. Abouleila, Y.; Onidani, K.; Ali, A.; Shoji, H.; Kawai, T.; Lim, C. T.; Kumar, V.; Okaya, S.; Kato, K.; Hiyama, E.; Yanagida, T.; Masujima, T.; Shimizu, Y.; Honda, K., Live single cell mass spectrometry reveals cancer-specific metabolic profiles of circulating tumor cells. *Cancer Science* **2019,** *110* (2), 697-706.
39. Fujii, T.; Matsuda, S.; Tejedor, M. L.; Esaki, T.; Sakane, I.; Mizuno, H.; Tsuyama, N.; Masujima, T., Direct metabolomics for plant cells by live single-cell mass spectrometry. *Nat Protoc* **2015,** *10* (9), 1445-1456.
40. Masujima, T., Live Single-cell Mass Spectrometry. *Analytical Sciences* **2009,** *25* (8), 953-960.
41. Hiyama, E.; Ali, A.; Amer, S.; Harada, T.; Shimamoto, K.; Furushima, R.; Abouleila, Y.; Emara, S.; Masujima, T., Direct Lipido-Metabolomics of Single Floating Cells for Analysis of Circulating Tumor Cells by Live Single-cell Mass Spectrometry. *Analytical Sciences* **2015,** *31* (12), 1215-1217.
42. Esaki, T.; Masujima, T., Fluorescence Probing Live Single-cell Mass Spectrometry for Direct Analysis of Organelle Metabolism. *Analytical Sciences* **2015,** *31* (12), 1211-1213.
43. Ali, A.; Abouleila, Y.; Amer, S.; Furushima, R.; Emara, S.; Equis, S.; Cotte, Y.; Masujima, T., Quantitative Live Single-cell Mass Spectrometry with Spatial Evaluation by Three-Dimensional Holographic and Tomographic Laser Microscopy. *Analytical Sciences* **2016,** *32* (2), 125-127.
44. Zhao, J. B.; Zhang, F.; Guo, Y. L., Quantitative Analysis of Metabolites at the Single-Cell Level by Hydrogen Flame Desorption Ionization Mass Spectrometry. *Analytical Chemistry* **2019,** *91* (4), 2752-2758.
45. Huang, G. M.; Li, G. T.; Cooks, R. G., Induced Nanoelectrospray Ionization for Matrix-Tolerant and High-Throughput Mass Spectrometry. *Angew Chem Int Edit* **2011,** *50* (42), 9907-9910.

46. Phelps, M.; Hamilton, J.; Verbeck, G. F., Nanomanipulation-coupled nanospray mass spectrometry as an approach for single cell analysis. *Rev Sci Instrum* **2014,** *85* (12).
47. Laforge, F. O.; Carpino, J.; Rotenberg, S. A.; Mirkin, M. V., Electrochemical attosyringe. *Proc Natl Acad Sci U S A* **2007,** *104* (29), 11895-900.
48. Yin, R. C.; Prabhakaran, V.; Laskin, J., Quantitative Extraction and Mass Spectrometry Analysis at a Single-Cell Level. *Analytical Chemistry* **2018,** *90* (13), 7937-7945.
49. Bergman, H. M.; Lanekoff, I., Profiling and quantifying endogenous molecules in single cells using nano-DESI MS. *Analyst* **2017,** *142* (19), 3639-3647.
50. Pan, N.; Rao, W.; Kothapalli, N. R.; Liu, R.; Burgett, A. W.; Yang, Z., The single-probe: a miniaturized multifunctional device for single cell mass spectrometry analysis. *Anal Chem* **2014,** *86* (19), 9376-80.
51. Pan, N.; Standke, S. J.; Kothapalli, N. R.; Sun, M.; Bensen, R. C.; Burgett, A. W. G.; Yang, Z. B., Quantification of Drug Molecules in Live Single Cells Using the Single-Probe Mass Spectrometry Technique. *Analytical Chemistry* **2019,** *91* (14), 9018-9024.
52. Standke, S. J.; Colby, D. H.; Bensen, R. C.; Burgett, A. W. G.; Yang, Z., Mass Spectrometry Measurement of Single Suspended Cells Using a Combined Cell Manipulation System and a Single-Probe Device. *Analytical Chemistry* **2019,** *91* (3), 1738-1742.
53. Liu, R. M.; Pan, N.; Zhu, Y. L.; Yang, Z. B., T-Probe: An Integrated Microscale Device for Online In Situ Single Cell Analysis and Metabolic Profiling Using Mass Spectrometry. *Analytical Chemistry* **2018,** *90* (18), 11078-11085.
54. Zhu, Y. L.; Liu, R. M.; Yang, Z. B., Redesigning the T-probe for mass spectrometry analysis of online lysis of non-adherent single cells. *Anal Chim Acta* **2019,** *1084*, 53-59.
55. Yin, R. C.; Burnum-Johnson, K. E.; Sun, X. F.; Dey, S. K.; Laskin, J., High spatial resolution imaging of biological tissues using nanospray desorption electrospray ionization mass spectrometry. *Nat Protoc* **2019,** *14* (12), 3445-3470.
56. Laskin, J.; Heath, B. S.; Roach, P. J.; Cazares, L.; Semmes, O. J., Tissue Imaging Using Nanospray Desorption Electrospray Ionization Mass Spectrometry. *Analytical Chemistry* **2012,** *84* (1), 141-148.
57. Pan, N.; Rao, W.; Standke, S. J.; Yang, Z. B., Using Dicationic Ion-Pairing Compounds To Enhance the Single Cell Mass Spectrometry Analysis Using the Single-Probe: A Microscale Sampling and Ionization Device. *Analytical Chemistry* **2016,** *88* (13), 6812-6819.
58. Standke, S. J.; Colby, D. H.; Bensen, R. C.; Burgett, A. W. G.; Yang, Z. B., Integrated Cell Manipulation Platform Coupled with the Single-probe for Mass Spectrometry Analysis of Drugs and Metabolites in Single Suspension Cells. *Jove-J Vis Exp* **2019,** (148).
59. Bensen, R. C.; Standke, S. J.; Colby, D. H.; Kothapalli, N. R.; Le-McClain, A. T.; Patten, M. A.; Tripathi, A.; Heinlen, J. E.; Yang, Z.; Burgett, A. W. G., Single Cell Mass Spectrometry Quantification of Anticancer Drugs: Proof of Concept in Cancer Patients. *ACS Pharmacol Transl Sci* **2021,** *4* (1), 96-100.
60. Sun, M.; Tian, X.; Yang, Z. B., Microscale Mass Spectrometry Analysis of Extracellular Metabolites in Live Multicellular Tumor Spheroids. *Analytical Chemistry* **2017,** *89* (17), 9069-9076.
61. Tian, X.; Zhang, G. W.; Zou, Z.; Yang, Z. B., Anticancer Drug Affects Metabolomic Profiles in Multicellular Spheroids: Studies Using Mass Spectrometry Imaging Combined with Machine Learning. *Analytical Chemistry* **2019,** *91* (9), 5802-5809.

62. Tian, X.; Zhang, G. W.; Shao, Y. H.; Yang, Z. B., Towards enhanced metabolomic data analysis of mass spectrometry image: Multivariate Curve Resolution and Machine Learning. *Anal Chim Acta* **2018,** *1037*, 211-219.
63. Rao, W.; Pan, N.; Yang, Z. B., High Resolution Tissue Imaging Using the Single-probe Mass Spectrometry under Ambient Conditions. *J Am Soc Mass Spectr* **2015,** *26* (6), 986-993.
64. Lee, J. K.; Jansson, E. T.; Nam, H. G.; Zare, R. N., High-Resolution Live-Cell Imaging and Analysis by Laser Desorption/Ionization Droplet Delivery Mass Spectrometry. *Analytical Chemistry* **2016,** *88* (10), 5453-5461.
65. Shrestha, B.; Vertes, A., In Situ Metabolic Profiling of Single Cells by Laser Ablation Electrospray Ionization Mass Spectrometry. *Anal. Chem.* **2009,** *81* (20), 8265-8271.
66. Shrestha, B.; Nemes, P.; Vertes, A., Ablation and analysis of small cell populations and single cells by consecutive laser pulses. *Appl Phys a-Mater* **2010,** *101* (1), 121-126.
67. Nemes, P.; Vertes, A., Laser ablation electrospray ionization for atmospheric pressure, in vivo, and imaging mass spectrometry. *Analytical Chemistry* **2007,** *79* (21), 8098-8106.
68. Stolee, J. A.; Shrestha, B.; Mengistu, G.; Vertes, A., Observation of Subcellular Metabolite Gradients in Single Cells by Laser Ablation Electrospray Ionization Mass Spectrometry. *Angew Chem Int Edit* **2012,** *51* (41), 10386-10389.
69. Shrestha, B.; Patt, J. M.; Vertes, A., In Situ Cell-by-Cell Imaging and Analysis of Small Cell Populations by Mass Spectrometry. *Analytical Chemistry* **2011,** *83* (8), 2947-2955.
70. Li, H.; Smith, B. K.; Shrestha, B.; Márk, L.; Vertes, A., Automated Cell-by-Cell Tissue Imaging and Single-Cell Analysis for Targeted Morphologies by Laser Ablation Electrospray Ionization Mass Spectrometry. In *Mass Spectrometry Imaging of Small Molecules*, He, L., Ed. Springer New York: New York, NY, 2015; pp 117-127.
71. Lapainis, T.; Rubakhin, S. S.; Sweedler, J. V., Capillary electrophoresis with electrospray ionization mass spectrometric detection for single-cell metabolomics. *Anal Chem* **2009,** *81* (14), 5858-64.
72. Nemes, P.; Knolhoff, A. M.; Rubakhin, S. S.; Sweedler, J. V., Metabolic differentiation of neuronal phenotypes by single-cell capillary electrophoresis-electrospray ionization-mass spectrometry. *Anal Chem* **2011,** *83* (17), 6810-7.
73. Nemes, P.; Rubakhin, S. S.; Aerts, J. T.; Sweedler, J. V., Qualitative and quantitative metabolomic investigation of single neurons by capillary electrophoresis electrospray ionization mass spectrometry. *Nat Protoc* **2013,** *8* (4), 783-99.
74. Onjiko, R. M.; Moody, S. A.; Nemes, P., Single-cell mass spectrometry reveals small molecules that affect cell fates in the 16-cell embryo. *Proc Natl Acad Sci U S A* **2015,** *112* (21), 6545-50.
75. Zhang, L. W.; Foreman, D. P.; Grant, P. A.; Shrestha, B.; Moody, S. A.; Villiers, F.; Kwake, J. M.; Vertes, A., In Situ metabolic analysis of single plant cells by capillary microsampling and electrospray ionization mass spectrometry with ion mobility separation. *Analyst* **2014,** *139* (20), 5079-5085.
76. Zhang, L. W.; Vertes, A., Energy Charge, Redox State, and Metabolite Turnover in Single Human Hepatocytes Revealed by Capillary Microsampling Mass Spectrometry. *Anal. Chem.* **2015,** *87* (20), 10397-10405.
77. Feng, D. S.; Xu, T. R.; Li, H.; Shi, X. Z.; Xu, G. W., Single-cell Metabolomics Analysis by Microfluidics and Mass Spectrometry: Recent New Advances. *J Anal Test* **2020,** *4* (3), 198-209.

78. Mellors, J. S.; Jorabchi, K.; Smith, L. M.; Ramsey, J. M., Integrated Microfluidic Device for Automated Single Cell Analysis Using Electrophoretic Separation and Electrospray Ionization Mass Spectrometry. *Analytical Chemistry* **2010,** *82* (3), 967-973.
79. Xie, W. Y.; Gao, D.; Jin, F.; Jiang, Y. Y.; Liu, H. X., Study of Phospholipids in Single Cells Using an Integrated Microfluidic Device Combined with Matrix-Assisted Laser Desorption/Ionization Mass Spectrometry. *Analytical Chemistry* **2015,** *87* (14), 7052-7059.
80. Feng, J. X.; Zhang, X. C.; Huang, L.; Yao, H.; Yang, C. D.; Ma, X. X.; Zhang, S. C.; Zhang, X. R., Quantitation of Glucose-phosphate in Single Cells by Microwell-Based Nanoliter Droplet Microextraction and Mass Spectrometry. *Analytical Chemistry* **2019,** *91* (9), 5613-5620.
81. Li, Q.; Tang, F.; Huo, X. M.; Huang, X.; Zhang, Y.; Wang, X. H.; Zhang, X. R., Native State Single-Cell Printing System and Analysis for Matrix Effects. *Analytical Chemistry* **2019,** *91* (13), 8115-8122.
82. Zhang, W. F.; Li, N.; Lin, L.; Huang, Q. S.; Uchiyama, K.; Lin, J. M., Concentrating Single Cells in Picoliter Droplets for Phospholipid Profiling on a Microfluidic System. *Small* **2020,** *16* (9).
83. Huang, Q. S.; Mao, S. F.; Khan, M.; Li, W. W.; Zhang, Q.; Lin, J. M., Single-cell identification by microfluidic-based in situ extracting and online mass spectrometric analysis of phospholipids expression. *Chem Sci* **2020,** *11* (1), 253-256.
84. Roddy, T. P.; Cannon, D. M.; Meserole, C. A.; Winograd, N.; Ewing, A. G., Imaging of freeze-fractured cells with in situ fluorescence and time-of-flight secondary ion mass spectrometry. *Analytical Chemistry* **2002,** *74* (16), 4011-4019.
85. Zhang, L. W.; Sevinsky, C. J.; Davis, B. M.; Vertes, A., Single-Cell Mass Spectrometry of Subpopulations Selected by Fluorescence Microscopy. *Analytical Chemistry* **2018,** *90* (7), 4626-4634.
86. Neumann, E. K.; Comi, T. J.; Rubakhin, S. S.; Sweedler, J. V., Lipid Heterogeneity between Astrocytes and Neurons Revealed by Single-Cell MALDI-MS Combined with Immunocytochemical Classification. *Angew Chem Int Edit* **2019,** *58* (18), 5910-5914.
87. Fagerer, S. R.; Schmid, T.; Ibanez, A. J.; Pabst, M.; Steinhoff, R.; Jefimovs, K.; Urban, P. L.; Zenobi, R., Analysis of single algal cells by combining mass spectrometry with Raman and fluorescence mapping. *Analyst* **2013,** *138* (22), 6732-6736.
88. Urban, P. L.; Schmid, T.; Amantonico, A.; Zenobi, R., Multidimensional Analysis of Single Algal Cells by Integrating Microspectroscopy with Mass Spectrometry. *Analytical Chemistry* **2011,** *83* (5), 1843-1849.

Chapter 2. Research Overview

In the past five years, my research has been focused on two aspects of single cell MS analysis: (1) the application of the Single-probe MS metabolomics studies of the synergistic effect between metformin and irinotecan on Irinotecan-resistant cells from the metabolomics approach, and (2) the integration of fluorescence microscopy with the Single-probe SCMS for the metabolomics studies of interactions between drug-resistant and drug-sensitive cells in co-culture systems.

This first project is described in Chapter 3. Irinotecan (IRI) is a chemotherapy drug widely used for the treatment of colon and lung cancers. Despite being an effective chemotherapy drug, clinical usage of irinotecan suffers from small population of cancer cells with drug resistance.[1] Our previous studies indicate irinotecan induces cancer stemness in irinotecan-resistant (IRI-resistant) cells.[2] Metformin, an oral antidiabetic drug, was recently reported for anticancer effects, likely due to its selective killing of CSCs (cancer stem cells).[3] Given IRI-resistant cells exhibited high cancer stemness, we hypothesize metformin can sensitize IRI-resistant cells and rescue the therapeutic effect. The combinational index values were first investigated the synergistic effect of metformin and irinotecan, then the Single-probe MS technique was utilized to study metabolomic profiles of IRI-resistant cells treated with mono-treatment (metformin) and co-treatment (metformin and IRI). The metabolites data shown that large numbers of cellular lipids, including glycerophosphoinositol lipids (PI), glycerophosphoserine (PS), and sphingomyelin (SM), were significantly decreased after combinational treatment (co-treatment). Correspondingly. We also observed different fatty acids (palmitic acid, stearic acid, etc.,) were significantly decreased after co-treatment. Using enzymatic

activity assay, we determined that the synergistic relationship of the co-treatment associates with the high inhibition on fatty acid synthase (FASN).

The second project is detailed in Chapter 4. Cell–cell interactions are critical for transmitting signals among cells and maintaining their normal functions from the single-cell level to tissues.[4] In cancer studies, interactions between drug-resistant and drug-sensitive cells play an important role in the development of chemotherapy resistance of tumors.[5] A variety of *in vitro* co-culture systems, either allowing indirect co-culture or direct co-culture, have been developed to study the mechanisms of cell-cell interactions.[6-8] Although a few direct co-culture systems have been developed, it is challenging to comprehensively analyze metabolomic profiles of individual cells among heterogeneous populations. Mass spectrometry (MS) is a powerful tool for the analysis of cellular metabolites. To study the cell-cell interactions among different types of cells, single cell MS (SCMS) metabolomics analysis is needed. A workflow was designed to combine the Single-probe SCMS technique with fluorescence microscopy to study cell-cell interactions in co-culture systems. Using the designed workflow, the metabolic profiles of drug-sensitive cells (HCT116 cells labeled with green fluorescent protein (GFP)) were found to be significantly changed by the drug-resistant cells (HCT116 cells with acquired IRI resistance) in the co-culture system with direct contact. Interestingly, both types of cells tend to exhibit increased similarities of metabolomic profiles after co-culture. Investigation of cell metabolites altered by co-culture shows that sphingomyelins (SM) lipids, lactic acid, TCA cycle intermediates and fatty acids were significantly regulated in drug-sensitive cells.

References

1. Petitprez, A.; Poindessous, V.; Ouaret, D.; Regairaz, M.; Bastian, G.; Guerin, E.; Escargueil, A. E.; Larsen, A. K., Acquired irinotecan resistance is accompanied by stable modifications of cell cycle dynamics independent of MSI status. *Int J Oncol* **2013,** *42* (5), 1644-1653.10.3892/ijo.2013.1868
2. Liu, R. M.; Sun, M.; Zhang, G. W.; Lan, Y. P.; Yang, Z. B., Towards early monitoring of chemotherapy-induced drug resistance based on single cell metabolomics: Combining single-probe mass spectrometry with machine learning. *Anal Chim Acta* **2019,** *1092*, 42-48.10.1016/j.aca.2019.09.065
3. Rattan, R.; Ali Fehmi, R.; Munkarah, A., Metformin: an emerging new therapeutic option for targeting cancer stem cells and metastasis. *J Oncol* **2012,** *2012*, 928127.10.1155/2012/928127
4. Gebhardt, R., Cell-Cell Interactions - Clues to Hepatocyte Heterogeneity and Beyond. *Hepatology* **1992,** *16* (3), 843-845
5. Holohan, C.; Van Schaeybroeck, S.; Longley, D. B.; Johnston, P. G., Cancer drug resistance: an evolving paradigm. *Nat Rev Cancer* **2013,** *13* (10), 714-26.10.1038/nrc3599
6. Hamilton, S. K.; Bloodworth, N. C.; Massad, C. S.; Hammoudi, T. M.; Suri, S.; Yang, P. J.; Lu, H.; Temenoff, J. S., Development of 3D hydrogel culture systems with on-demand cell separation. *Biotechnol J* **2013,** *8* (4), 485-95.10.1002/biot.201200200
7. Renaud, J.; Martinoli, M. G., Development of an Insert Co-culture System of Two Cellular Types in the Absence of Cell-Cell Contact. *Jove-J Vis Exp* **2016,** (113).ARTN e54356 10.3791/54356
8. Pandurangan, M.; Hwang, I., Application of cell co-culture system to study fat and muscle cells. *Appl Microbiol Biotechnol* **2014,** *98* (17), 7359-64.10.1007/s00253-014-5935-9

Chapter 3. Single Cell Mass Spectrometry Analysis of Drug-resistant Cancer Cells: Metabolomics Studies of Synergetic Effect of Combinational Treatment

Author Contributions: Studies included in Chapter 3 are mainly conducted by Xingxiu Chen. Mei Sun assisted cell viability measurements.

Copyright permission: The material in chapter 3 is adapted from Xingxiu Chen, Mei Sun, and Zhibo Yang, 'Single cell mass spectrometry analysis of drug-resistant cancer cells: metabolomics studies of synergetic effect of combinational treatment'. Anal. Chim. Acta, 2022, 1201, 339621. Copyright permission is obtained from Elsevier, and the detail is included in Appendix III.

3.1 Abstract

Irinotecan (IRI), a topoisomerase I inhibitor blocking DNA synthesis, is a widely used chemotherapy drug for metastatic colorectal cancer. Despite being an effective chemotherapy drug, its clinical effectiveness is limited by both intrinsic and acquired drug resistance. Previous studies indicate IRI induces cancer stemness in irinotecan-resistant (IRI-resistant) cells. Metformin, an oral antidiabetic drug, was recently reported for anticancer effects, likely due to its selective killing of cancer stem cells (CSCs). Given IRI-resistant cells exhibiting high cancer stemness, we hypothesize metformin can sensitize IRI-resistant cells and rescue the therapeutic effect. In this work, we utilized the Single-probe mass spectrometry technique to analyze live IRI-resistant cells under different

treatment conditions. We discovered that metformin treatment was associated with the downregulation of lipids and fatty acids, potentially through the inhibition of fatty acid synthase (FASN). Importantly, certain species can be only detected from cells in their living status. The level of synergistic effect of metformin and IRI in their co-treatment of IRI-resistant cells was evaluated using Chou-Talalay combinational index. Using enzymatic activity assay, we determined that the co-treatment exhibit the highest FASN inhibition compared with the mono-treatment of IRI or metformin. To our knowledge, this is the first single-cell MS metabolomics study demonstrating metformin-IRI synergistic effect overcoming drug resistance in IRI-resistant cells.

3.2 Introduction

Drug resistance, classified as intrinsic resistance (pre-existent) and acquired resistance (induced by drug), occurs in almost all cancer patients in chemotherapy, decreasing the therapeutic effect of the treatment.[1] Acquired drug resistance is one of the major challenges of treating metastatic colorectal cancer (mCRC) patients. Among all cancers, colorectal cancer is the third most common cancer diagnosed and the fourth leading cause of cancer death worldwide.[2] GLOBOCAN estimates colorectal cancer accounted for 6.1% of all cancer incidence and 9.2% of all cancer deaths in 2018.[3] It is estimated approximately 60% of patients will ultimately develop into mCRC,[4] whereas more than 30% of patients were first diagnosed with mCRC in their early stages without showing any symptoms.[4]

Irinotecan (IRI) is a widely used chemotherapy drug for the treatment of mCRC. Chemotherapy regimens using IRI (e.g., FOLFIRI and FOLFOXIRI) are standard first-line therapies for mCRC. As an effective chemotherapy drug, IRI containing regimens give

an average response rate of 31–65% and overall median survival of 14–31 months.[5-7] However, the effectiveness of IRI treatment suffers from small populations of cancer cells with acquired drug resistance, which is a common reason for treatment failure. Numerous studies have been performed to explain the mechanisms of IRI drug resistance. The proposed theories include drug inactivation by IRI glucuronidation[8], reduced drug accumulation in subcellular localization caused by active drug efflux[9], drug-target interaction reduction by decreased topoisomerase I expression[10], DNA damage minimization by decreasing topo I-DNA interaction[11], and the induction of cancer stem-like cells to escape cytotoxic effect.[12-13] To gain an insight into the cellular mechanism of IRI resistance in colorectal cancer cells, we studied the changes in metabolites and proteins of IRI-resistant cells, which were derived from colorectal cancer cell line HCT-116 through low-does (1 μM) IRI treatment.[14] Compared with the parental HCT-116 cells, the resistance index (RI = $\frac{IC_{50(drug-resistant\ cell)}}{IC_{50(parental\ cell)}}$) increased from 1.9 to 3.6 after HCT-116 cells were exposed to IRI for 10 and 20 days, respectively.[14] Further studies found the IRI-resistant cells exhibited certain levels of similarities of lipid compositions as cancer stem cells. In addition, we discovered that IRI-resistant cells possess cancer stemness, including the enriched proteins and overexpressed mRNAs of cancer stem cells (CSCs) biomarkers such as CD133, CD24, and ALDH1A1.

Metformin is a classical biguanide antidiabetic drug. Recently, it was reported that the chemotherapy involving metformin showed enhanced anticancer effects,[15] arising from its ability of selectively killing CSCs.[16-18] Metformin exhibits pharmacological activities on CSCs by disrupting their energy metabolism (e.g., glycolysis, TCA cycle, and electron transport chain) to inhibit oxidative phosphorylation and ATP synthesis.[19]

Eventually, metformin induces energy crisis to CSCs by preventing cellular metabolism shifting from mitochondrial-dependent metabolism to aerobic glycolysis.[19] In fact, the antitumor capability of metformin was reflected from the decreased expression of CSCs biomarkers, such as CD44, EZH2, Oct4, in cells treated by this compound.[20]

The combined treatment of metformin and IRI in mCRC patients has been previously proposed, and Phase 2 clinical trial of this combination showed improved disease control and better overall survival for patients.[21] However, studies of the combined treatment of IRI-resistant cells have not been performed, and the molecular mechanisms of the synergistic effect remain unclear. Based on the facts that metformin targeting CSCs and IRI-resistant cells exhibiting high cancer stemness, we predict metformin can rescue the therapeutic effect of IRI in IRI-resistant cells.

Metabolites are the end products of cellular activities, and they directly and sensitively reflect the genetic and environmental changes of cells. Cellular metabolomics studies have become an indispensable approach to determining alterations in metabolic pathways induced by environmental stimuli, including physical and chemical changes. Owing to its high sensitivity and accuracy, mass spectrometry (MS) has become a powerful tool for metabolomics studies. MS metabolomics studies have been generally performed using samples prepared from populations of cells. However, this strategy becomes ineffective when analyzing specific types of cells among heterogeneous populations. Tumor heterogeneity in cancer is characterized by the diversity of cancer cells consisting of a broad spectrum of morphologies, gene expression profiles, and functional features.[22-23] Cancer cell heterogeneity is driven by both intrinsic (e.g., epigenetic mutation) and extrinsic factors (e.g., drug-related stimuli during treatment).[23]

Because metabolites have rapid turnover rates, they promptly reflect the status of live cells, and any environment perturbation may affect their native compositions.[24-25] Thus, traditional HPLC-MS based methods requiring multi-step sample preparation (e.g., cell pellet preparation, cell lysis, and metabolite extraction) cannot accurately reflect intrinsic compositions of metabolites in live cells. An obvious choice to use ambient single cell MS (SCMS) techniques to measure of individual cells in their living status.

A variety of ambient single cell MS (SCMS) techniques have been developed and utilized in numerous studies. Example of these techniques include Live single-cell MS[26], capillary microsampling ESI-IMS-MS[27], patch clamp technique combined nano-ESI-MS[28], nano-DESI single cell MS[29], and laser ablation based single cell MS[30]. In this work, we utilized the Single-probe SCMS technique to study the metabolomic changes of IRI-resistant cells upon metformin treatment and metformin-IRI co-treatment. The Single-probe SCMS technique is a versatile tool that can be used to study cellular metabolism of individual cells and to quantify drug compounds inside live single cells in ambient conditions.[31-35] To further verify the mechanisms of the synergistic effect, enzymatic activity assay of fatty acid synthase (FASN) was performed to compare the inhibition levels of FASN between the mono-treatment (IRI or metformin) and co-treatment (IRI combined with metformin).

3.3 Experimental section

3.3.1 Cell culture

The establishment of IRI-resistant cells followed our previously published protocols.[14] Briefly, HCT-116 cells were cultured with 1 μM IRI in McCoy's 5a Medium (Fisher Scientific Company LLC, IL, USA) supplemented with 10% fetal bovine serum

(FBS, GE Healthcare Bio-science Corp, Marlborough, MA, USA) and 1% penicillin streptomycin (Life Technologies Corporation, Grand Island, NY, USA). HCT-116 cells were split when their confluency reached 80%. For the cell passaging, 2 mL trypsin–EDTA (Life Technologies Corporation, Grand Island, NY, USA) was incubated into a petri dish at 37°C for 3 minutes, and then 8 mL cell culture medium was added to quench trypsin enzymatic activity. Sub-culture was performed by pipetting 1 mL cell suspending solution into 9 mL fresh culture medium. IRI-resistant cells were harvested after culturing HCT-116 cells in the culture medium containing 1 μM IRI for 30 days.

3.3.2 The Single-probe SCMS analysis

The Single-probe was fabricated according to the previously established protocols.[33] The Single-probe is composed of three major parts: a nano-ESI emitter, a dual-bore quartz needle, and a fused silica capillary. A dual-bore quartz tubing (O.D. 500 μm; I.D. 127 μm, Friedrich & Dimmock, Millville, NJ) was pulled into needle with a sharp needle (tip size is approximately 10 μm) using a laser micropipette puller (Sutter P-2000, Sutter Instrument, Novato, CA). The Nano-ESI emitter was produced by pulling the fused silica capillary (O.D. 105μm; I.D. 40 μm, Polymicro Technologies, Phoenix, AZ) using a butane micro torch. Fabrication of the Single-probe requires inserting the fused silica capillary and nano-ESI emitter into the dual-bore quartz needle. To conveniently conduct experiment, the Single-probe was attached to a microscope glass slide using epoxy glue. The Single-probe was then attached to an XYZ-stage system coupled to the Thermo LTQ Orbitrap XL mass spectrometer (Thermo Scientific, Waltham, MA) for the SCMS analysis. Acetonitrile (1% formic acid) was used as the solvent for the SCMS experiments. The mass range of the mass spectrometer was set as m/z 150─2000 and m/z 50─800 in the

positive and negative ion mode, respectively. Other mass spectrometer parameter settings are mass resolution 60,000, ionization voltage 4.5kV (positive ion mode)/- 4.5kV (negative ion mode), 1 microscan, 100 ms max injection time, and AGC (target $5E^5$) on.

3.3.3 Cell viability analysis

The cell viability measurements of IRI-resistant cells were performed using the MTT (3-(4,5-dimethylthoazol-2-yl)-2,5-diphenyltetrazolium bromide) assay. . The assay was conducted according to the previous publication with a few modifications.[36] Briefly after settling down the IRI-resistant cells (cell density ~ 10,000 cells/well) into 96-well plates, drug treatments were carried out using different concentrations of IRI (1.0, 4.0, 8.0, 16, 64, and 128 μM) combined with metformin (2.0, 4.0, and 8.0 mM). MTT (BIOTIUM Inc., Hayward, CA) was added into each well of 96-well plates, and then absorbance signal at 570 nm and background absorbance at 630 nm were measured using a microplate reader (Synergy H1, BioTek, Winooski, VE). Five replicates were measured for each drug treatment, and the cell viability values are summarized in Fig. 1A. MTT assay was used to measure cell viability of IRI-resistant cells under metformin and IRI mono-treatments, and the IC_{50} values of these two drugs were determined using Prism (GraphPad Software Inc.).

3.3.4 Enzymatic activity analysis

There are two major steps in measuring enzymatic activities of IRI-resistant cells in the current studies. First, we extracted enzyme from the IRI-resistant cells. Cells under different treatment conditions were harvested and washed with cold PBS. To obtain the protein fraction, cells were mixed with ice-cold enzyme lysis buffer (20 mM Tris-HCl, pH = 7.5, 1mM dithiothreitol, and 1mM EDTA) and sonicated at 4 ^oC for 10 min. Cell lysates

were centrifuged for 10 min at 100,000g, and the supernatants were collected. Second, we conducted NADPH absorbance assay of the supernatant to measure FASN activity following the published protocols.[37-39] Briefly, the concentrations of cellular proteins in the supernatant were measured using Piece BCA protein assay (Thermo Scientific, Waltham, MA). The supernatant was added in to 96-well plate and diluted by the assay buffer (25 mM K_2HPO_4-KH_2PO_4, pH = 7, 250 μM EDTA, and 250 μM dithiothreitol) to reach the final concentration of 100 μg protein/well (with 300 μL total volume). The background oxidation rate of NADPH was obtained from the absorbance (at 340 nm for 3 min) after the addition of 30 μM Acetyl-CoA (Sigma-Aldrich, St. Louis, MO) and 350 μM NADPH (Sigma-Aldrich, St. Louis, MO) into wells. The oxidation reaction of NADPH was then initiated by adding 100 μM Malonyl-CoA (Sigma-Aldrich, St. Louis, MO), and the absorption was monitored (at 340 nm for 10 min). The net oxidation rate of NADPH was then determined from the decreased rate of absorbance with the correction of background oxidation rate. The results were expressed as one enzymatic unit equals the oxidation for 1 nmol NADPH/min/μg. Statistical analysis of enzymatic activities was conducted with one-way ANOVA (analysis of variance) using GraphPad Prism (GraphPad Software Inc.).

3.3.5 HPLC-MS

HPLC-MS analyses of cell lysates were performed to provide complementary information to identify ions of interest. Cell lysates were prepared using the Folch's extraction method. Briefly, the IRI-resistant cells were suspended into PBS solution after trypsinization, chloroform and methanol (3:1, v/v) were added, and then the mix was vortexed on ice for 10 mins. After separating two layers by centrifuge, the organic layer

was transferred and dried under the vacuum. The samples were then stored in -80°C refrigerator prior to HPLC-MS analysis.

An UltiMate 3000 HPLC system (Thermo Scientific, San Jose, CA) was coupled to the LTQ Orbitrap XL mass spectrometer for metabolites separation and MS^2 identification. A Luca 3u C18 column (50 X 2.00 mm, 3 μm, Phenomenex, Torrance, CA) was used for chromatographic separation. The settings of HPLC include injection volume: 5 μL; column oven: 50 °C; Flow rate: 350 μl/min; mobile phase A: acetonitrile/water (60/40, v/v); mobile phase B: isopropanol/acetonitrile/water (90/8/2, v/v). Both mobile phases contain 10 mM ammonium formate and 0.1% formic acid. The total run time was 80 mins, including 5 mins' equilibrium. The MS^2 analyses were carried out in data independent mode, and the normalized collision energy (NCE) was set as 24-25 (factory unit) for collision induced dissociation (CID) experiments.

3.3.6 Data analysis

Adopted from our previous studies,[40] a customized R script was used for data preprocessing, including background signals removal (e.g., from solvent and cell culture medium) and normalization of ion intensities to the total ion current (TIC)[40], followed by peak alignment of MS data from all cells using Geena 2.[41] Multivariate analysis, performed using the partial least squares discriminant analysis (PLS-DA) in MetaboAnalyst 4.0,[42] was carried out to compare the overall metabolic profiles of cells in different groups. Levene's test was conducted, and the results indicated equal variance of the data across samples. Thus, Student's t-test (in MetaboAnalyst) was applied to obtain metabolites with significantly different abundances in cells from two groups. One-way ANOVA and post-hoc test (Tukey's test) were performed to reveal the cellular

metabolites changes among three groups.[40] To tentatively label ions, we used three different online databases, METLIN[43], HMDB[44] and GNPS[45], to search for potential metabolites (mass error < 5 ppm). The identification of chemical structures of ions of interest was based on the tandem MS (MS^2) results.

3.4 Results and Discussion

3.4.1 Co-treatment of metformin and IRI exhibited synergistic effect in IRI-resistant cells.

To quantitatively evaluate the enhanced potency of metformin and IRI in the combined treatment of IRI-resistant cells, we measured the combinational treatment effect of these two compounds. Solutions with different final concentrations of IRI (1.0, 4.0, 8.0, 16, 64, and 128 μM) and metformin (2.0, 4.0, and 8.0 mM) were used to measure cell viability using the MTT assay. As shown in Fig. 1A, both IRI and metformin inhibited cell proliferation in a dose-dependent manner. The combination of IRI and metformin resulted in higher death degrees of IRI-resistant cells. To quantitatively evaluate the synergistic effect between IRI and metformin, we calculated the combinational index (CI) values of these two compounds using Chow-Talalay method integrated in CompuSyn software.[46] The degrees of synergetic effect of any two compounds are reflected from the CI values: synergism (CI < 1), additive effect (CI = 1), or antagonism (CI > 1).[46-48] Our measurements show that the CI values for the co-treatment of IRI and metformin are less than 1 (Fig. 1B), indicating the presence of synergistic effects of these two compounds in the treatment of IRI-resistant cells. The relationships between CI values and Fa (i.e., faction affected) are summarized in Fig. 1B. Although all combinational treatments showed synergetic effects, most of them resulted in strong or very strong synergism (Fig.

S2C), according to the previously established standard of assessment (i.e., very strong synergism (CI<0.1), strong synergism (0.1<CI<0.3), and synergism (0.3<CI<0.7)).[49]

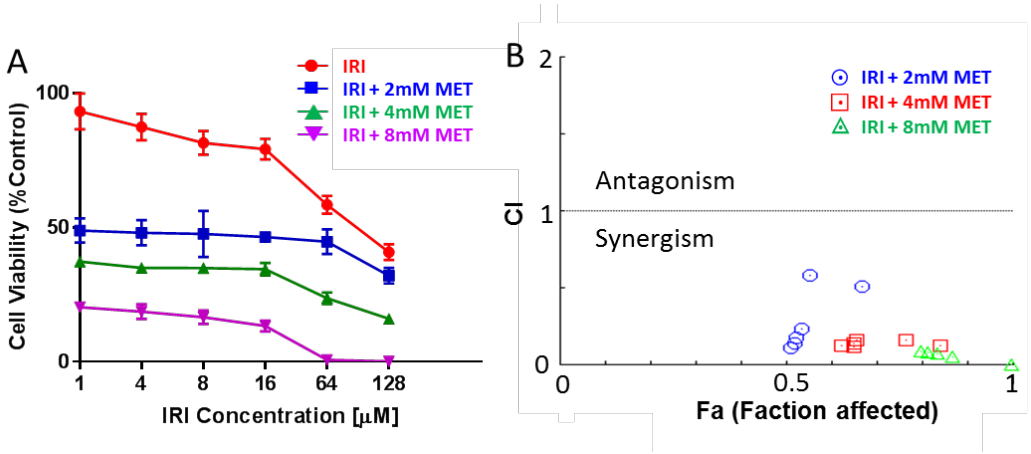


Fig. 1. Measurements of cell viability and combinational index (CI). (A) Cell viability plot of IRI-resistant cells treated using combined irinotecan (IRI) and metformin (MET). Cell viabilities in co-treatments are corelative to the measurements from IRI monotreatment. (B) The CI-Fa (faction affected) plot for IRI and metformin in IRI-resistant cell.

3.4.2 Metformin treatment resulted in downregulated fatty acids and lipids.

To study the influence of metformin on metabolites in IRI-resistant cells, 8.7 mM metformin, which is its IC_{50} determined from the MTT assay (Fig. S2A), was utilized to treat IRI-resistant cells followed by the Single-probe SCMS metabolomic analysis in both the positive and negative ion modes. In the comparison studies, the same measurements were conducted using cells without metformin treatment. As reported in our previous studies, the technical variance of the Single-probe SCMS technique (i.e., ion intensity fluctuation due to technical factors during the SCMS experiments) is insignificant compared with the biological variance (i.e., mass spectra difference due to the variation

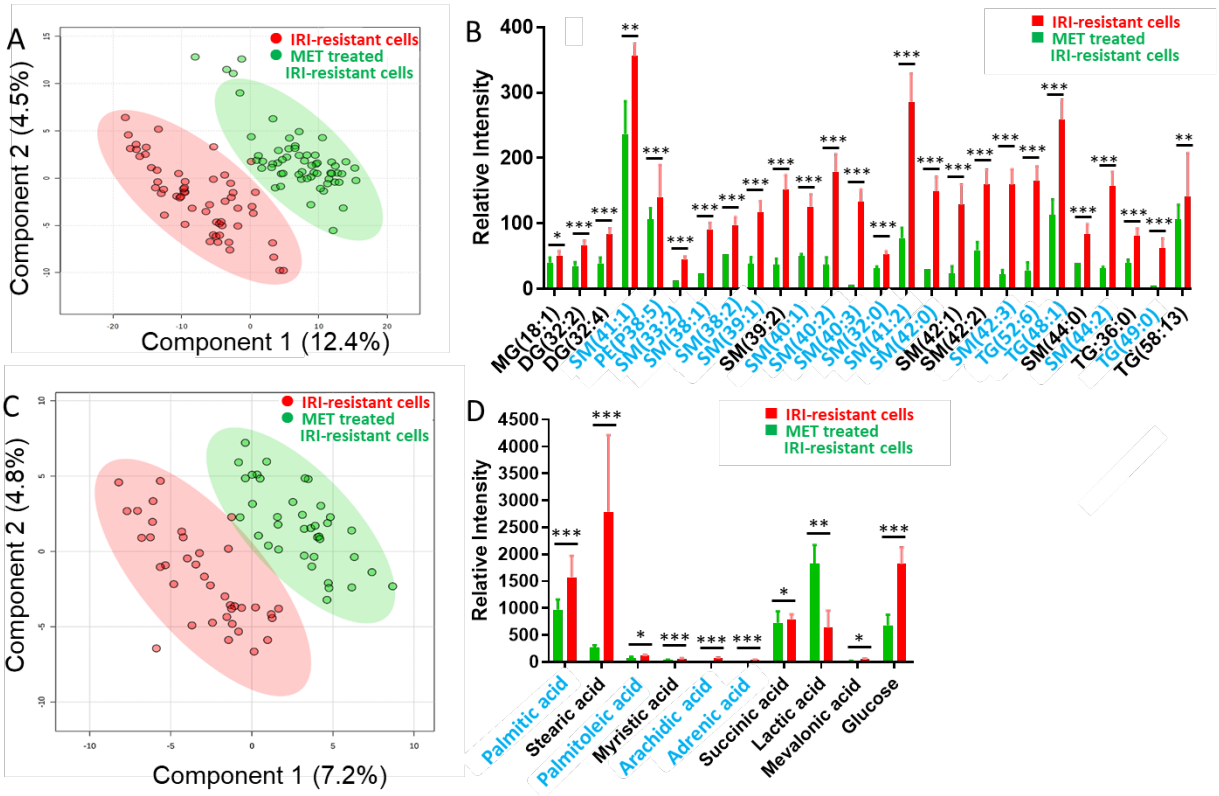


Fig. 2. SCMS results revealing the influence of metformin (8.7 mM) mono-treatment on metabolites of IRI-resistant cells. (A) PLS-DA of positive ion mode results shows the metabolomics profiles were significantly changed ($p = 0.009$ from permutation test), and (B) representative lipids with significant abundance change ($p < 0.05$ from Student's t-test). (C) PLS-DA of negative ion mode results shows the metabolomics profiles were significantly changed ($p < 0.003$ from permutation test), and (D) representative fatty acids with significant abundance change ($p < 0.05$, ** $p < 0.01$, *** $p < 0.001$ from Student's t-test). Species labeled in blue font were identified using MS^2 analysis both from single cells and cell lysates. (MG: monoglycerides; DG: diglyceride; TG: triglyceride; PI: phosphatidylinositol; PS: Phosphatidylserine; SM: sphingomyelin).*

of heterogeneous cellular metabolites).[14] PLS-DA can be utilized to illustrate the within-group cell heterogeneity (i.e., data point distribution of each group) and difference of cells

in different groups (i.e., overlap between different groups). PLS-DA was utilized to evaluate the difference of metabolomic profiles of individual cells in different treatment groups. In the positive ion mode, significantly different ($p=0.009$ from permutation test) metabolic profiles were observed upon metformin treatment (Fig. 2A). Furthermore, we performed the Student's t-test and found a large number of cellular lipids significantly downregulated by metformin (e.g., Fig. 2B). Similarly, significantly different ($p<0.003$ from permutation test) metabolic profiles were obtained between these two groups in the negative ion mode (Fig. 2C). A number of fatty acids, including palmitic acid, stearic acid, palmitoleic acid, myristic acid, arachidic acid, and adrenic acid, were significantly downregulated (Fig. 2D).

3.4.3 Metformin and IRI co-treatment resulted in downregulated lipids, fatty acids, and ceramide phosphoethanolamine.

To understand the influence of synergistic effect on cell metabolites, the Single-probe SCMS experiments were performed in both the positive and negative ion modes to analyze IRI-resistant cells after mono- and co-treatment. IC_{50} of IRI (22 μM, Fig. S2B) or metformin (8.7 mM, Fig. S2A) was selected as the monotreatment concentration. In the co-treatment, we selected IRI (0.56 μM) and metformin (4.0 mM) as a representative combination, because a sharply decreased cell viability was observed around these concentrations. In the positive ion mode, significantly different ($p < 0.001$) metabolic profiles were observed from PLS-DA (Fig. 3A). Furthermore, ANAVO results indicate that metformin-containing treatments, including both the mono- and co-treatment, lead to significant downregulation of lipids in IRI-resistant cells (Fig. 3B). Among all treatment

conditions, the co-treatment showed the lowest expression of both polar and nonpolar lipids.

To acquire broader ranges of molecular coverage, we also performed the SCMS measurements in the negative ion mode. Around 30 IRI-resistant cells in the metformin monotreatment, IRI monotreatment, and co-treatment groups were analyzed. PLS-DA results showed significantly distinct ($p = 0.004$) metabolic features among these three groups (Fig. 3C). Using the combined ANOVA and Tukey's test, which was demonstrated as a rigorous method to determine metabolite biomarkers in our previous studies[40], we discovered species exhibiting significantly different abundances (i.e., $p < 0.05$ from both tests) among them. We were able to tentatively label 49 ions based on the accurate mass search the online databases. A number of fatty acids (e.g., palmitic acid, palmitoleic acid, oleic acid, stearic acid, and arachidonic acid) exhibited lower expression levels after metformin mono-treatment compared with those with IRI mono-treatment (Fig. 3D). Particularly, the lowest abundances of fatty acids were found in cells from the co-treatment, and this trend is similar to that of lipids discovered in the positive ion mode (Fig. 3B). While a higher IRI concentration (IC_{50} of IRI) was applied for the IRI mono-treatment cells compared with IRI-resistant cells (low IRI concentration, 1μM) in Fig. 2B, different lipids species were still significantly downregulated compared with MET mono-treatment.

Due to the extremely limited amounts (in picoliter range) and complex compositions of contents in single cells, MS^2 analyses at the single-cell level can be only performed for relatively abundant ions. To provide supplementary information for structure identification of lipids, we prepared cell lysates for targeted analysis of ions of interest (i.e., species with significantly different abundances among different groups)

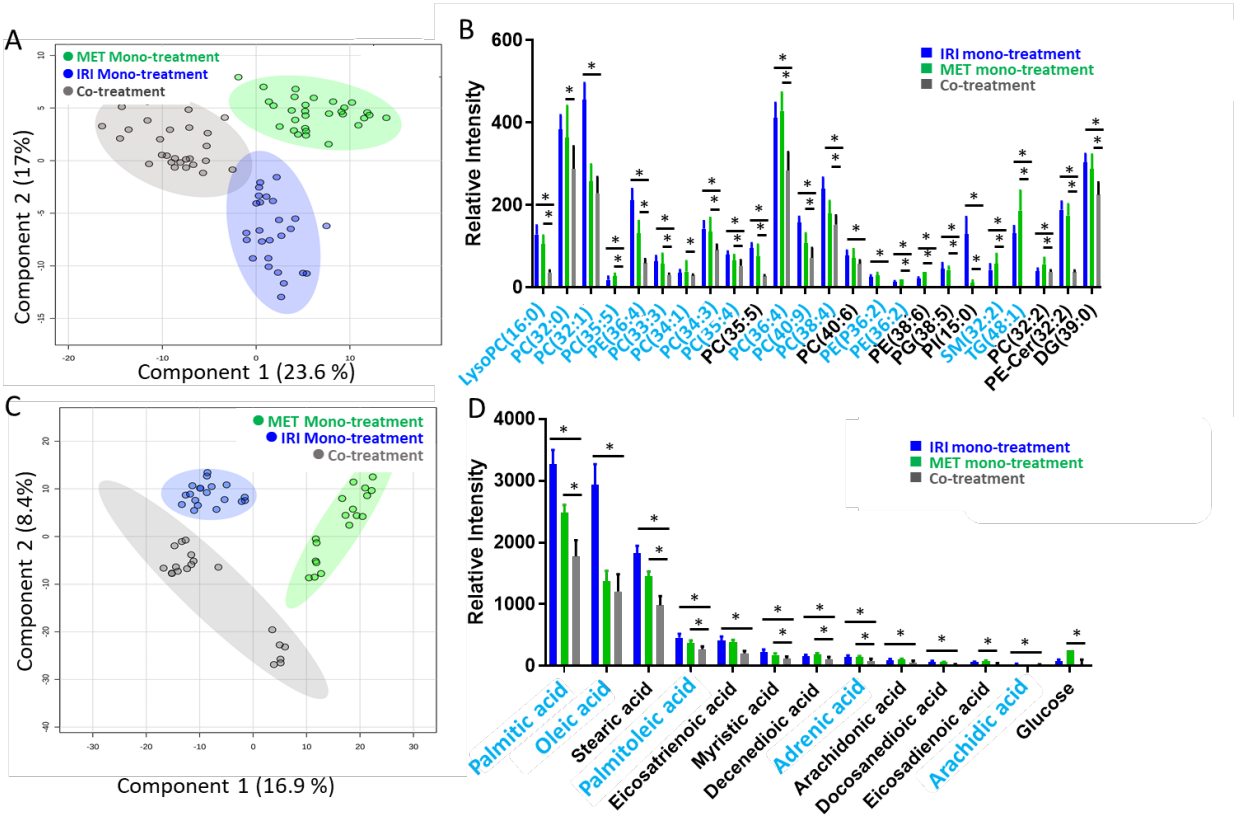


Fig. 3. SCMS results of IRI-resistant cells from the co-treatment (0.56 μM IRI + 4.0 mM MET), IRI mono-treatment (22 μM IRI), and metformin mono-treatment (8.7 mM MET). (A) PLS-DA of positive ion mode results shows the metabolomics profiles were significantly changed by three different treatments (p<0.001 from permutation test), and (B) representative lipids with significant abundance change (, p < 0.05 from both ANOVA and Tukey's test) among three treatment groups. (C) PLS-DA of negative ion mode results shows metabolomics profiles were significantly changed by three different treatments (p = 0.004 from permutation test), and (D) representative fatty acids with significantly different abundances (* p < 0.05 from both ANOVA and Tukey's test) among three treatment groups. Species labeled in blue font were identified using MS^2 analyses using both single cells and cell lysates. (LysoPC: lysophosphatidylcholine; PC: phosphatidylcholine; PE: phosphatidylethanolamine; PI: phosphatidylinositol; PE-Cer: ceramide phosphoethanolamine; PG: phosphatidylglycerol; DG: diglyceride).*

using HPLC-MS^2 method in the positive ion mode. Because the majority of ions of interest were downregulated in all treatment groups, IRI-resistant cells were used for lysate preparation. The retention time was determined from the full scan mode in the first run (Fig. S5), and then the precursor ions were isolated for the MS^2 analysis in the second run. HPLC/MS analyses provided the identification of 9 metabolites that cannot be identified at the single-cell level due to their low abundances. Combining the MS^2 mass spectra from single cells and cell lysates, we were able to identify 32 out of 49 tentatively labeled ions as illustrated in Figures 2B and 3B. Importantly, we noticed that 17 ions can only be detected from the SCMS experiments. This likely indicates that these species are fragile or have rapid turnover rate in live cells, and they are potentially lost during the preparation of cell lysate.[40]

3.4.4 Co-treatment of metformin and IRI more efficiently reduced FASN enzymatic activity compared with the mono-treatment.

Our SCMS experimental results indicate that the treatment involving metformin greatly reduced the levels of fatty acids and lipids. It is very likely that these downregulations are related to the inhibition of lipogenic enzymes by metformin. Among all lipogenic enzymes, the overexpressed FASN is generally observed in broad types of cancer cells.[50-52] FASN is a key enzyme controlling *de novo* fatty acids biosynthesis in cells.[53] FASN utilizes Acetyl-CoA and Malonyl-CoA as the starting materials to synthesize saturated fatty acids through condensation reactions. The major product from FASN is palmitic acid, and the byproducts include saturated fatty acids, which can be further processed to synthesize more functional and complex fatty acids (e.g., unsaturated fatty acids and long-chain fatty acids).[53] *De novo* lipid synthesis requires fatty acids for the

production of glycerophospholipids (e.g., phosphatidylcholine (PC), phosphatidylserine (PS), and phosphatidylinositol (PI)), glycerolipids (e.g., diacylglyceride (DG) and triacylglyceride (TG)), and sphingolipids utilized by cells for energy storage and cellular membrane synthesis.[54] Because FASN synthesizes fatty acids are required for cell divisions, the hyperactivity and overexpression of FASN are tightly related to the malignancy of cancer cells.[55-56]

Based on our studies of synergetic effect and metabolomics, we hypothesized that metformin inhibits the activities of FASN and further sensitizes IRI-resistant cells to the therapeutic effect of IRI. As one of the most well accepted molecular mechanisms, metformin affects cancer cells by initializing the AMPK (AMP-activated protein kinase) signaling pathway.[57-58] Metformin induces energy deficiency in cancer cells by promoting ATP depletion mainly through inhibiting glycolysis, TCA cycle, and electron transport chain complex I.[59] The energy crisis stress imposed by metformin activates the AMPK signaling pathway (Fig. 4A). Among all downstream actions of AMPK, one is to regulate cancer cell death by inhibiting the expression of FASN and hindering the biosynthesis of fatty acid and lipids.[60] Eventually, without adequate lipids and fatty acids to provide cellular energy and building blocks, cancer cell proliferation is decreased.

In order to compare the degree of FASN inhibition in IRI-resistant cells among four different groups (i.e., IRI mono-treatment, metformin mono-treatment, co-treatment using both compounds, and IRI-resistant cells), we studied FASN activities by measuring the Malonyl-CoA-dependent oxidation rate of NADPH (Fig. 4B). We found the FASN activity in the co-treatment (7.5 ± 0.6 nmol NADPH oxidized min^{-1} mg $protein^{-1}$) is the lowest among all four different groups (Fig. 4). The FASN activity in metformin mono-treatment

(9.0 ± 0.4 nmol NADPH oxidized min^{-1} mg $protein^{-1}$) is higher than that in the co-treatment but lower than those in both IRI mono-treatment (9.8 ± 0.2 nmol NADPH oxidized min^{-1} mg $protein^{-1}$) and control cells (10.2 ± 0.7 nmol NADPH oxidized min^{-1} mg $protein^{-1}$). These findings agree with the above results obtained from the SCMS and cell viability measurements, suggesting higher degrees of FASN inhibition is likely responsible for the enhanced antitumor ability in the co-treatment.

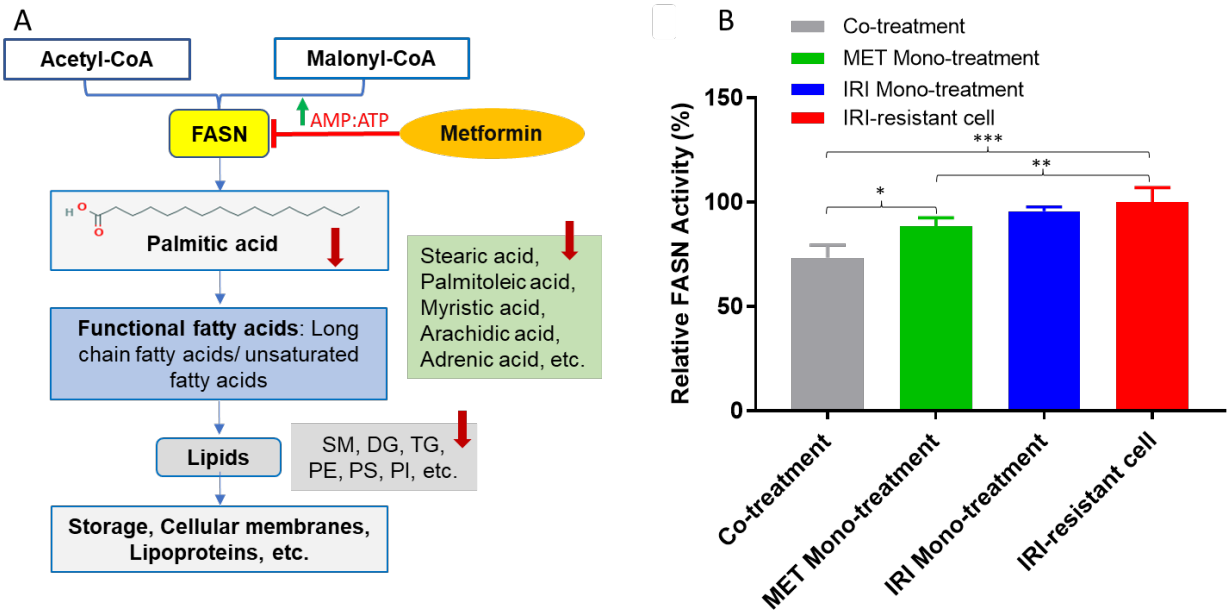


Fig. 4. The proposed mechanisms of metformin in the treatment of IRI-resistant cells and results from FASN activity assay. (A) Schematic pharmacological pathways of metformin in IRI-resistant cells. Metformin inhibits FASN by activating AMPK pathway, and the downstream products, including fatty acids and lipids, are decreased. (B) The relative FASN enzymatic activities of IRI-resistant cells in four different treatments. Results represent four replicates in each treatment for FASN enzymatic activity assay. Standard deviations are labeled as error bars in the histogram ($p < 0.05$; ** $p < 0.01$; *** $p < 0.001$ from one-way ANOVA).*

FASN, a key lipogenic enzyme, is an important biomarker, and its overexpression correlates with high malignancy and poor prognosis in cancer pathogenesis.[61] The

development of cancer stemness is also associated with FASN overexpression.[62] Suppressing the activity of FASN can induce apoptosis of cancer cells and decrease their viability. Furthermore, the inhibition of FASN was believed to help restore cancer cells membrane to a non-malignant architecture, resulting in enhanced chemotherapy efficacy of treating drug-resistant cell lines.[63] In fact, combining FASN inhibitors with other chemotherapy agents has been proven as an effective strategy to resensitize anticancer drugs.[63] Our studies indicate that the enhanced potency of metformin containing co-treatment is likely due to its capability of suppressing FASN activity.

Although the current studies are performed using the IRI-resistant cells, drug resistance induced by metformin is also clinically relevant. It is known that diabetes (primarily type 2) is associated with increased risk of multiple cancers such as in liver, pancreas, colon, and breast.[64] Because metformin is a commonly used for treatment of diabetes, anti-metformin is generally observed in diabetes treatment for patients, including those with cancers. It has been reported that long-term exposure of cancer cells to metformin can lead to resistance to chemotherapy.[65-66] It is worth comprehensively studying cancer cells with resistance to both metformin and anticancer drugs; however, these studies are beyond the scope of current work.

3.5 Conclusion

The oral antidiabetic drug metformin exhibits anticancer effects for its ability of selectively killing CSCs. To understand its influence on metabolites and synergetic effect with anticancer drug IRI, we conducted both metformin mono-treatment and metformin/IRI co-treatment for IRI-resistant cells, which are used the model system for drug-resistant cells. The Single-probe SCMS metabolomics studies were performed to

investigate the influence of metformin on metabolites in IRI-resistant cells. Traditional HPLC/MS analyses of cell lysates were performed to provide complementary information for molecular identification. In addition, we carried out measurements of synergetic effect between metformin and IRI in co-treatment and studied the enzymatic activity of FASN. Our results indicate that metformin mono-treatment induced the downregulation of lipids and fatty acids, whereas the co-treatment resulted in further reduced production of glycosylated ceramides. Importantly, some species can be only detected and identified in live single cells. The measurement of CI demonstrated a synergistic interaction between metformin and IRI in the co-treatment. Enzymatic activity assay confirmed that the co-treatment led to the lowest FASN activity compared with the mono-treatment of metformin or IRI. Collectively, our studies indicate that metformin sensitizes IRI-resistant cells, and its pharmacological action is related to its capability of inhibiting FASN.

Reference

1. Zahreddine, H.; Borden, K. L. B., Mechanisms and insights into drug resistance in cancer. *Front Pharmacol* **2013,** *4*.ARTN 28 10.3389/fphar.2013.00028
2. Favoriti, P.; Carbone, G.; Greco, M.; Pirozzi, F.; Pirozzi, R. E. M.; Corcione, F., Worldwide burden of colorectal cancer: a review. *Updates Surg* **2016,** *68* (1), 7-11.10.1007/s13304-016-0359-y
3. Bray, F.; Ferlay, J.; Soerjomataram, I.; Siegel, R. L.; Torre, L. A.; Jemal, A., Global cancer statistics 2018: GLOBOCAN estimates of incidence and mortality worldwide for 36 cancers in 185 countries. *Ca-Cancer J Clin* **2018,** *68* (6), 394-424.10.3322/caac.21492
4. Van Cutsem, E.; Twelves, C.; Cassidy, J.; Allman, D.; Bajetta, E.; Boyer, M.; Bugat, R.; Findlay, M.; Frings, S.; Jahn, M.; McKendrick, J.; Osterwalder, B.; Perez-Manga, G.; Rosso, R.; Rougier, P.; Schmiegel, W. H.; Seitz, J. F.; Thompson, P.; Vieitez, J. M.; Weitzel, C.; Harper, P.; Grp, X. C. C. S., Oral capecitabine compared with intravenous fluorouracil plus leucovorin in patients with metastatic colorectal cancer: Results of a large phase III study. *J Clin Oncol* **2001,** *19* (21), 4097-4106.Doi 10.1200/Jco.2001.19.21.4097
5. Colucci, G.; Gebbia, V.; Paoletti, G.; Giuliani, F.; Caruso, M.; Gebbia, N.; Carteni, G.; Agostara, B.; Pezzella, G.; Manzione, L.; Borsellino, N.; Misino, A.; Romito, S.; Durini, E.; Cordio, S.; Di Seri, M.; Lopez, M.; Maiello, E., Phase III randomized trial of FOLFIRI versus FOLFOX4 in the treatment of advanced colorectal cancer: A Multicenter study of the Gruppo Oncologico Dell'Italia Meridionale. *J Clin Oncol* **2005,** *23* (22), 4866-4875.10.1200/Jco.2005.07.113
6. Saltz, L. B.; Cox, J. V.; Blanke, C.; Rosen, L. S.; Fehrenbacher, L.; Moore, M. J.; Maroun, J. A.; Ackland, S. P.; Locker, P. K.; Pirotta, N.; Elfring, G. L.; Miller, L. L.; Group, I. S., Irinotecan plus fluorouracil and leucovorin for metastatic colorectal cancer. *New Engl J Med* **2000,** *343* (13), 905-914.Doi 10.1056/Nejm200009283431302
7. Loupakis, F.; Cremolini, C.; Masi, G.; Lonardi, S.; Zagonel, V.; Salvatore, L.; Cortesi, E.; Tomasello, G.; Ronzoni, M.; Spadi, R.; Zaniboni, A.; Tonini, G.; Buonadonna, A.; Amoroso, D.; Chiara, S.; Carlomagno, C.; Boni, C.; Allegrini, G.; Boni, L.; Falcone, A., Initial Therapy with FOLFOXIRI and Bevacizumab for Metastatic Colorectal Cancer. *New Engl J Med* **2014,** *371* (17), 1609-1618.10.1056/NEJMoa1403108
8. Chen, S. J.; Yueh, M. F.; Bigo, C.; Barbier, O.; Wang, K. P.; Karin, M.; Nguyen, N.; Tukey, R. H., Intestinal glucuronidation protects against chemotherapy-induced toxicity by irinotecan (CPT-11). *P Natl Acad Sci USA* **2013,** *110* (47), 19143-19148.10.1073/pnas.1319123110
9. Beretta, G. L.; Perego, P.; Zunino, F., Mechanisms of cellular resistance to camptothecins. *Curr Med Chem* **2006,** *13* (27), 3291-3305.Doi 10.2174/092986706778773121
10. Petitprez, A.; Poindessous, V.; Ouaret, D.; Regairaz, M.; Bastian, G.; Guerin, E.; Escargueil, A. E.; Larsen, A. K., Acquired irinotecan resistance is accompanied by stable modifications of cell cycle dynamics independent of MSI status. *Int J Oncol* **2013,** *42* (5), 1644-1653.10.3892/ijo.2013.1868
11. Saleem, A.; Edwards, T. K.; Rasheed, Z.; Rubin, E. H., Mechanisms of resistance to camptothecins. *Ann Ny Acad Sci* **2000,** *922*, 46-55

12. Yang, Y.; Wang, G. X.; Zhu, D. J.; Huang, Y. F.; Luo, Y.; Su, P. F.; Chen, X. W.; Wang, Q., Epithelial-mesenchymal transition and cancer stem cell-like phenotype induced by Twist1 contribute to acquired resistance to irinotecan in colon cancer. *Int J Oncol* **2017,** *51* (2), 515-524.10.3892/ijo.2017.4044
13. Emmink, B. L.; Van Houdt, W. J.; Vries, R. G.; Hoogwater, F. J.; Govaert, K. M.; Verheem, A.; Nijkamp, M. W.; Steller, E. J.; Jimenez, C. R.; Clevers, H.; Borel Rinkes, I. H.; Kranenburg, O., Differentiated human colorectal cancer cells protect tumor-initiating cells from irinotecan. *Gastroenterology* **2011,** *141* (1), 269-78.10.1053/j.gastro.2011.03.052
14. Liu, R. M.; Sun, M.; Zhang, G. W.; Lan, Y. P.; Yang, Z. B., Towards early monitoring of chemotherapy-induced drug resistance based on single cell metabolomics: Combining single-probe mass spectrometry with machine learning. *Anal Chim Acta* **2019,** *1092*, 42-48.10.1016/j.aca.2019.09.065
15. Vancura, A.; Bu, P. L.; Bhagwat, M.; Zeng, J.; Vancurova, I., Metformin as an Anticancer Agent. *Trends Pharmacol Sci* **2018,** *39* (10), 867-878.10.1016/j.tips.2018.07.006
16. Rattan, R.; Ali Fehmi, R.; Munkarah, A., Metformin: an emerging new therapeutic option for targeting cancer stem cells and metastasis. *J Oncol* **2012,** *2012*, 928127.10.1155/2012/928127
17. Hirsch, H. A.; Iliopoulos, D.; Tsichlis, P. N.; Struhl, K., Metformin selectively targets cancer stem cells, and acts together with chemotherapy to block tumor growth and prolong remission. *Cancer Res* **2009,** *69* (19), 7507-7511.10.1158/0008-5472.CAN-09-2994
18. Bao, B.; Azmi, A. S.; Ali, S.; Zaiem, F.; Sarkar, F. H., Metformin may function as anti-cancer agent via targeting cancer stem cells: the potential biological significance of tumor-associated miRNAs in breast and pancreatic cancers. *Ann Transl Med* **2014,** *2* (6), 59-59.10.3978/j.issn.2305-5839.2014.06.05
19. Mayer, M. J.; Klotz, L. H.; Venkateswaran, V., Metformin and prostate cancer stem cells: a novel therapeutic target. *Prostate Cancer P D* **2015,** *18* (4), 303-309.10.1038/pcan.2015.35
20. Gong, J.; Kelekar, G.; Shen, J.; Shen, J.; Kaur, S.; Mita, M., The expanding role of metformin in cancer: an update on antitumor mechanisms and clinical development. *Target Oncol* **2016,** *11* (4), 447-467.10.1007/s11523-016-0423-z
21. Bragagnoli, A.; Araujo, R.; Abdalla, K.; Comar, F.; Santos, F.; Ferraz, M.; dos Santos, L. V.; Carvalheira, J.; Lima, J. P. S. D. N., Final results of a phase II of metformin plus irinotecan for refractory colorectal cancer. *J Clin Oncol* **2018,** *36* (15).DOI 10.1200/JCO.2018.36.15_suppl.e15527
22. Buikhuisen, J. Y.; Torang, A.; Medema, J. P., Exploring and modelling colon cancer inter-tumour heterogeneity: opportunities and challenges. *Oncogenesis* **2020,** *9* (7).ARTN 66 10.1038/s41389-020-00250-6
23. Teeuwssen, M.; Fodde, R., Cell Heterogeneity and Phenotypic Plasticity in Metastasis Formation: The Case of Colon Cancer. *Cancers* **2019,** *11* (9).ARTN 1368 10.3390/cancers11091368
24. Muschet, C.; Moller, G.; Prehn, C.; de Angelis, M. H.; Adamski, J.; Tokarz, J., Removing the bottlenecks of cell culture metabolomics: fast normalization procedure, correlation of metabolites to cell number, and impact of the cell harvesting method. *Metabolomics* **2016,** *12* (10).ARTN 151 10.1007/s11306-016-1104-8

25. Zhang, L. W.; Vertes, A., Energy Charge, Redox State, and Metabolite Turnover in Single Human Hepatocytes Revealed by Capillary Microsampling Mass Spectrometry. *Analytical Chemistry* **2015,** *87* (20), 10397-10405.10.1021/acs.analchem.5b02502
26. Abouleila, Y.; Onidani, K.; Ali, A.; Shoji, H.; Kawai, T.; Lim, C. T.; Kumar, V.; Okaya, S.; Kato, K.; Hiyama, E.; Yanagida, T.; Masujima, T.; Shimizu, Y.; Honda, K., Live single cell mass spectrometry reveals cancer-specific metabolic profiles of circulating tumor cells. *Cancer Sci* **2019,** *110* (2), 697-706.10.1111/cas.13915
27. Zhang, L.; Foreman, D. P.; Grant, P. A.; Shrestha, B.; Moody, S. A.; Villiers, F.; Kwak, J. M.; Vertes, A., In situ metabolic analysis of single plant cells by capillary microsampling and electrospray ionization mass spectrometry with ion mobility separation. *Analyst* **2014,** *139* (20), 5079-85.10.1039/c4an01018c
28. Zhu, H. Y.; Zou, G. C.; Wang, N.; Zhuang, M. H.; Xiong, W.; Huang, G. M., Single-neuron identification of chemical constituents, physiological changes, and metabolism using mass spectrometry. *P Natl Acad Sci USA* **2017,** *114* (10), 2586-2591.10.1073/pnas.1615557114
29. Bergman, H. M.; Lanekoff, I., Profiling and quantifying endogenous molecules in single cells using nano-DESI MS. *Analyst* **2017,** *142* (19), 3639-3647.10.1039/c7an00885f
30. Shrestha, B.; Vertes, A., In Situ Metabolic Profiling of Single Cells by Laser Ablation Electrospray Ionization Mass Spectrometry. *Analytical Chemistry* **2009,** *81* (20), 8265-8271.10.1021/ac901525g
31. Pan, N.; Standke, S. J.; Kothapalli, N. R.; Sun, M.; Bensen, R. C.; Burgett, A. W. G.; Yang, Z. B., Quantification of Drug Molecules in Live Single Cells Using the Single-Probe Mass Spectrometry Technique. *Analytical Chemistry* **2019,** *91* (14), 9018-9024.10.1021/acs.analchem.9b01311
32. Pan, N.; Rao, W.; Yang, Z., Single-Probe Mass Spectrometry Analysis of Metabolites in Single Cells. *Methods Mol Biol* **2020,** *2064*, 61-71.10.1007/978-1-4939-9831-9_5
33. Pan, N.; Rao, W.; Kothapalli, N. R.; Liu, R.; Burgett, A. W.; Yang, Z., The single-probe: a miniaturized multifunctional device for single cell mass spectrometry analysis. *Anal Chem* **2014,** *86* (19), 9376-80.10.1021/ac5029038
34. Sun, M.; Yang, Z. B., Metabolomic Studies of Live Single Cancer Stem Cells Using Mass Spectrometry. *Analytical Chemistry* **2019,** *91* (3), 2384-2391.10.1021/acs.analchem.8b05166
35. Standke, S. J.; Colby, D. H.; Bensen, R. C.; Burgett, A. W. G.; Yang, Z. B., Mass Spectrometry Measurement of Single Suspended Cells Using a Combined Cell Manipulation System and a Single-Probe Device. *Analytical Chemistry* **2019,** *91* (3), 1738-1742.10.1021/acs.analchem.8b05774
36. van Meerloo, J.; Kaspers, G. J.; Cloos, J., Cell sensitivity assays: the MTT assay. *Methods Mol Biol* **2011,** *731*, 237-45.10.1007/978-1-61779-080-5_20
37. Nepokroeff, C. M.; Lakshmanan, M. R.; Porter, J. W., Fatty-acid synthase from rat liver. *Methods Enzymol* **1975,** *35*, 37-44.10.1016/0076-6879(75)35136-7
38. Lee, K. H.; Lee, M. S.; Cha, E. Y.; Sul, J. Y.; Lee, J. S.; Kim, J. S.; Park, J. B.; Kim, J. Y., Inhibitory effect of emodin on fatty acid synthase, colon cancer proliferation and apoptosis. *Mol Med Rep* **2017,** *15* (4), 2163-2173.10.3892/mmr.2017.6254
39. Dils, R.; Carey, E. M., Fatty acid synthase from rabbit mammary gland. *Methods Enzymol* **1975,** *35*, 74-83.10.1016/0076-6879(75)35140-9

40. Liu, R. M.; Zhang, G. W.; Sun, M.; Pan, X. L.; Yang, Z. B., Integrating a generalized data analysis workflow with the Single-probe mass spectrometry experiment for single cell metabolomics. *Anal Chim Acta* **2019,** *1064*, 71-79.10.1016/j.aca.2019.03.006
41. Romano, P.; Profumo, A.; Rocco, M.; Mangerini, R.; Ferri, F.; Facchiano, A., Geena 2, improved automated analysis of MALDI/TOF mass spectra. *Bmc Bioinformatics* **2016,** *17*.ARTN 61
10.1186/s12859-016-0911-2
42. Xia, J.; Wishart, D. S., Using MetaboAnalyst 3.0 for Comprehensive Metabolomics Data Analysis. *Current Protocols in Bioinformatics* **2016,** *55* (1), 14.10.1-14.10.91.10.1002/cpbi.11
43. Smith, C. A.; O'Maille, G.; Want, E. J.; Qin, C.; Trauger, S. A.; Brandon, T. R.; Custodio, D. E.; Abagyan, R.; Siuzdak, G., METLIN: a metabolite mass spectral database. *Ther Drug Monit* **2005,** *27* (6), 747-51.10.1097/01.ftd.0000179845.53213.39
44. Wishart, D. S.; Feunang, Y. D.; Marcu, A.; Guo, A. C.; Liang, K.; Vazquez-Fresno, R.; Sajed, T.; Johnson, D.; Li, C.; Karu, N.; Sayeeda, Z.; Lo, E.; Assempour, N.; Berjanskii, M.; Singhal, S.; Arndt, D.; Liang, Y.; Badran, H.; Grant, J.; Serra-Cayuela, A.; Liu, Y.; Mandal, R.; Neveu, V.; Pon, A.; Knox, C.; Wilson, M.; Manach, C.; Scalbert, A., HMDB 4.0: the human metabolome database for 2018. *Nucleic Acids Res* **2018,** *46* (D1), D608-D617.10.1093/nar/gkx1089
45. Wang, M.; Carver, J. J.; Phelan, V. V.; Sanchez, L. M.; Garg, N.; Peng, Y.; Nguyen, D. D.; Watrous, J.; Kapono, C. A.; Luzzatto-Knaan, T.; Porto, C.; Bouslimani, A.; Melnik, A. V.; Meehan, M. J.; Liu, W. T.; Crusemann, M.; Boudreau, P. D.; Esquenazi, E.; Sandoval-Calderon, M.; Kersten, R. D.; Pace, L. A.; Quinn, R. A.; Duncan, K. R.; Hsu, C. C.; Floros, D. J.; Gavilan, R. G.; Kleigrewe, K.; Northen, T.; Dutton, R. J.; Parrot, D.; Carlson, E. E.; Aigle, B.; Michelsen, C. F.; Jelsbak, L.; Sohlenkamp, C.; Pevzner, P.; Edlund, A.; McLean, J.; Piel, J.; Murphy, B. T.; Gerwick, L.; Liaw, C. C.; Yang, Y. L.; Humpf, H. U.; Maansson, M.; Keyzers, R. A.; Sims, A. C.; Johnson, A. R.; Sidebottom, A. M.; Sedio, B. E.; Klitgaard, A.; Larson, C. B.; P, C. A. B.; Torres-Mendoza, D.; Gonzalez, D. J.; Silva, D. B.; Marques, L. M.; Demarque, D. P.; Pociute, E.; O'Neill, E. C.; Briand, E.; Helfrich, E. J. N.; Granatosky, E. A.; Glukhov, E.; Ryffel, F.; Houson, H.; Mohimani, H.; Kharbush, J. J.; Zeng, Y.; Vorholt, J. A.; Kurita, K. L.; Charusanti, P.; McPhail, K. L.; Nielsen, K. F.; Vuong, L.; Elfeki, M.; Traxler, M. F.; Engene, N.; Koyama, N.; Vining, O. B.; Baric, R.; Silva, R. R.; Mascuch, S. J.; Tomasi, S.; Jenkins, S.; Macherla, V.; Hoffman, T.; Agarwal, V.; Williams, P. G.; Dai, J.; Neupane, R.; Gurr, J.; Rodriguez, A. M. C.; Lamsa, A.; Zhang, C.; Dorrestein, K.; Duggan, B. M.; Almaliti, J.; Allard, P. M.; Phapale, P.; Nothias, L. F.; Alexandrov, T.; Litaudon, M.; Wolfender, J. L.; Kyle, J. E.; Metz, T. O.; Peryea, T.; Nguyen, D. T.; VanLeer, D.; Shinn, P.; Jadhav, A.; Muller, R.; Waters, K. M.; Shi, W.; Liu, X.; Zhang, L.; Knight, R.; Jensen, P. R.; Palsson, B. O.; Pogliano, K.; Linington, R. G.; Gutierrez, M.; Lopes, N. P.; Gerwick, W. H.; Moore, B. S.; Dorrestein, P. C.; Bandeira, N., Sharing and community curation of mass spectrometry data with Global Natural Products Social Molecular Networking. *Nat Biotechnol* **2016,** *34* (8), 828-837.10.1038/nbt.3597
46. Chou, T. C., Drug Combination Studies and Their Synergy Quantification Using the Chou-Talalay Method. *Cancer Res* **2010,** *70* (2), 440-446.10.1158/0008-5472.Can-09-1947
47. Chou, T. C., Theoretical basis, experimental design, and computerized simulation of synergism and antagonism in drug combination studies. *Pharmacol Rev* **2006,** *58* (3), 621-681.10.1124/pr.58.3.10
48. Chou, T. C., Preclinical versus clinical drug combination studies. *Leukemia Lymphoma* **2008,** *49* (11), 2059-2080.10.1080/10428190802353591

49. Chou, T. C., Preclinical versus clinical drug combination studies. *Leuk Lymphoma* **2008,** *49* (11), 2059-80.10.1080/10428190802353591
50. Mashima, T.; Seimiya, H.; Tsuruo, T., De novo fatty-acid synthesis and related pathways as molecular targets for cancer therapy. *Brit J Cancer* **2009,** *100* (9), 1369-1372.10.1038/sj.bjc.6605007
51. Kuhajda, F. P., Fatty acid synthase and cancer: New application of an old pathway. *Cancer Res* **2006,** *66* (12), 5977-5980.10.1158/0008-5472.Can-05-4673
52. Menendez, J. A.; Lupu, R., Fatty acid synthase and the lipogenic phenotype in cancer pathogenesis. *Nature Reviews Cancer* **2007,** *7* (10), 763-777.10.1038/nrc2222
53. Menendez, J. A.; Lupu, R., Fatty acid synthase and the lipogenic phenotype in cancer pathogenesis. *Nat Rev Cancer* **2007,** *7* (10), 763-77.10.1038/nrc2222
54. Santos, C. R.; Schulze, A., Lipid metabolism in cancer. *The FEBS Journal* **2012,** *279* (15), 2610-2623.10.1111/j.1742-4658.2012.08644.x
55. Baron, A.; Migita, T.; Tang, D.; Loda, M., Fatty acid synthase: A metabolic oncogene in prostate cancer? *Journal of Cellular Biochemistry* **2004,** *91* (1), 47-53.10.1002/jcb.10708
56. Flavin, R.; Peluso, S.; Nguyen, P. L.; Loda, M., Fatty acid synthase as a potential therapeutic target in cancer. *Future Oncol* **2010,** *6* (4), 551-562.10.2217/fon.10.11
57. Luo, Z. J.; Zang, M. W.; Guo, W., AMPK as a metabolic tumor suppressor: control of metabolism and cell growth. *Future Oncology* **2010,** *6* (3), 457-470.10.2217/Fon.09.174
58. Hadad, S. M.; Hardie, D. G.; Appleyard, V.; Thompson, A. M., Effects of metformin on breast cancer cell proliferation, the AMPK pathway and the cell cycle. *Clin Transl Oncol* **2014,** *16* (8), 746-752.10.1007/s12094-013-1144-8
59. Cantoria, M. J.; Boros, L. G.; Meuillet, E. J., Contextual inhibition of fatty acid synthesis by metformin involves glucose-derived acetyl-CoA and cholesterol in pancreatic tumor cells. *Metabolomics* **2014,** *10* (1), 91-104.10.1007/s11306-013-0555-4
60. Loubière, C.; Goiran, T.; Laurent, K.; Djabari, Z.; Tanti, J.-F.; Bost, F., Metformin-induced energy deficiency leads to the inhibition of lipogenesis in prostate cancer cells. *Oncotarget* **2015,** *6* (17), 15652-15661.10.18632/oncotarget.3404
61. Cao, Z.; Xu, Y. L.; Guo, F.; Chen, X.; Ji, J.; Xu, H.; He, J. Y.; Yu, Y. W.; Sun, Y. H.; Lu, X.; Wang, F. B., FASN Protein Overexpression Indicates Poor Biochemical Recurrence-Free Survival in Prostate Cancer. *Dis Markers* **2020,** *2020*.Artn 3904947
10.1155/2020/3904947
62. Yasumoto, Y.; Miyazaki, H.; Vaidyan, L. K.; Kagawa, Y.; Ebrahimi, M.; Yamamoto, Y.; Ogata, M.; Katsuyama, Y.; Sadahiro, H.; Suzuki, M.; Owada, Y., Inhibition of Fatty Acid Synthase Decreases Expression of Stemness Markers in Glioma Stem Cells. *Plos One* **2016,** *11* (1).ARTN e0147717
10.1371/journal.pone.0147717
63. Buckley, D.; Duke, G.; Heuer, T. S.; O'Farrell, M.; Wagman, A. S.; McCulloch, W.; Kemble, G., Fatty acid synthase - Modern tumor cell biology insights into a classical oncology target. *Pharmacology & Therapeutics* **2017,** *177*, 23-31.10.1016/j.pharmthera.2017.02.021
64. Giovannucci, E.; Harlan, D. M.; Archer, M. C.; Bergenstal, R. M.; Gapstur, S. M.; Habel, L. A.; Pollak, M.; Regensteiner, J. G.; Yee, D., Diabetes and cancer: a consensus report. *Diabetes Care* **2010,** *33* (7), 1674-85.10.2337/dc10-0666

65. Scherbakov, A. M.; Sorokin, D. V.; Tatarskiy, V. V.; Prokhorov, N. S.; Semina, S. E.; Berstein, L. M.; Krasil'nikov, M. A., The phenomenon of acquired resistance to metformin in breast cancer cells: The interaction of growth pathways and estrogen receptor signaling. *Iubmb Life* **2016,** *68* (4), 281-292.10.1002/iub.1481
66. Andrzejewski, S.; Siegel, P. M.; St-Pierre, J., Metabolic Profiles Associated With Metformin Efficacy in Cancer. *Front Endocrinol* **2018,** *9*.ARTN 372 10.3389/fendo.2018.00372

Chapter 4. Metabolomics Studies of Cell-Cell Interactions using Single Cell Mass Spectrometry Combined with Fluorescence Microscopy

Author Contributions: The project of Chapter 4 is mainly conducted by Xingxiu Chen. Zongkai Peng assisted data collection from cell viability measurements and SCMS experiments.

4.1 Abstract

Cell–cell interactions are critical for transmitting signals among cells and maintaining their normal functions from the single-cell level to tissues. In cancer studies, interactions between drug-resistant and drug-sensitive cells play an important role in the development of chemotherapy resistance of tumors. As metabolites directly reflect cell status, metabolomics studies provide insight into cell-cell communication. Mass spectrometry (MS) is a powerful tool for metabolomics studies, whereas single cell MS (SCMS) analysis can provide unique information for understanding interactions among heterogeneous cells. In the current studies, we utilized a direct co-culture system with cell contact to study metabolomics of single cells affected by cell-cell interactions in their living status. A fluorescence microscope was utilized to distinguish these two types of cells for SCMS metabolomics studies using the Single-probe SCMS technique under ambient

conditions. Our results show that, through interactions with drug-resistant cells, drug-sensitive cancer cells acquired significantly increased drug resistance and exhibited drastically altered metabolites. Further investigation found the increased drug resistance was associated with multiply metabolism regulations in drug-sensitive cells through co-culture, such as the upregulation of sphingomyelins lipids and lactic acid, the downregulation of TCA cycle intermediates and saturated fatty acids. The method reported here allows for metabolomics studies of cells labeled with fluorescent proteins or dyes among heterogeneous populations.

4.2 Introduction

Biological variability of cells not only exhibits among different types of cells characterized by the expression of specific biomarkers, but also presents in the individuals of the same type of cells, where the gene expression, protein synthesis, and cell metabolism are diverse at the single-cell level.[1-4] In addition, the degree of cell heterogeneity is related to other types of cells in the cellular microenvironment through cell-cell interaction, as the function, survival and proliferation of cells can be determined by their neighbors in the same niche.[5-6]

The importance of cell-cell heterogeneity has been appreciated in many disease studies, especially drug resistance research in cancer. Resistance to chemotherapy medicine is a major cause of clinical cancer treatment failure.[7] Understanding drug resistance mechanisms lays the foundation for the development of effective clinical intervention for drug resistance. Over the past few decades, numerous studies have been conducted to tackle molecular mechanisms of resistance in drug-resistant cells. The proposed mechanisms include drug inactivation, drug target alternation, drug efflux, DNA

damage repair, epithelial-mesenchymal transition (EMT), and cell death inhibition.[8] Although drug-resistant cells themselves exhibit resistance to anticancer drugs, their communications with drug-sensitive cells in tumor microenvironments can enhance chemotherapy resistance of the latter.[9-10] The mechanisms are attributed to intercellular transfer of molecules, including P-glycoproteins[11], midkine[12], small RNAs[13], and metabolites[10] that can protect drug-sensitive cells from chemotherapy-induced apoptosis.

There are two major mechanisms of transmitting molecules during cell-cell communication: secreting soluble molecules[14] (including but not limited to chemokines, cytokines, and growth factors) and transferring extracellular vesicles[15] (e.g., microvesicles, exosomes, and apoptotic bodies). Different *in vitro* co-culture systems have been developed to study cell-cell interactions, and these systems can be generally classified into two categories: indirect co-culture (i.e., co-culture without cell contact) and direct co-culture (i.e., co-culture with cell contact).[16-20] In the indirect co-culture systems, different types of cells are physically segregated (e.g., cells cultured in different devices or different chambers of the same device[21]), whereas cell-cell communication is through the shared culture medium (e.g., via permeable membrane in culture device or channels in microfluidic device[22-23]) or conditioned medium harvested from the other type of cells[24]. This type of co-culture methods is commonly used due to their high reproducibility and commercial availability. Particularly, different types of cells can be conveniently separated for molecular analysis. However, due to the lack of direct cell-cell contact, these systems cannot vividly mimic the actual physiological environment, considering intercellular transfer of some proteins and small RNA are achieved in contact- or distance-dependent manners.[25-26] In contrast, in the direct co-culture systems, different types of cells are

cultured in the same device with cell-cell contact, indicating they are better models representing natural cell-cell interactions.[27] Several techniques (e.g., micropatterning[28], temporary divider[29], and degradable hydrogel[30]) have been previously developed for indirect co-culture. However, these less-than-ideal methods necessitate a temporary seal between different cell types, and intercellular response is hindered due to impacted molecular diffusion from separation between cells.[25] Alternatively, direct co-culture systems, which allow for direct contact among different types of cells, have been achieved in multiple studies. However, *in situ* molecular analysis of different types of cells is challenging due to heterogeneous cell populations.[20] Single cell analysis is inevitably needed to overcome these challenges.

As the end products of cellular processes, metabolites directly reflect the genetic and environmental changes of cells. Mass spectrometry (MS) has become the major analytical platform for metabolomics studies. Traditional MS metabolomics research, e.g., liquid chromatography–mass spectrometry (LC–MS), relies on samples prepared from populations of cells. Apparently, it is intractable to use these traditional methods for *in situ* studies of the cell-cell interactions among coexisting cells in the living status. Although fluorescence-activated cell sorting (FACS) has been commonly used for cell isolation and molecular analysis, FACS-treated cells possess different compositions of metabolites.[31-32]

The inevitable approach to overcome the above challenges is to conduct single cell metabolomics analysis. A variety of sampling and ionization techniques, including vacuum- and ambient-based methods, have been developed for MS single cell

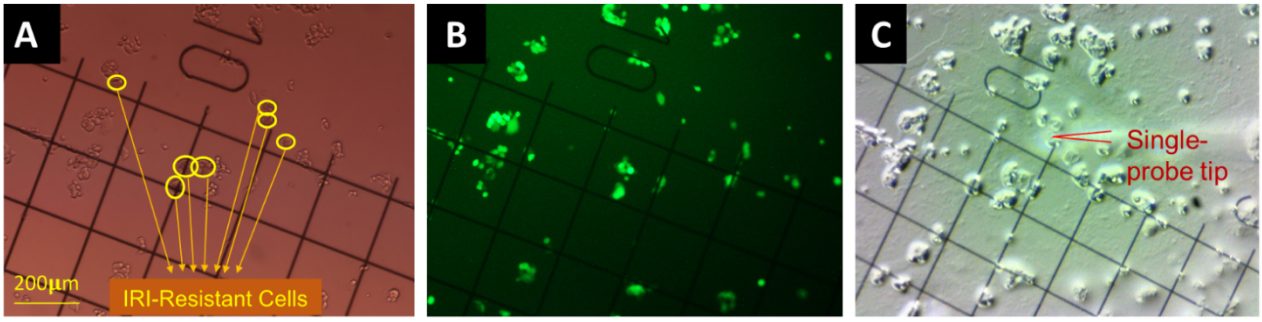


Fig. 1 Determination of different types of single cells in the direct co-culture for the Single-probe SCMS analysis. Both drug-sensitive (HCT116-GFP) and drug-resistant (IRI-HCT116) cells were co-cultured and attached on the gridded glass coverslips. Coordinates of single cells in each group were determined by comparing (A) bright-field and (B) fluorescence images of the same coverslip. (C) Metabolomics measurement analysis of both types of cells were conducted using the Single-probe SCMS technique.

metabolomics studies. MALDI (matrix-assisted laser desorption/ionization) and SIMS(secondary ion mass spectrometry), two common vacuum-based ionization techniques, have been used to measure metabolites at the cellular and subcellular scales.[33-34] Alternatively, the development of ambient-based sampling and ionization techniques (such as live single cell video MS[35], probe ESI MS[36], nano-DESI MS[37], and LAESI MS[38]) created opportunities to study live single cells in their native or near-native environment. We have developed a number of microscale devices, including the Single-probe[39-45], T-probe[46-47], and micropipette needle[48], that can be coupled to a mass spectrometer for single cell MS (SCMS) metabolomics studies in ambient conditions. In this work, we designed a workflow to combine the Single-probe SCMS technique[39] with fluorescence microscopy to study cell-cell interactions in co-culture systems using cells with different levels of anticancer drug resistance (Fig. 1). Our experimental setup

enables direct, *in situ* metabolomics studies of cell-cell interactions, eliminating potential interference of materials (e.g., membranes or dividers needed for cell separation) in cell growth. Particularly, different types of cells can be labeled with dyes or fluorescent proteins, allowing for selecting the cell of interest for SCMS metabolomics studies.

4.3 Methods

4.3.1 Materials and chemicals

Device utilized for the indirect co-culture system is Corning Transwell inserts (Corning Incorporated Life Science, Tewsbury, MA, USA) in the format of 6-well plate with permeable membrane (pore size: 0.4 μm). The gridded glass coverslips (ibidi USA Incorporation, Fitchburg, WI, USA) were used for cell attachment in the direct co-culture system. Materials to fabricate the Single-probe include the dual-bore quartz tubing (O.D 500 μm, I.D. 127 μm, Friedrich & Dimmock, Inc. Millville, NJ, USA) and fused silica capillary (O.D 105 μm, I.D. 40 μm, Polymicro technologies, Phoenix, AZ, USA). Chemicals used include acetonitrile (EMD Millipore corporation, Burlington, MA, USA), formic acid (Sigma-Aldrich, St. Louis, MO, USA), and irinotecan hydrochloride (BioVision Incorporated, Milpitas, CA, USA). Reagents needed to culture cancer cells include McCoy's 5A cell culture media, Penicillin streptomycin (Pen Strep), 0.25% Trypsin-EDTA (Life Technologies Corporation, Grand Island, NY, USA), and FBS (Global Life Sciences Solutions, Marlborough, MA, USA).

4.3.2 Mono-culture systems

Human colorectal cancer HCT116 cells, which are defined as drug-sensitive cells in the current study, were purchased from American Type Culture Collection (ATCC; Rockville, MD, USA). HCT116 cells were cultured (at 37 ^{o}C in 5% CO_2) in the petri dishes

using McCoy's 5A media supplemented with 10% FBS and 1% Pen Strep. HCT116 cells were split once the confluency reaches 80%.

Multiple methods have been reported to induce drug resistance in cancer cell lines: continuous treatment with stepwise dose, continuous treatment with constant dose, pulsed treatment with stepwise dose, and pulsed treatment with constant dose.[49] Among them, continuous treatment of chemotherapy is an effective method to induce early-stage resistance. The protocols of preparing the irinotecan (IRI)-resistant cells were adopted from previous publications using continuous drug treatment.[50] Briefly, HCT116 cells were cultured in complete growth medium containing 1 μM IRI for 20 days, and cells survived from this elongated treatment were regarded as IRI-resistant cells. To minimize the influence of intracellular IRI compound in the co-culture, the IRI-resistant cells were cultured in the regular complete growth medium (without IRI) for one week prior to the co-culture with drug-sensitive HCT116 cells.

Stable HCT116-GFP cells, generated from HCT116 cells by lentiviral vector transduction, were purchased from company (Cellomics Technology, Halethorpe, MD, USA). Because GFP (green fluorescent protein) labeling has no significant influence on cell metabolism and functions[51], HCT116-GFP cells are also defined as drug-sensitive cells in the current study. To maintain the ability of expressing green fluorescent protein, HCT116-GFP cells were cultured in complete growth medium containing 1 μg/mL puromycin. Cells were maintained in puromycin-free complete growth medium for three days before being used in co-culture systems.

4.3.3 Indirect and direct co-culture systems

Two different types of co-culture systems, i.e., indirect and direct coculture methods, were utilized to co-culture IRI-resistant and drug-sensitive HCT116 cells.

(a) Indirect cell co-culture. Cells in this co-culture system were cultured without direct cell-cell contact using Corning Transwell inserts combined with 6-well culture plates. Three different ratios of IRI-resistant to sensitive cells (1:1, 5:1, and 25:1) were used to investigate the influence of the number of drug-resistant cells on the drug resistance level of drug-sensitive cells. Briefly, the IRI-resistant cells (1x 10^5, 5x 10^5, or 2.5x 10^6 cells suspended in 1.5 mL medium) were added into the inserts, whereas the parental HCT116 cells (1x 10^5 cells suspended in 2.6 mL medium) were added in the 6-well plates. The cell-containing inserts and 6-well plates were then combined for co-culture. After being incubated for 3 or 4 days at 37^{o}C, the HCT116 cells in 6-well plates were harvested for IC_{50} measurement using MTT assay.

(b) Direct cell co-culture. Cells in this co-culture system were cultured with direct cell-cell contact. HCT116-GFP and IRI-resistant HCT116 cell lines were used as models to represent drug-sensitive and drug-resistant cancer cells, respectively. Both types of cells were cultured in the same well of a multi-well plate. Two different types of experiments, i.e., fluorescence microscopy observation and SCMS measurement, were performed using these co-cultured cells. First, we monitored cell growth under IRI treatment using the fluorescence microscope. 1,400 HCT116-GFP cells (suspended in 40 µl medium) and 1,400 IRI-resistant cells (suspended in 40 µl medium) were added into the same wells of a 384-well plate. The mixed cells were incubated for one day, treated by IRI (5 or 10 µM), and then observed using the fluorescence microscope to evaluate the density of HCT116-GFP cells. objective lens (4X) was used to ensure all cells in one

well of the 384-well plate were captured in a fluorescence image. The fluorescent microscope images were processed using ImageJ (ImageJ for windows, Version 1.53m; NIH, Bethasda, MD, USA) to quantify the fluorescence intensities, which were used to compare the relative densities (i.e., viabilities) of HCT116-GFP cells under different co-culture conditions. Photos with a higher magnification (with a 10X objective lens) were also captured for better views of single cells. Second, we conducted the SCMS experiments on direct co-cultured cells. 5,000 IRI-resistant and 5,000 HCT116-GFP cells were added into the same wells of a 12-well plate, in which gridded glass coverslips were placed at the bottom. Cells were attached to the glass coverslips after an overnight incubation for the Single-probe SCMS analysis.

4.3.4 MTT assay

The MTT assays were conducted according to the manufacture's recommendations. The HCT116 cells from indirect co-culture were harvested, rinsed using fresh culture medium, and seeded into 96-well plates (~10,000 cells/well). Drug treatments were carried out using different concentrations of IRI (0.1, 1, 5, 10, or 50 μM). MTT (3-(4,5-dimethylthoazol-2-yl)-2,5-diphenyltetrazolium bromide) was added into each well in 96-well plates, and absorbance values at 570nm were measured using a microplate reader (Synergy H1, BioTek, Winooski, VT). The IC_{50} values were determined using Prism (GraphPad Software, San Diego, CA), and Microsoft Excel was used to construct dose-response curves.

4.3.5 LC-MS/MS Identification

Cell lysis and lipids extraction. The Folch method was adopted to extract lipids from HCT116-GFP cell lines for LC-MS study. After detaching cells from petri dish using

trypsin, cells were collected for lipids extraction. 10,000 cells were mixed with 3 mL chloroform/method (2:1, v/v), vortexed on ice for 10 mins, and then centrifuged for 15 min. The organic layer was transferred to dry under vacuum, and the sample was then reconstituted in 150 mL chloroform for the following LC-MS analysis.

LC-MS. LC-MS/MS was carried out as a complementary method to identify ions of interest. A UltiMate 3000 HPLC system (Thermo Scientific, San Jose, CA) was coupled with the LTQ Orbitrap XL mass spectrometer for separation and MS^2 identification. A Luca 3u C18 column (50 X 2.00 mm, 3 µm, Phenomenex, Torrance, CA) was used for chromatographic separation. The HPLC was set as follows: injection volume: 5 µL; column oven: 50 ^oC; Flow rate: 350 µl/min; mobile phase A: water/methanol (95/5, v/v); mobile phase B: isopropanol/methanol/water (60/35/5, v/v). Both mobile phases contain 10 mM ammonium formate and 0.1% formic acid. The total run time was 80 mins, including 5 mins' equilibrium. The MS^2 was carried out in data independent mode, and the normalized collision energy (NCE) was set between 24-25 x.

4.3.6 The single-probe SCMS setup

The fabrication method of the Single-probe was similar to Chapter 3, where we follow our published protocols for the fabrication.[39] Briefly, three major components (i.e., a Nano-ESI emitter, a dual-bore quartz tip, and a fused silica capillary) were integrated to prepare a Single-probe. The Single-probe was then coupled to a Thermo LTQ Orbitrap XL mass spectrometer for SCMS analysis (Fig. 1). The sampling solvent (acetonitrile supplemented with 1% formic acid) was used for SCMS experiment at a flowrate of ~0.05 µl/min. The MS parameter settings included mass range m/z 200-1500 for positive ion

mode and m/z 50-900 for negative ion mode, mass resolution 60,000, ionization voltage 4.5kV, 1 microscan, and 100 ms max injection time.

4.3.7 SCMS analyses of cells in direct co-culture

The gridded glass coverslip containing co-cultured IRI-resistant and HCT116-GFP cells were used for the SCMS experiments. First, we obtained the optical images of the co-cultured cells to determine the locations of each type cells on the gridded glass slides. A Nikon Eclipse Ti microscope was used to take both bright-field (Fig. 1A) and fluorescence images (Fig. 1B) of cells attached on the gridded glass coverslips, which are maintained in 12-well plates during image capture. Based on the comparison of these two types of images, we manually determined the coordinates of each type of cells on gridded glass cover slips (Fig. 1). Second, the gridded glass coverslips containing cells were taken out from 6-well plates, rinsed with FBS-free culture medium, and placed onto the XYZ-stage for the Single-probe SCMS measurements (Fig. 1C). Guided by the digital microscope, we analyzed both types of cells on the gridded glass slides. To compare the changed metabolites due to cell-cell communication in the direct co-culture, SCMS experiments were also carried out using HCT116-GFP and IRI-resistant cells obtained from the mono-culture.

4.3.8 SCMS data analysis

We adopted our previously established SCMS data analysis workflow, including data pretreatment, statistical analysis, and database searching, to analyze experimental results.[52] First, we conducted SCMS data pretreatment, including noise removal, background subtraction, ion intensity normalization, and peak alignment. Noise removal is performed to remove instrument noise; background subtraction can eliminate

contaminants (e.g., ions from the solvent and cell culture medium); ion intensity normalization provides an effective approach to comparing the relative abundances of species from different cells. Although quantitative Single-probe SCMS experiments can be performed to measure the absolute quantity or concentration of target molecules (e.g., anticancer drugs) in single cells, the internal standard (e.g., isotopically labelled anticancer drug) is needed in each study.[41, 53] It is impractical to obtain the absolute quantitative information of large numbers of species from single cells. In our studies, ion intensities were normalized to the total ion current (TIC), a commonly used normalization method in MS studies, and then multiplied by an arbitrary scaling factor of 10^5. Peak alignment was then performed to correct minor mass shift in different measurements. The first three steps were performed using our customized R script[52], whereas peak alignment was achieved using Geena 2.[54] Second, statistical analyses, including multivariate analysis (e.g., principle component analysis (PCA) and partial least squares-discriminant analysis (PLS-DA)) and univariate analysis (e.g., Student's t test), were conducted using MetaboAnalyst.[55] Last, three online metabolomics databases, Metlin[56] HMDB[57], and GNPS[58] were utilized to tentatively label all ions. MS^2 structure verification of ions of interest was conducted through three different approaches: at the single-cell level using single-probe SCMS method, MS analysis of cell lysate using direct injection, and LC-MS/MS analysis of cell lysate.

4.4 Results and discussions

4.4.1 Changes of drug-resistance levels by IRI-resistant cells in drug-free medium.

IRI-resistant HCT116 cells were produced by culturing the parental HCT116 in medium containing low-dose of IRI (IC_{50} = 16.6 ± 1.4 μM). It was reported that drug-resistance levels of drug-resistant cells can gradually decline when cultured in drug-free medium over time.[59] To determine if culturing IRI-resistant cells in drug-free medium can significantly affect their drug-resistance levels, we incubated IRI-resistant HCT116 cells under normal conditions (i.e., using regular IRI-free medium) for 1 and 2 weeks. We then performed IC_{50} measurements, and evaluated their IRI-resistance level using the resistance index (RI), which is the ratio of IC_{50} of IRI-resistance and parental HCT116 cells (IC_{50} = 2.90 ± 0.1 μM).[49] Our results indicate that their IRI-resistance levels were slightly reduced after 1 week (RI = 5.0) and 2 weeks (RI = 4.0) culture in IRI-free medium, compared with the original IRI-resistant cells (RI = 5.7) (Fig. S1).

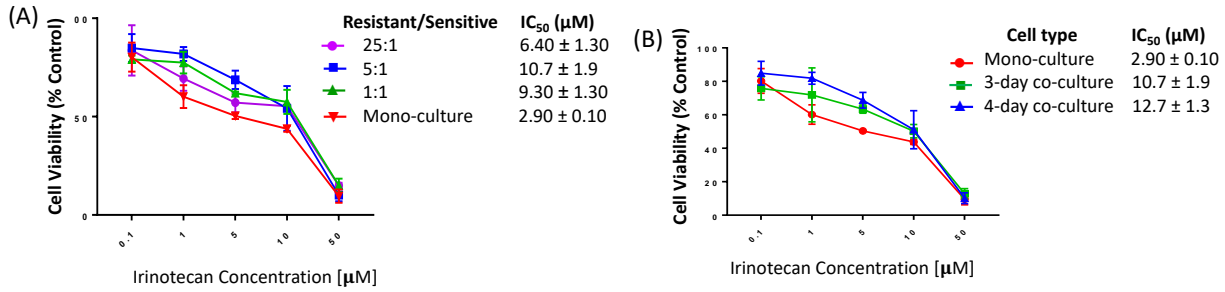


Fig. 2 The viability measurements of drug-sensitive HCT116 cells in the indirect co-culture with IRI- HCT116 cells under (A) difference cell density ratios and (B) different co-culture times. Cell viability was reported relatives to control cells (mono-cultured HCT116 cells) from 5 measurements.

4.4.2 Changes of drug-resistance levels of drug-sensitive cells in co-culture conditions.

The IRI-resistance levels of HCT116 cells in the indirect co-culture system were also evaluated using MTT assay. Cells were co-cultured using different cell density ratios and co-culture times. To study the influence of the relative cell populations on drug resistance, the IRI-resistant and parental HCT116 cells at different ratios (1:1, 5:1, 25:1) were added into the indirect co-culture devices. MTT assay was then carried out to determine the drug resistance levels of HCT116 cells after 2, 3, and 4 days of co-culture. Our results indicate that the ratio of IRI-resistant to HCT116 cells has a negligible influence when it was increased from 1:1 (IC_{50} = 9.30 ± 1.30 μM) to 5:1 (IC_{50} = 10.7 ± 1.9 μM) (Fig. 2A). However, a noticeable decrease of IRI-resistance (IC_{50} = 6.40 ± 1.30 μM) was observed when this ratio was increased to 25:1. Based on our observation using microscope, this change is likely due to the formation of 3D spheroids, instead of maintaining the 2D monolayer in other conditions, from excessive numbers of IRI-resistant cells. The 3D structure of spheroids is expected to limit interactions between IRI-resistance cells in inner spheroids and HCT116 cells, whereas only those on the outer layer, which account for small portions of total cell numbers, can more effectively participate in such interactions. The influence of co-culture time on IRI-resistance has also been investigated. Our results indicate that HCT116 (IC_{50} = 2.90 ± 0.10 μM) acquired significantly higher levels of drug resistance after being co-cultured for 3 (IC_{50} = 10.7 ± 1.9 μM) and 4 days (IC_{50} = 12.7 ± 1.3 μM) (Fig. 2B).

Although IC_{50} measurements cannot be conveniently conducted for cells in the direct co-culture systems, cell density was visually inspected to approximately evaluate

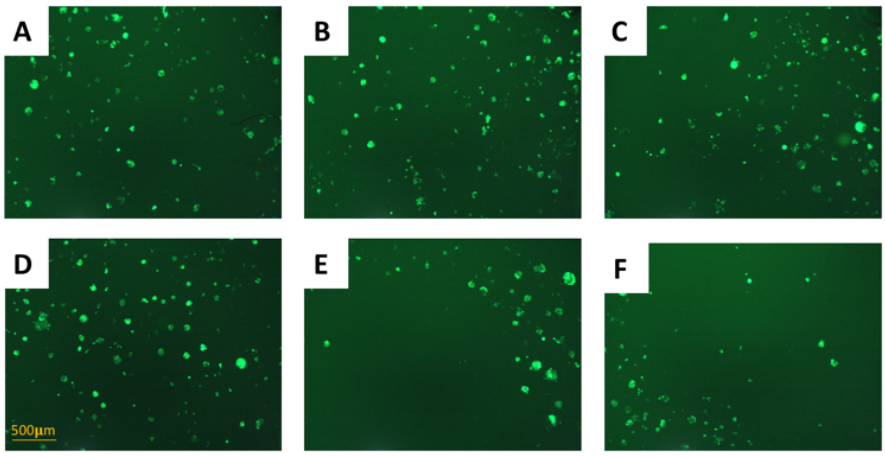


Fig. 3 Using fluorescence microscopy to evaluate drug resistance of HCT116-GFP cells in the direct co-culture with (A-C) drug-resistant or (D-F) drug–sensitive HCT116 cells, λexcitation = 495 nm, λemission = 519 nm. (A) Abundant HCT116-GFP cells (light-green spots) were observed in the co-culture system with IRI-HCT116 cells (no fluorescence). Densities of HCT116-GFP were slightly reduced after IRI treatment at (B) 5 μM or (C) 10 μM for 24 hrs. (D) Abundant HCT116-GFP cells were observed in the co-culture system with regular HCT116 cells. Densities of HCT116-GFP were significantly reduced after IRI treatment at (B) 5 μM or (C) 10 μM for 24 hrs.

changes of drug-resistance level under irinotecan treatment. The IRI-resistant cells and HCT116-GFP (with cell density ratio of 1:1) were cultured in the same well containing IRI (0, 5, or 10 μM). We used the fluorescence microscope to monitor the growth of HCT116-GFP cells under IRI treatment. In the comparison studies, regular HCT116 and HCT116-GFP cells were co-cultured under the same conditions (Fig. 3). Fluorescence images of each system were taken after 24hrs of treatment. It is evident that HCT116-GFP cells acquired certain levels of drug resistance through interactions with IRI-resistant HCT116 cell (Fig 3A-C), whereas those co-cultured with regular HCT116 (Fig. 3D-F) exhibited

poorer viability under IRI treatment. In more quantitative analyses, the relative intensities of fluorescence (calculated using ImageJ) from HCT116-GFP cells were used to compare the viability of HCT116-GPF cells under different IRI treatment concentrations (Fig. S2). Our experimental results suggest that IRI-resistance cells can foster drug-sensitive cells to improve their IRI-resistance levels through cell-cell interactions with or without direct cell-cell contact.

4.4.3 Metabolomics profile change of cells in co-culture systems

We performed the SCMS experiments for cells in five different groups, including the mono-culture (HCT116, HCT116-GFP, and IRI-resistant HCT116) and co-culture (HCT116-GFP and IRI-resistant HCT116) cells. Approximately 30 cells in each group were analyzed, and the obtained data were subjected to the pretreatment and statistical analyses to extract molecular information (Fig. 4). To minimize the variance of experimental conditions (e.g., instrument tuning and cell status) on the SCMS results, we performed three batches of experiments on three different days.

In the first batch of experiment, we compared the metabolomics profiles between mono-cultured HCT116 and HCT 116-GFP cells, as we used HCT 116-GPF to represent HCT116 cells in the direct co-culture system. We performed PCA, an unsupervised multivariate analysis method, and results indicate that HCT116 and HCT116-GFP cells possess very similar molecular profiles (i.e., ellipses of cells in these two groups are largely overlapped) (Fig. S3A and S3B). To quantitatively confirm these results, we subjected these SCMS data to PLS-DA, a supervised method, and results show that there is no significantly different ($p=0.698$) molecular composition between these two cell lines (Fig. S3B). Our experimental results agree well with the previous report that GFP labeling

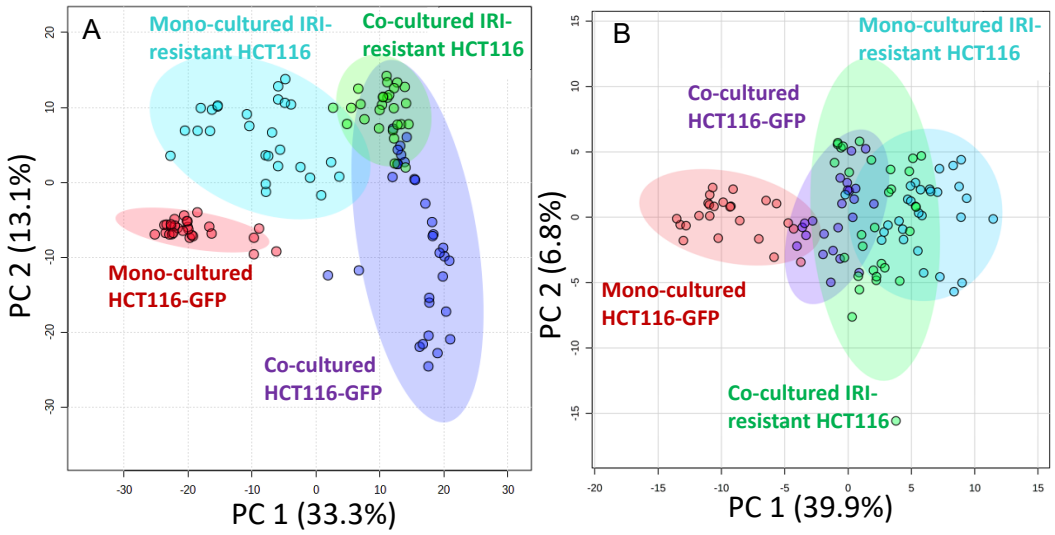


Fig. 4 PCA results illustrating metabolomics profiles of HCT116-GFP and IRI-HCT116 cells in the mono-culture and direct co-culture systems under positive ion mode (A) and negative ion mode (B). Metabolites of HCT116-GFP were significantly changed by IRI-HCT116 cells in both systems, and these two types of cells tended to possess similar metabolomics profiles in the direct co-culture.

has negligible influence on cell metabolism.[51] Therefore, it is valid to use HCT116-GFP cells to represent HCT116 cells for the co-culture studies.

In the second batch of experiments, we studied IRI-resistant and HCT116-GFP cells in the direct co-culture, along with the mono-culture counterparts, using the Single-probe SCMS in the positive ion mode and negative ion modes. Similar to the above data analysis, we conducted PCA, and the results indicate that the metabolic profiles of HCT116-GFP cells were significantly changed by the IRI-resistant cells through cell-cell interactions (Fig. 4). Interestingly, both HCT116-GFP and IRI-resistant cells tend to exhibit increased similarities of metabolomics profiles after direct co-culture.

To investigate molecules altered by co-culture, we compared the SCMS data of HCT116-GFP cells in the mono-culture and direct co-culture. Typical background-subtracted mass spectra of single HCT116-GFP cells in these two culture conditions are shown in Fig. S4, illustrating the overall cellular metabolites of drug-sensitive cells were altered by IRI-resistant cells. In general, HCT116-GFP cells from direct co-culture contain higher abundances of SMs (e.g., SM(40:1), SM(41:1)) than triglycerides (TGs) (e.g., TG(52:2), TG(54:3)), whereas an opposite trend was observed in mono-cultured HCT116-GFP cells. Student's t-test was further performed to discover species altered by co-culture. 19 sphingomyelins (SMs) lipids and two phosphatidylcholines (PCs) were significantly upregulated in HCT116-GFP cells from direct co-culture (Fig. 5). The structure identifications were performed using tandem MS (MS/MS) both at the single-cell level and using cell lysate (Fig. S6-S8).

To improve the detection coverage of cellular metabolites, we conducted the third batch of SCMS experiments in the negative ion mode. HCT116-GFP and IRI-resistant cells in both the direct co-culture and mono-culture were analyzed. Similar to the trend observed from positive ion mode results, metabolites detected in the negative ion mode indicated HCT116-GFP and IRI-resistant cells tend to exhibit increased similarities (Fig. 4B). The olverlap degrees among different cell groups are different in two ion modes, likely because fewer metabolites were observed in the negative ion mode (Fig. S5).

T-test was conducted to determine metabolites with significant changes between mono-cultured and co-cultured HCT116-GFP cells. As illustrated in Fig. 5B, the top-10 metabolites with significantly different abundances include amino acids, fatty acids, and

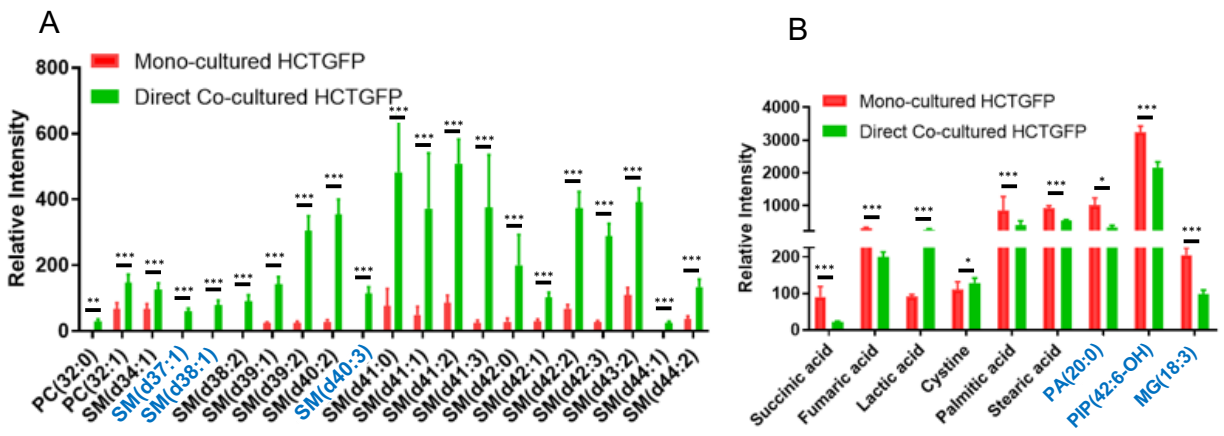


*Fig. 5 Metabolites significantly altered in HCT116-GFP cells through direct co-culture with IRI-HCT116 cells under (A) positive ion mode and (B) negative ion mode. Results were obtained from n> 30 cells in each group. SM (sphingomyelin), PC (phosphatidylcholine), PA (phosphatidic acid), and MG (monoglyceride). (From t-test: * p<0.05; **p<0.01, ***p<0.005). Species in black font were identified from MS^2 analyses.*

species involved in TCA (tricarboxylic acid) cycle. Molecular identification was preformed by annotating MS/MS spectra from single cells and lysates (Fig. S6-S7).

To study the influence of drug treatment on cell metabolites, SCMS experiments were conducted using HCT116-GFP and IRI-resistant cells with and without IRI treatment (Fig. S6). As expected, drug treatment has more influence on drug-sensitive cells than drug-resistant cells (Fig. S6A). T-test results indicate that species altered by IRI treatment in HCT116-GFP cells and IRI-resistant cells are primarily phospholipids (e.g., PC, PE, and LysoPC lipids), which agree with previous studies.[47, 60-61] Our results suggest that molelcules changed in co-culture conditions are primarily due to cell-to-cell interactions rather than the influence of drug compound.

4.4.4 Potential metabolic mechanisms of spreading drug resistance by drug-resistant cells

Tumor microenvironment, composed of different types of cells, plays an important role in spreading drug resistance, resulting in cancer relapse and metastasis.[62] Growing evidence shows that the metabolic cooperation between different types of cells promotes the development of drug resistance.[63-64] In particular, cell communication between drug-resistant cells and drug-sensitive cells can assist the progression of chemotherapy resistance in tumor cells.[10] The attainment of drug resistance in drug-sensitive cells from drug-resistant cells can be achieved by exchanging signaling factors.[10, 12-13, 65] For example, drug resistance levels of drug-sensitive cells can be enhanced by intercellular transfer of P-glycoprotein (P-gp) from drug-resistant cells.[11, 66-69] The acquirement of these mediators elevates drug resistance, and subsequently induces metabolic regulation in drug-sensitive cells.[70]

In the current studies, we detected lipid reprograming in drug-sensitive cells after acquiring drug resistance from neighboring drug-resistant cells. Lipids are a major constituent of cell membrane, which is the signaling platform of transporters, and they control the structure and permeability of the membrane. Our results indicate that, compared with the mono-cultured HCT116-GFP cells, the major alternation of lipids in co-cultured HCT116-GFP cells is attributed to significantly upregulated SMs. Similar results have been reported in previous studies, with higher levels of SM lipids being associated with drug resistance in many cancer resistant cell lines (e.g., 5-FU-resistant human colorectal cancer cells[71], doxorubicin-resistant ovarium carcinoma cells[72], and vinblastine-resistant leukemia T lymphoblast cells[73]). Particularly, the increased levels of

SM in drug-resistant cells can alter biophysical properties of cell membrane by increasing its structural order and decreasing its fluidity, possibly due to SMs' high affinities to cholesterols.[74] Passive diffusion of drugs across the cell membrane, which is one of the most efficient drug uptake methods, is thus impaired by the decreased membrane fluidity.[74] This mechanism of biophysical alternation on the cell membrane could possibly explain the elevated SMs' expression in co-cultured HCT116-GFP cells in our study. However, more experiments need to be conducted to verify the proposed mechanism.

Additional information can be obtained from the negative ion mode results (Fig. 5A). It is possible that cell-cell communication can also induce drug resistance through other pathways such as TCA cycle, amino acids metabolism, and fatty acids expression. For example, succinic acid and fumaric acid, two small molecules in TCA cycle metabolism, were significantly downregulated in HCT116-GFP cells after co-culturing with IRI-resistant cells. TCA cycle is known to play a central role in the development of drug resistance.[75] Our findings are consistent with previous studies: genes involved in TCA cycle are significantly downregulated in the IRI-resistant cells compared to the sensitive cells.[76] Succinic acid and fumaric acid are also classified as oncometabolites, and their downregulation is tightly correlated with the development of drug resistance in cisplatin-resistant cells.[77] The suppressed TCA cycle impels in cancer cells to rely more on glycolysis for obtaining energy, thus producing larger amounts of lactic acid (Fig. 5B). In fact, accumulation of lactic acid is related to increased cancer resistance and malignancy.[78] Amino acid metabolism is also associated with the development of drug resistance in cancer. For example, the overexpression of cystine transport system assists cancer cells decreasing drug sensitivity.[79]

4.5 Conclusion

In summary, we provided a new method to study cellular metabolism alteration due to direct cell-cell interactions among different types of cells by combing the Single-probe SCMS and fluorescence microscopy. Our method allows for ambient SCMS metabolomics studies of different types of cells growing under the same conditions with direct cell-cell contact. We used model systems representing drug-sensitive (i.e., parental HCT116 or HCT116-GFP) and drug-resistant (i.e., IRI-resistant HCT116) cells in both indirect (without cell-cell contact) and direct (with cell-cell contact) co-culture systems. This study is focused on the influence of drug-resistant cells on the drug-resistance level and metabolism of drug-sensitive cells in co-culture conditions. Fluorescence microscope was used to locate individual HCT116-GFP cells in direct co-culture system, and then the Single-probe SCMS technique was used to measure cellular metabolites. Our results indicate that drug-sensitive cancer cells acquired significantly improved drug-resistance levels and drastically altered metabolomics profiles through cell-cell communication with drug-resistant cancer cells. In particular, the drug-sensitive cancer cells tend to acquire metabolites similar to drug-resistant cells through direct co-culture. The acquirement of enhanced drug resistance is associated with multiple metabolism regulations such as higher expression of SM lipids and lactic acid as well as downregulation of TCA cycle intermediates. Detailed structure characterization of lipids (e.g., the determination of cis/trans isomers and positions of carbon-carbon double bonds) was not performed, because these studies are beyond our current research scope. Future studies are necessary to fill this knowledge gap. We expect our methods can be potentially utilized to study metabolic responses of single cells to microenvironment change (e.g., physical

and chemical stimuli) or cell-cell interactions using cells labeled with fluorescence proteins or dyes.

References

1. Bakken, T.; Cowell, L.; Aevermann, B. D.; Novotny, M.; Hodge, R.; Miller, J. A.; Lee, A.; Chang, I.; McCorrison, J.; Pulendran, B.; Qian, Y.; Schork, N. J.; Lasken, R. S.; Lein, E. S.; Scheuermann, R. H., Cell type discovery and representation in the era of high-content single cell phenotyping. *Bmc Bioinformatics* **2017,** *18* (Suppl 17), 559.10.1186/s12859-017-1977-1
2. Sanchez, A.; Golding, I., Genetic determinants and cellular constraints in noisy gene expression. *Science* **2013,** *342* (6163), 1188-93.10.1126/science.1242975
3. Rubakhin, S. S.; Romanova, E. V.; Nemes, P.; Sweedler, J. V., Profiling metabolites and peptides in single cells. *Nat Methods* **2011,** *8* (4), S20-S29.10.1038/Nmeth.1549
4. Papalexi, E.; Satija, R., Single-cell RNA sequencing to explore immune cell heterogeneity. *Nat Rev Immunol* **2018,** *18* (1), 35-45.10.1038/nri.2017.76
5. Gebhardt, R., Cell-Cell Interactions - Clues to Hepatocyte Heterogeneity and Beyond. *Hepatology* **1992,** *16* (3), 843-845
6. Komohara, Y.; Jinushi, M.; Takeya, M., Clinical significance of macrophage heterogeneity in human malignant tumors. *Cancer Sci* **2014,** *105* (1), 1-8.10.1111/cas.12314
7. Holohan, C.; Van Schaeybroeck, S.; Longley, D. B.; Johnston, P. G., Cancer drug resistance: an evolving paradigm. *Nat Rev Cancer* **2013,** *13* (10), 714-26.10.1038/nrc3599
8. Housman, G.; Byler, S.; Heerboth, S.; Lapinska, K.; Longacre, M.; Snyder, N.; Sarkar, S., Drug resistance in cancer: an overview. *Cancers (Basel)* **2014,** *6* (3), 1769-92.10.3390/cancers6031769
9. Brucher, B. L.; Jamall, I. S., Cell-cell communication in the tumor microenvironment, carcinogenesis, and anticancer treatment. *Cell Physiol Biochem* **2014,** *34* (2), 213-43.10.1159/000362978
10. Frankfurt, O. S.; Seckinger, D.; Sugarbaker, E. V., Intercellular Transfer of Drug-Resistance. *Cancer Res* **1991,** *51* (4), 1190-1195
11. Levchenko, A.; Mehta, B. M.; Niu, X. L.; Kang, G.; Villafania, L.; Way, D.; Polycarpe, D.; Sadeain, M.; Larson, S. M., Intercellular transfer of P-glycoprotein mediates acquired multidrug resistance in tumor cells. *P Natl Acad Sci USA* **2005,** *102* (6), 1933-1938.10.1073/pnas.0401851102
12. Chu, F.; Naiditch, J. A.; Clark, S.; Qiu, Y. Y.; Zheng, X.; Lautz, T. B.; Holub, J. L.; Chou, P. M.; Czurylo, M.; Madonna, M. B., Midkine Mediates Intercellular Crosstalk between Drug-Resistant and Drug-Sensitive Neuroblastoma Cells In Vitro and In Vivo. *ISRN Oncol* **2013,** *2013*, 518637.10.1155/2013/518637
13. Menachem, A.; Makovski, V.; Bodner, O.; Pasmanik-Chor, M.; Stein, R.; Shomron, N.; Kloog, Y., Intercellular transfer of small RNAs from astrocytes to lung tumor cells induces resistance to chemotherapy. *Oncotarget* **2016,** *7* (11), 12489-12504.DOI 10.18632/oncotarget.7273
14. Korkaya, H.; Liu, S.; Wicha, M. S., Breast cancer stem cells, cytokine networks, and the tumor microenvironment. *J Clin Invest* **2011,** *121* (10), 3804-9.10.1172/JCI57099
15. Lindoso, R. S.; Collino, F.; Vieyra, A., Extracellular vesicles as regulators of tumor fate: crosstalk among cancer stem cells, tumor cells and mesenchymal stem cells. *Stem Cell Investigation* **2017,** *4* (9),

16. Vis, M. A. M.; Ito, K.; Hofmann, S., Impact of Culture Medium on Cellular Interactions in in vitro Co-culture Systems. *Front Bioeng Biotechnol* **2020,** *8*, 911.10.3389/fbioe.2020.00911
17. Pandurangan, M.; Hwang, I., Application of cell co-culture system to study fat and muscle cells. *Appl Microbiol Biotechnol* **2014,** *98* (17), 7359-64.10.1007/s00253-014-5935-9
18. Kuppusamy, P.; Kim, D.; Soundharrajan, I.; Hwang, I.; Choi, K. C., Adipose and Muscle Cell Co-Culture System: A Novel In Vitro Tool to Mimic the In Vivo Cellular Environment. *Biology (Basel)* **2020,** *10* (1).10.3390/biology10010006
19. Goers, L.; Freemont, P.; Polizzi, K. M., Co-culture systems and technologies: taking synthetic biology to the next level. *J R Soc Interface* **2014,** *11* (96).10.1098/rsif.2014.0065
20. Borciani, G.; Montalbano, G.; Baldini, N.; Cerqueni, G.; Vitale-Brovarone, C.; Ciapetti, G., Co-culture systems of osteoblasts and osteoclasts: Simulating in vitro bone remodeling in regenerative approaches. *Acta Biomater* **2020,** *108*, 22-45.10.1016/j.actbio.2020.03.043
21. Renaud, J.; Martinoli, M. G., Development of an Insert Co-culture System of Two Cellular Types in the Absence of Cell-Cell Contact. *Jove-J Vis Exp* **2016,** (113).ARTN e54356 10.3791/54356
22. Li, W. W.; Khan, M.; Mao, S. F.; Feng, S.; Lin, J. M., Advances in tumor-endothelial cells co-culture and interaction on microfluidics. *J Pharm Anal* **2018,** *8* (4), 210-218.10.1016/j.jpha.2018.07.005
23. Pagella, P.; Neto, E.; Lamghari, M.; Mitsiadis, T. A., Investigation of Orofacial Stem Cell Niches and Their Innervation through Microfluidic Devices. *Eur Cells Mater* **2015,** *29*, 213-223.DOI 10.22203/eCM.v029a16
24. Jiang, J.; Leong, N. L.; Mung, J. C.; Hidaka, C.; Lu, H. H., Interaction between zonal populations of articular chondrocytes suppresses chondrocyte mineralization and this process is mediated by PTHrP. *Osteoarthr Cartilage* **2008,** *16* (1), 70-82.10.1016/j.joca.2007.05.014
25. Bogdanowicz, D. R.; Lu, H. H., Studying cell-cell communication in co-culture. *Biotechnol J* **2013,** *8* (4), 395-6.10.1002/biot.201300054
26. Heng, B. C.; Cao, T.; Lee, E. H., Directing stem cell differentiation into the chondrogenic lineage in vitro. *Stem Cells* **2004,** *22* (7), 1152-1167.10.1634/stemcells.2004-0062
27. Goers, L.; Freemont, P.; Polizzi, K. M., Co-culture systems and technologies: taking synthetic biology to the next level. *J R Soc Interface* **2014,** *11* (96).ARTN 20140065 10.1098/rsif.2014.0065
28. Efremov, A. N.; Stanganello, E.; Welle, A.; Scholpp, S.; Levkin, P. A., Micropatterned superhydrophobic structures for the simultaneous culture of multiple cell types and the study of cell-cell communication. *Biomaterials* **2013,** *34* (7), 1757-63.10.1016/j.biomaterials.2012.11.034
29. Jiang, J.; Nicoll, S. B.; Lu, H. H., Co-culture of osteoblasts and chondrocytes modulates cellular differentiation in vitro. *Biochem Biophys Res Commun* **2005,** *338* (2), 762-70.10.1016/j.bbrc.2005.10.025
30. Hamilton, S. K.; Bloodworth, N. C.; Massad, C. S.; Hammoudi, T. M.; Suri, S.; Yang, P. J.; Lu, H.; Temenoff, J. S., Development of 3D hydrogel culture systems with on-demand cell separation. *Biotechnol J* **2013,** *8* (4), 485-95.10.1002/biot.201200200
31. Binek, A.; Rojo, D.; Godzien, J.; Ruperez, F. J.; Nunez, V.; Jorge, I.; Ricote, M.; Vazquez, J.; Barbas, C., Flow Cytometry Has a Significant Impact on the Cellular Metabolome. *J Proteome Res* **2019,** *18* (1), 169-181.10.1021/acs.jproteome.8b00472

32. Llufrio, E. M.; Wang, L. J.; Naser, F. J.; Patti, G. J., Sorting cells alters their redox state and cellular metabolome. *Redox Biol* **2018,** *16*, 381-387.10.1016/j.redox.2018.03.004
33. Boggio, K. J.; Obasuyi, E.; Sugino, K.; Nelson, S. B.; Agar, N. Y. R.; Agar, J. N., Recent advances in single-cell MALDI mass spectrometry imaging and potential clinical impact. *Expert Rev Proteomic* **2011,** *8* (5), 591-604.10.1586/Epr.11.53
34. Jungnickel, H.; Laux, P.; Luch, A., Time-of-Flight Secondary Ion Mass Spectrometry (ToF-SIMS): A New Tool for the Analysis of Toxicological Effects on Single Cell Level. *Toxics* **2016,** *4* (1).ARTN 5
10.3390/toxics4010005
35. Masujima, T., Live Single-cell Mass Spectrometry. *Analytical Sciences* **2009,** *25* (8), 953-960.DOI 10.2116/analsci.25.953
36. Gong, X. Y.; Zhao, Y. Y.; Cai, S. Q.; Fu, S. J.; Yang, C. D.; Zhang, S. C.; Zhang, X. R., Single Cell Analysis with Probe ESI-Mass Spectrometry: Detection of Metabolites at Cellular and Subcellular Levels. *Analytical Chemistry* **2014,** *86* (8), 3809-3816.10.1021/ac500882e
37. Bergman, H. M.; Lanekoff, I., Profiling and quantifying endogenous molecules in single cells using nano-DESI MS. *Analyst* **2017,** *142* (19), 3639-3647.10.1039/c7an00885f
38. Shrestha, B.; Vertes, A., In Situ Metabolic Profiling of Single Cells by Laser Ablation Electrospray Ionization Mass Spectrometry. *Anal. Chem.* **2009,** *81* (20), 8265-8271.DOI 10.1021/ac901525g
39. Pan, N.; Rao, W.; Kothapalli, N. R.; Liu, R.; Burgett, A. W.; Yang, Z., The single-probe: a miniaturized multifunctional device for single cell mass spectrometry analysis. *Anal Chem* **2014,** *86* (19), 9376-80.10.1021/ac5029038
40. Pan, N.; Rao, W.; Yang, Z., Single-Probe Mass Spectrometry Analysis of Metabolites in Single Cells. *Methods Mol Biol* **2020,** *2064*, 61-71.10.1007/978-1-4939-9831-9_5
41. Pan, N.; Standke, S. J.; Kothapalli, N. R.; Sun, M.; Bensen, R. C.; Burgett, A. W. G.; Yang, Z. B., Quantification of Drug Molecules in Live Single Cells Using the Single-Probe Mass Spectrometry Technique. *Analytical Chemistry* **2019,** *91* (14), 9018-9024.10.1021/acs.analchem.9b01311
42. Sun, M.; Yang, Z. B., Metabolomic Studies of Live Single Cancer Stem Cells Using Mass Spectrometry. *Anal. Chem.* **2019,** *91* (3), 2384-2391.10.1021/acs.analchem.8b05166
43. Standke, S. J.; Colby, D. H.; Bensen, R. C.; Burgett, A. W. G.; Yang, Z., Mass Spectrometry Measurement of Single Suspended Cells Using a Combined Cell Manipulation System and a Single-Probe Device. *Analytical Chemistry* **2019,** *91* (3), 1738-1742.10.1021/acs.analchem.8b05774
44. Pan, N.; Rao, W.; Standke, S. J.; Yang, Z. B., Using Dicationic Ion-Pairing Compounds To Enhance the Single Cell Mass Spectrometry Analysis Using the Single-Probe: A Microscale Sampling and Ionization Device. *Analytical Chemistry* **2016,** *88* (13), 6812-6819.10.1021/acs.analchem.6b01284
45. Standke, S. J.; Colby, D. H.; Bensen, R. C.; Burgett, A. W. G.; Yang, Z. B., Integrated Cell Manipulation Platform Coupled with the Single-probe for Mass Spectrometry Analysis of Drugs and Metabolites in Single Suspension Cells. *Jove-J Vis Exp* **2019,** (148).ARTN e59875
10.3791/59875

46. Liu, R. M.; Pan, N.; Zhu, Y. L.; Yang, Z. B., T-Probe: An Integrated Microscale Device for Online In Situ Single Cell Analysis and Metabolic Profiling Using Mass Spectrometry. *Analytical Chemistry* **2018,** *90* (18), 11078-11085.10.1021/acs.analchem.8b02927
47. Zhu, Y. L.; Liu, R. M.; Yang, Z. B., Redesigning the T-probe for mass spectrometry analysis of online lysis of non-adherent single cells. *Anal Chim Acta* **2019,** *1084*, 53-59.10.1016/j.aca.2019.07.059
48. Zhu, Y. L.; Wang, W. H.; Yang, Z. B., Combining Mass Spectrometry with Paterno-Buchi Reaction to Determine Double-Bond Positions in Lipids at the Single-Cell Level. *Analytical Chemistry* **2020,** *92* (16), 11380-11387.10.1021/acs.analchem.0c02245
49. McDermott, M.; Eustace, A. J.; Busschots, S.; Breen, L.; Crown, J.; Clynes, M.; O'Donovan, N.; Stordal, B., In vitro Development of Chemotherapy and Targeted Therapy Drug-Resistant Cancer Cell Lines: A Practical Guide with Case Studies. *Front Oncol* **2014,** *4*, 40.10.3389/fonc.2014.00040
50. Liu, R. M.; Sun, M.; Zhang, G. W.; Lan, Y. P.; Yang, Z. B., Towards early monitoring of chemotherapy-induced drug resistance based on single cell metabolomics: Combining single-probe mass spectrometry with machine learning. *Anal Chim Acta* **2019,** *1092*, 42-48.10.1016/j.aca.2019.09.065
51. Yang, J.; Wang, N.; Chen, D.; Yu, J.; Pan, Q.; Wang, D.; Liu, J.; Shi, X.; Dong, X.; Cao, H.; Li, L.; Li, L., The Impact of GFP Reporter Gene Transduction and Expression on Metabolomics of Placental Mesenchymal Stem Cells Determined by UHPLC-Q/TOF-MS. *Stem Cells Int* **2017,** *2017*, 3167985.10.1155/2017/3167985
52. Liu, R. M.; Zhang, G. W.; Sun, M.; Pan, X. L.; Yang, Z. B., Integrating a generalized data analysis workflow with the Single-probe mass spectrometry experiment for single cell metabolomics. *Anal Chim Acta* **2019,** *1064*, 71-79.10.1016/j.aca.2019.03.006
53. Bensen, R. C.; Standke, S. J.; Colby, D. H.; Kothapalli, N. R.; Le-McClain, A. T.; Patten, M. A.; Tripathi, A.; Heinlen, J. E.; Yang, Z.; Burgett, A. W. G., Single Cell Mass Spectrometry Quantification of Anticancer Drugs: Proof of Concept in Cancer Patients. *ACS Pharmacol Transl Sci* **2021,** *4* (1), 96-100.10.1021/acsptsci.0c00156
54. Romano, P.; Profumo, A.; Rocco, M.; Mangerini, R.; Ferri, F.; Facchiano, A., Geena 2, improved automated analysis of MALDI/TOF mass spectra. *Bmc Bioinformatics* **2016,** *17*.ARTN 61
10.1186/s12859-016-0911-2
55. Xia, J.; Wishart, D. S., Using MetaboAnalyst 3.0 for Comprehensive Metabolomics Data Analysis. *Current Protocols in Bioinformatics* **2016,** *55* (1), 14.10.1-14.10.91.10.1002/cpbi.11
56. Smith, C. A.; O'Maille, G.; Want, E. J.; Qin, C.; Trauger, S. A.; Brandon, T. R.; Custodio, D. E.; Abagyan, R.; Siuzdak, G., METLIN: a metabolite mass spectral database. *Ther Drug Monit* **2005,** *27* (6), 747-51.10.1097/01.ftd.0000179845.53213.39
57. Wishart, D. S.; Feunang, Y. D.; Marcu, A.; Guo, A. C.; Liang, K.; Vazquez-Fresno, R.; Sajed, T.; Johnson, D.; Li, C.; Karu, N.; Sayeeda, Z.; Lo, E.; Assempour, N.; Berjanskii, M.; Singhal, S.; Arndt, D.; Liang, Y.; Badran, H.; Grant, J.; Serra-Cayuela, A.; Liu, Y.; Mandal, R.; Neveu, V.; Pon, A.; Knox, C.; Wilson, M.; Manach, C.; Scalbert, A., HMDB 4.0: the human metabolome database for 2018. *Nucleic Acids Res* **2018,** *46* (D1), D608-D617.10.1093/nar/gkx1089
58. Wang, M.; Carver, J. J.; Phelan, V. V.; Sanchez, L. M.; Garg, N.; Peng, Y.; Nguyen, D. D.; Watrous, J.; Kapono, C. A.; Luzzatto-Knaan, T.; Porto, C.; Bouslimani, A.; Melnik, A. V.; Meehan,

M. J.; Liu, W. T.; Crusemann, M.; Boudreau, P. D.; Esquenazi, E.; Sandoval-Calderon, M.; Kersten, R. D.; Pace, L. A.; Quinn, R. A.; Duncan, K. R.; Hsu, C. C.; Floros, D. J.; Gavilan, R. G.; Kleigrewe, K.; Northen, T.; Dutton, R. J.; Parrot, D.; Carlson, E. E.; Aigle, B.; Michelsen, C. F.; Jelsbak, L.; Sohlenkamp, C.; Pevzner, P.; Edlund, A.; McLean, J.; Piel, J.; Murphy, B. T.; Gerwick, L.; Liaw, C. C.; Yang, Y. L.; Humpf, H. U.; Maansson, M.; Keyzers, R. A.; Sims, A. C.; Johnson, A. R.; Sidebottom, A. M.; Sedio, B. E.; Klitgaard, A.; Larson, C. B.; P, C. A. B.; Torres-Mendoza, D.; Gonzalez, D. J.; Silva, D. B.; Marques, L. M.; Demarque, D. P.; Pociute, E.; O'Neill, E. C.; Briand, E.; Helfrich, E. J. N.; Granatosky, E. A.; Glukhov, E.; Ryffel, F.; Houson, H.; Mohimani, H.; Kharbush, J. J.; Zeng, Y.; Vorholt, J. A.; Kurita, K. L.; Charusanti, P.; McPhail, K. L.; Nielsen, K. F.; Vuong, L.; Elfeki, M.; Traxler, M. F.; Engene, N.; Koyama, N.; Vining, O. B.; Baric, R.; Silva, R. R.; Mascuch, S. J.; Tomasi, S.; Jenkins, S.; Macherla, V.; Hoffman, T.; Agarwal, V.; Williams, P. G.; Dai, J.; Neupane, R.; Gurr, J.; Rodriguez, A. M. C.; Lamsa, A.; Zhang, C.; Dorrestein, K.; Duggan, B. M.; Almaliti, J.; Allard, P. M.; Phapale, P.; Nothias, L. F.; Alexandrov, T.; Litaudon, M.; Wolfender, J. L.; Kyle, J. E.; Metz, T. O.; Peryea, T.; Nguyen, D. T.; VanLeer, D.; Shinn, P.; Jadhav, A.; Muller, R.; Waters, K. M.; Shi, W.; Liu, X.; Zhang, L.; Knight, R.; Jensen, P. R.; Palsson, B. O.; Pogliano, K.; Linington, R. G.; Gutierrez, M.; Lopes, N. P.; Gerwick, W. H.; Moore, B. S.; Dorrestein, P. C.; Bandeira, N., Sharing and community curation of mass spectrometry data with Global Natural Products Social Molecular Networking. *Nat Biotechnol* **2016,** *34* (8), 828-837.10.1038/nbt.3597

59. Biedler, J. L.; Spengler, B. A., Reverse transformation of multidrug-resistant cells. *Cancer Metastasis Rev* **1994,** *13* (2), 191-207.10.1007/BF00689636

60. Cui, D. N.; Wang, X.; Chen, J. Q.; Lv, B.; Zhang, P.; Zhang, W.; Zhang, Z. J.; Xu, F. G., Quantitative Evaluation of the Compatibility Effects of Huangqin Decoction on the Treatment of Irinotecan-Induced Gastrointestinal Toxicity Using Untargeted Metabolomics. *Front Pharmacol* **2017,** *8*.ARTN 211
10.3389/fphar.2017.00211

61. Tian, X.; Zhang, G. W.; Zou, Z.; Yang, Z. B., Anticancer Drug Affects Metabolomic Profiles in Multicellular Spheroids: Studies Using Mass Spectrometry Imaging Combined with Machine Learning. *Analytical Chemistry* **2019,** *91* (9), 5802-5809.10.1021/acs.analchem.9b00026

62. Li, Z. W.; Dalton, W. S., Tumor microenvironment and drug resistance in hematologic malignancies. *Blood Rev* **2006,** *20* (6), 333-42.10.1016/j.blre.2005.08.003

63. Morin, P. J., Drug resistance and the microenvironment: nature and nurture. *Drug Resist Update* **2003,** *6* (4), 169-172.10.1016/S1368-7646(03)00059-1

64. Shekhar, M. P. V., Drug Resistance: Challenges to Effective Therapy. *Curr Cancer Drug Tar* **2011,** *11* (5), 613-623

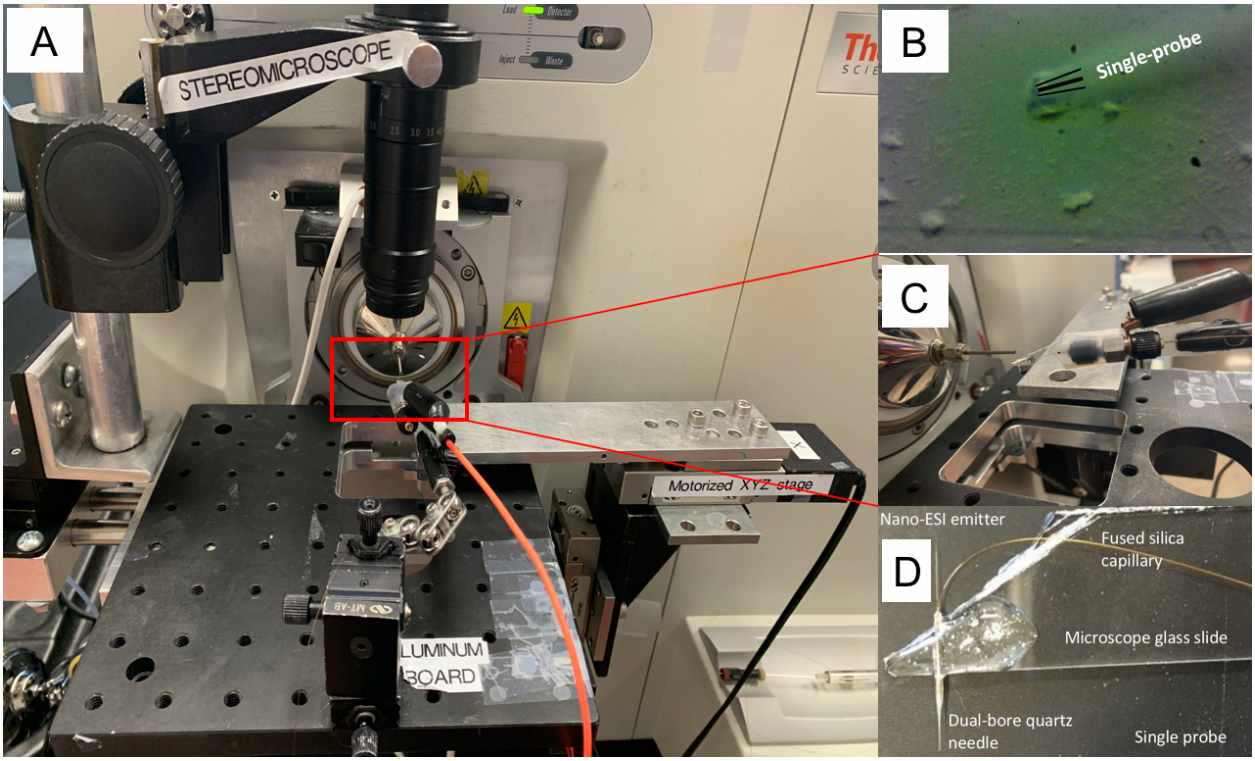
65. Mirkin, B. L.; Clark, S.; Zheng, X.; Chu, F.; White, B. D.; Greene, M.; Rebbaa, A., Identification of midkine as a mediator for intercellular transfer of drug resistance. *Oncogene* **2005,** *24* (31), 4965-4974.10.1038/sj.onc.1208671

66. Cheng, X. Z.; Zhou, H. L.; Tang, S. X.; Jiang, T.; Chen, Q.; Gao, R.; Ding, Y. L., Intercellular transfer of P-glycoprotein mediates the formation of stable multi-drug resistance in human bladder cancer BIU-87 cells. *Biol Open* **2019,** *8* (5).ARTN bio041889
10.1242/bio.041889

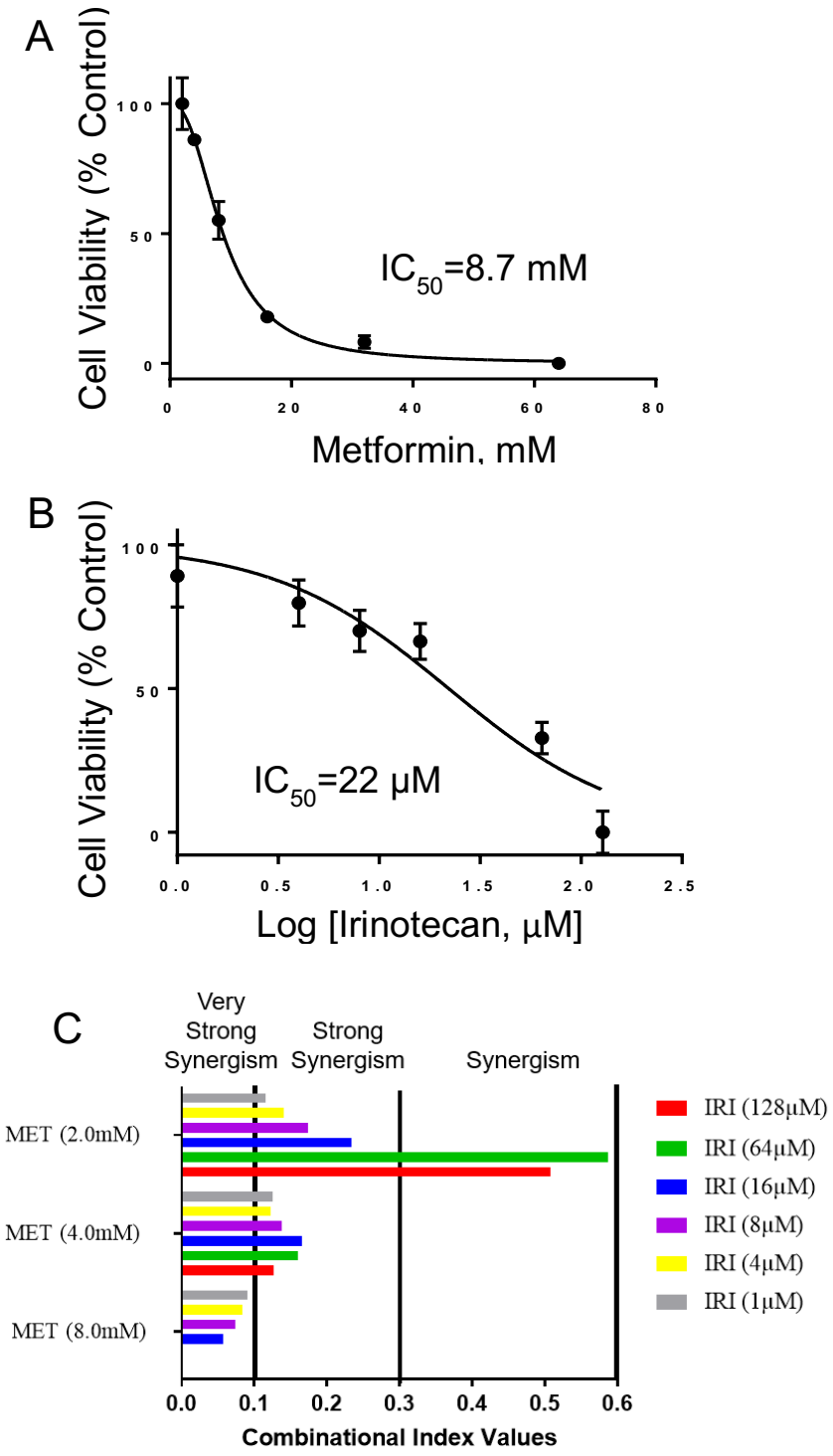
67. Ambudkar, S. V.; Sauna, Z. E.; Gottesman, M. M.; Szakacs, G., A novel way to spread drug resistance in tumor cells: functional intercellular transfer of P-glycoprotein (ABCB1). *Trends Pharmacol Sci* **2005,** *26* (8), 385-387.10.1016/j.tips.2005.06.001

68. Bebawy, M.; Combes, V.; Lee, E.; Jaiswal, R.; Gong, J.; Bonhoure, A.; Grau, G. E. R., Membrane microparticles mediate transfer of P-glycoprotein to drug sensitive cancer cells. *Leukemia* **2009,** *23* (9), 1643-1649.10.1038/leu.2009.76
69. Becker, M.; Levy, D., Modeling the Transfer of Drug Resistance in Solid Tumors. *B Math Biol* **2017,** *79* (10), 2394-2412.10.1007/s11538-017-0334-x
70. Peetla, C.; Vijayaraghavalu, S.; Labhasetwar, V., Biophysics of cell membrane lipids in cancer drug resistance: Implications for drug transport and drug delivery with nanoparticles. *Adv Drug Deliver Rev* **2013,** *65* (13-14), 1686-1698.10.1016/j.addr.2013.09.004
71. Jung, J. H.; Taniguchi, K.; Lee, H. M.; Lee, M.; Bandu, R.; Komura, K.; Lee, K.; Akao, Y.; Kim, K. P., Comparative lipidomics of 5-Fluorouracil-sensitive and -resistant colorectal cancer cells reveals altered sphingomyelin and ceramide controlled by acid sphingomyelinase (SMPD1). *Sci Rep-Uk* **2020,** *10* (1).ARTN 6124
10.1038/s41598-020-62823-0
72. Veldman, R. J.; Klappe, K.; Hinrichs, J.; Hummel, I.; van der Schaaf, G.; Sietsma, H.; Kok, J. W., Altered sphingolipid metabolism in multidrug-resistant ovarian cancer cells is due to uncoupling of glycolipid biosynthesis in the Golgi apparatus. *Faseb J* **2002,** *16* (7), 1111-+.10.1096/fj.01-0863fje
73. May, G. L.; Wright, L. C.; Dyne, M.; Mackinnon, W. B.; Fox, R. M.; Mountford, C. E., Plasma membrane lipid composition of vinblastine sensitive and resistant human leukaemic lymphoblasts. *Int J Cancer* **1988,** *42* (5), 728-33.10.1002/ijc.2910420517
74. Lee, W. K.; Kolesnick, R. N., Sphingolipid abnormalities in cancer multidrug resistance: Chicken or egg? *Cell Signal* **2017,** *38*, 134-145.10.1016/j.cellsig.2017.06.017
75. Eniafe, J.; Jiang, S., The functional roles of TCA cycle metabolites in cancer. *Oncogene* **2021,** *40* (19), 3351-3363.10.1038/s41388-020-01639-8
76. Poorebrahim, M.; Sadeghi, S.; Ghanbarian, M.; Kalhor, H.; Mehrtash, A.; Teimoori-Toolabi, L., Identification of candidate genes and miRNAs for sensitizing resistant colorectal cancer cells to oxaliplatin and irinotecan. *Cancer Chemother Pharmacol* **2020,** *85* (1), 153-171.10.1007/s00280-019-03975-3
77. Guo, J.; Yu, J.; Peng, F.; Li, J.; Tan, Z.; Chen, Y.; Rao, T.; Wang, Y.; Peng, J.; Zhou, H., In vitro and in vivo analysis of metabolites involved in the TCA cycle and glutamine metabolism associated with cisplatin resistance in human lung cancer. *Expert Rev Proteomics* **2021,** *18* (3), 233-240.10.1080/14789450.2021.1915775
78. Steliou, K.; Perrine, S. P.; Faller, D. V., Lactic Acid in Cancer and Mitochondrial Disease. *Drug Develop Res* **2009,** *70* (7), 499-511.10.1002/ddr.20342
79. Yoo, H. C.; Han, J. M., Amino Acid Metabolism in Cancer Drug Resistance. *Cells-Basel* **2022,** *11* (1).10.3390/cells11010140

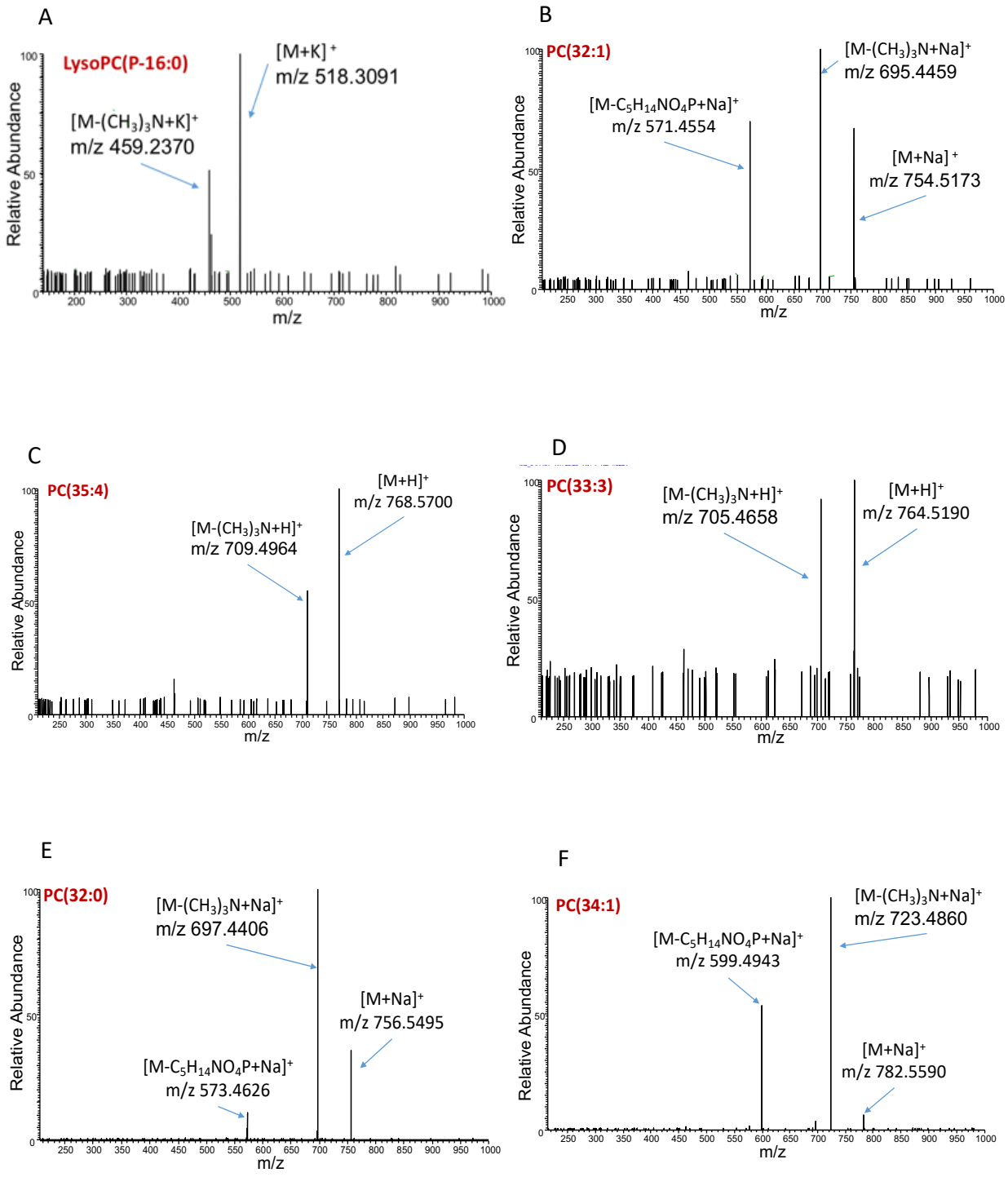
Appendix I: Support Information of Chapter 3

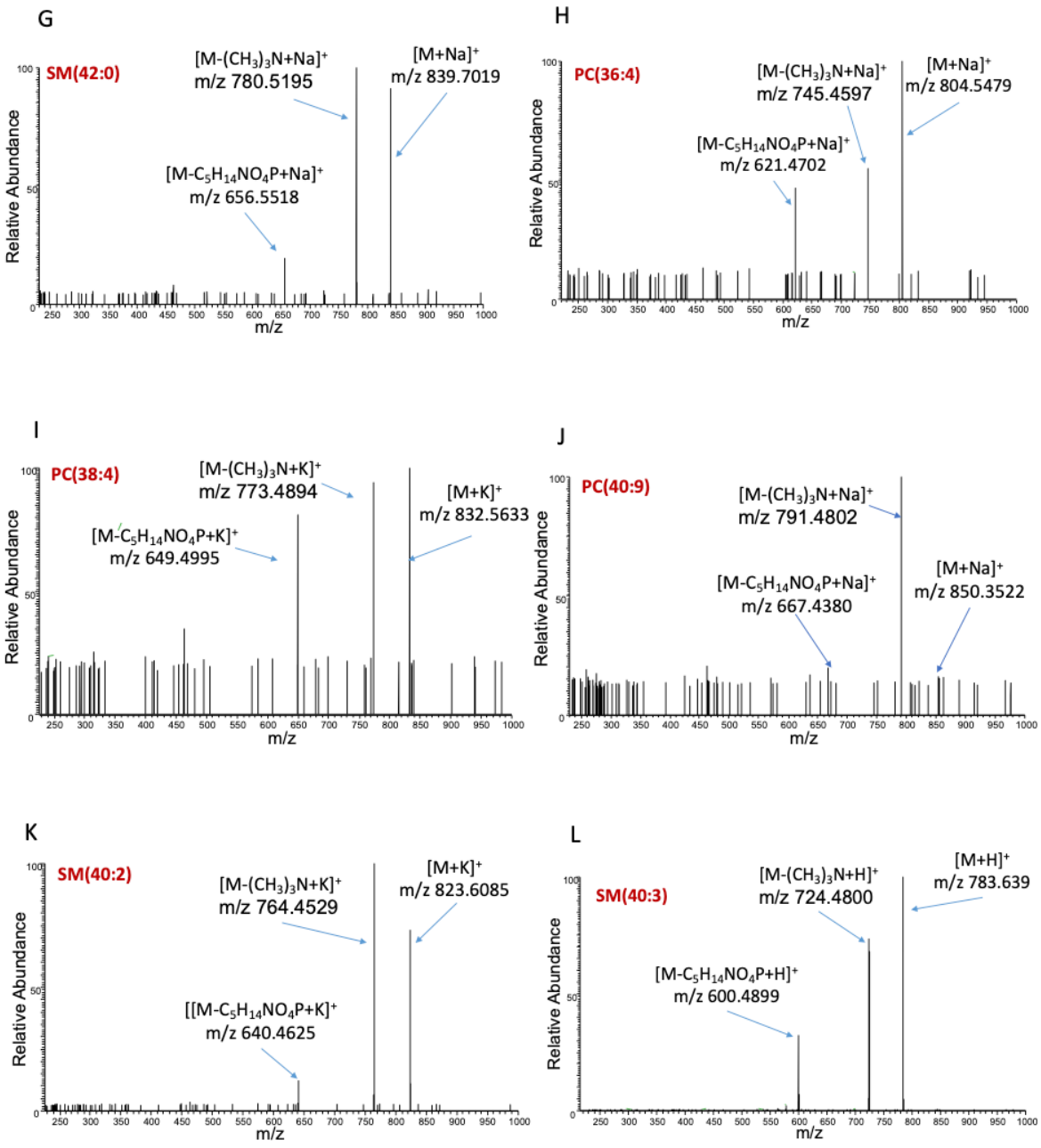


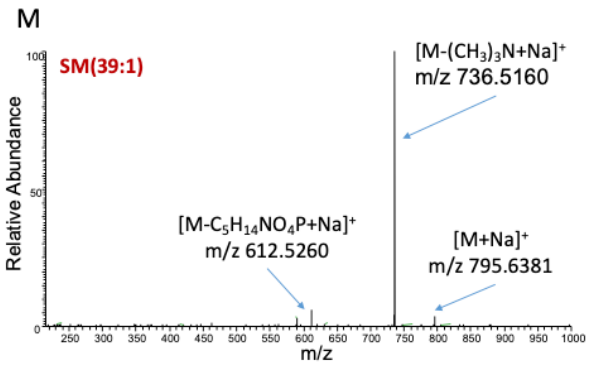
S1. (A) Instrumental setup of the Single-probe SCMS studies. The Single-probe is connected with the solvent-providing capillary through a conductive union, and the sampling solvent is delivered by a syringe pump with controlled flowrate. The ionization voltage is applied on the Single-probe via the conductive union. Single cells are selected and sampled by precisely moving the motorized XYZ-stage system, and the entire process is monitored using a digital stereomicroscope. (B) A typical microscopy image of single cells analysis using the Single-probe device. (C) A sideview of the Single-probe coupled with the mass spectrometer. (D) Image of a fabricated Single-probe, which has a dual-bore quartz tubing, a fused silica capillary, and a nano-ESI.

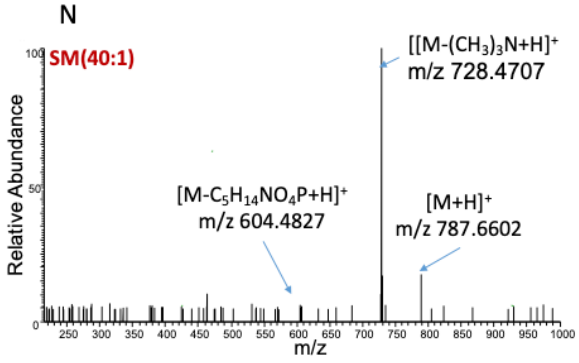


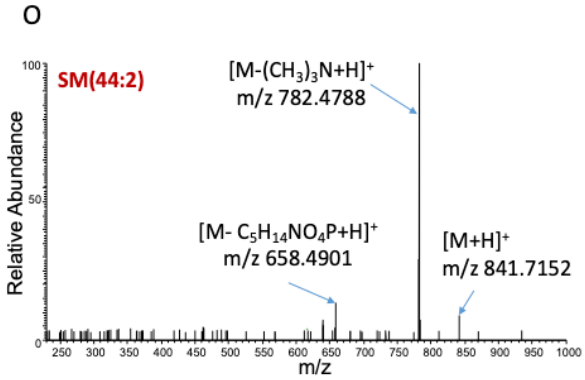
S2. (A) Cell viability measurement of irinotecan (IRI)-resistant cells treated by metformin (MET). (B) Cell viability measurement of IRI-resistant cells treated by IRI. (C) Histogram of combinational index values assessing the degree of synergism: very strong (CI < 0.1), strong (0.1<CI<0.3), and synergism (0.3<CI<0.7).[1-2]

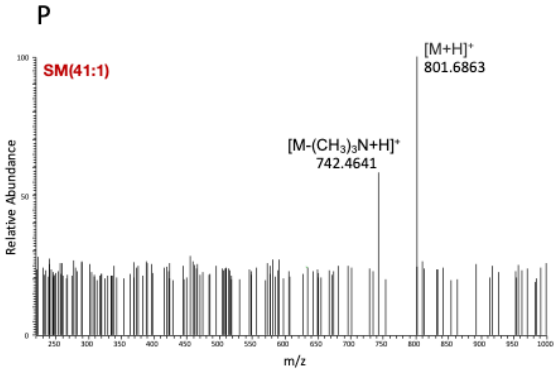

A
LysoPC(P-16:0)
[M+K]+
m/z 518.3091
[M-(CH3)3N+K]+
m/z 459.2370
Relative Abundance
m/z
B
PC(32:1)
[M-(CH3)3N+Na]+
m/z 695.4459
[M-C5H14NO4P+Na]+
m/z 571.4554
[M+Na]+
m/z 754.5173
Relative Abundance
m/z
C
PC(35:4)
[M+H]+
m/z 768.5700
[M-(CH3)3N+H]+
m/z 709.4964
Relative Abundance
m/z
D
PC(33:3)
[M-(CH3)3N+H]+
m/z 705.4658
[M+H]+
m/z 764.5190
Relative Abundance
m/z
E
PC(32:0)
[M-(CH3)3N+Na]+
m/z 697.4406
[M+Na]+
m/z 756.5495
[M-C5H14NO4P+Na]+
m/z 573.4626
Relative Abundance
m/z
F
PC(34:1)
[M-(CH3)3N+Na]+
m/z 723.4860
[M-C5H14NO4P+Na]+
m/z 599.4943
[M+Na]+
m/z 782.5590
Relative Abundance
m/z

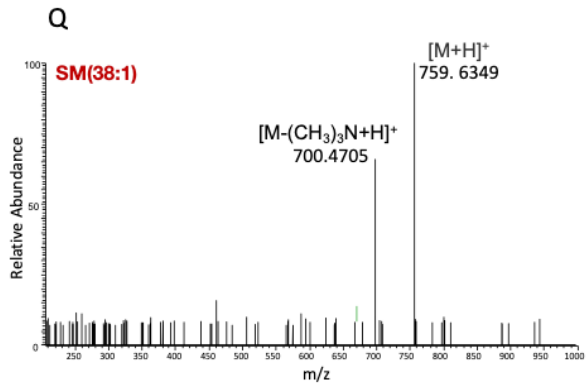

G
SM(42:0)
[M-(CH3)3N+Na]+
m/z 780.5195
[M+Na]+
m/z 839.7019
[M-C5H14NO4P+Na]+
m/z 656.5518
H
PC(36:4)
[M-(CH3)3N+Na]+
m/z 745.4597
[M+Na]+
m/z 804.5479
[M-C5H14NO4P+Na]+
m/z 621.4702
I
PC(38:4)
[M-(CH3)3N+K]+
m/z 773.4894
[M+K]+
m/z 832.5633
[M-C5H14NO4P+K]+
m/z 649.4995
J
PC(40:9)
[M-(CH3)3N+Na]+
m/z 791.4802
[M+Na]+
m/z 850.3522
[M-C5H14NO4P+Na]+
m/z 667.4380
K
SM(40:2)
[M-(CH3)3N+K]+
m/z 764.4529
[M+K]+
m/z 823.6085
[[M-C5H14NO4P+K]+
m/z 640.4625
L
SM(40:3)
[M-(CH3)3N+H]+
m/z 724.4800
[M+H]+
m/z 783.639
[M-C5H14NO4P+H]+
m/z 600.4899
Relative Abundance
m/z

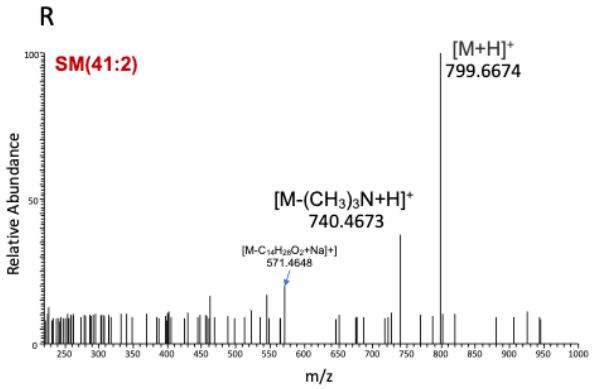

M
SM(39:1)
[M-(CH3)3N+Na]+
m/z 736.5160
[M-C5H14NO4P+Na]+
m/z 612.5260
[M+Na]+
m/z 795.6381
Relative Abundance
m/z


N
SM(40:1)
[[M-(CH3)3N+H]+
m/z 728.4707
[M-C5H14NO4P+H]+
m/z 604.4827
[M+H]+
m/z 787.6602
Relative Abundance
m/z

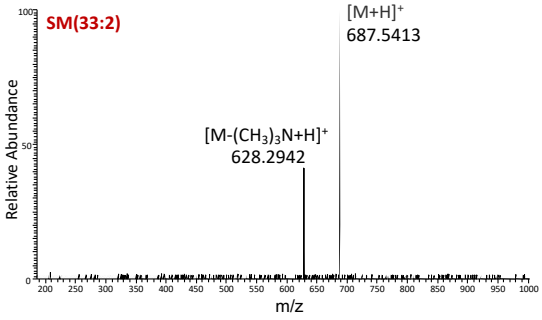

O
SM(44:2)
[M-(CH3)3N+H]+
m/z 782.4788
[M- C5H14NO4P+H]+
m/z 658.4901
[M+H]+
m/z 841.7152
Relative Abundance
m/z


P
SM(41:1)
[M+H]+
801.6863
[M-(CH3)3N+H]+
742.4641
Relative Abundance
m/z

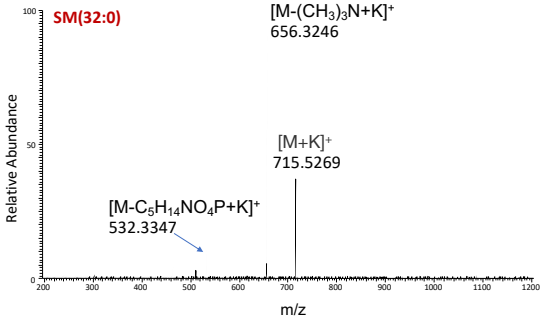

Q
SM(38:1)
[M+H]+
759. 6349
[M-(CH3)3N+H]+
700.4705
Relative Abundance
m/z


R
SM(41:2)
[M+H]+
799.6674
[M-(CH3)3N+H]+
740.4673
[M-C14H28O2+Na]+
571.4648
Relative Abundance
m/z

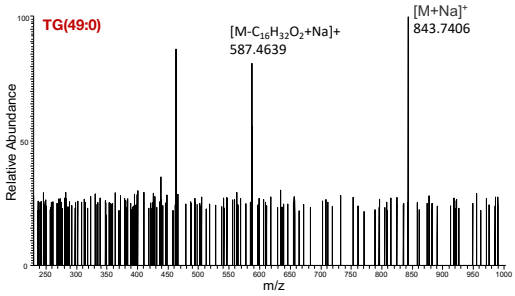
S


SM(33:2)
[M+H]+
687.5413
[M-(CH3)3N+H]+
628.2942
Relative Abundance
m/z

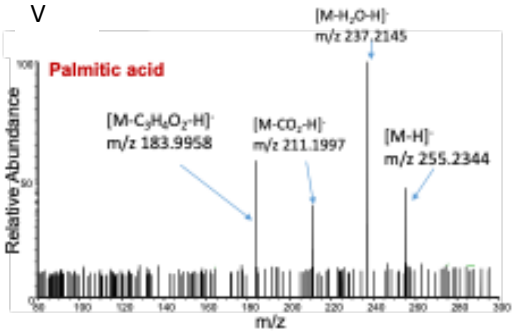
T


SM(32:0)
[M-(CH3)3N+K]+
656.3246
[M+K]+
715.5269
[M-C5H14NO4P+K]+
532.3347
Relative Abundance
m/z

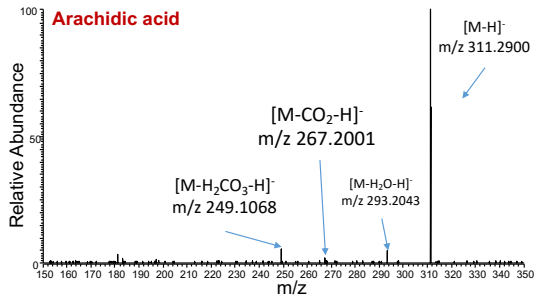
U


TG(49:0)
[M-C16H32O2+Na]+
587.4639
[M+Na]+
843.7406
Relative Abundance
m/z

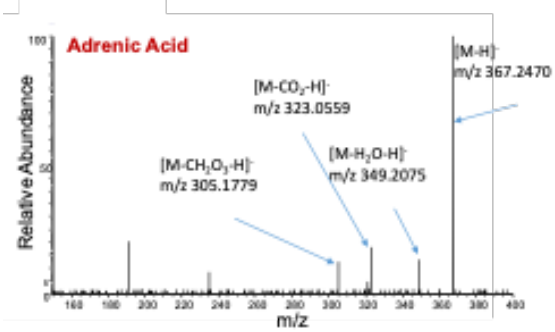
V

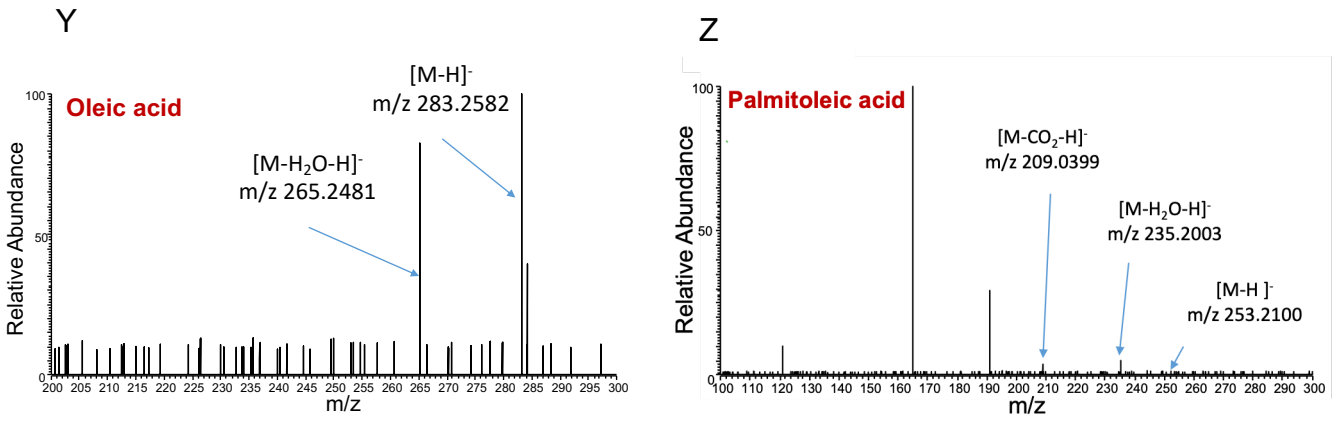

Palmitic acid
[M-H2O-H]-
m/z 237.2145
[M-C3H6O2-H]-
m/z 183.9958
[M-CO2-H]-
m/z 211.1997
[M-H]-
m/z 255.2344
Relative Abundance
m/z

W

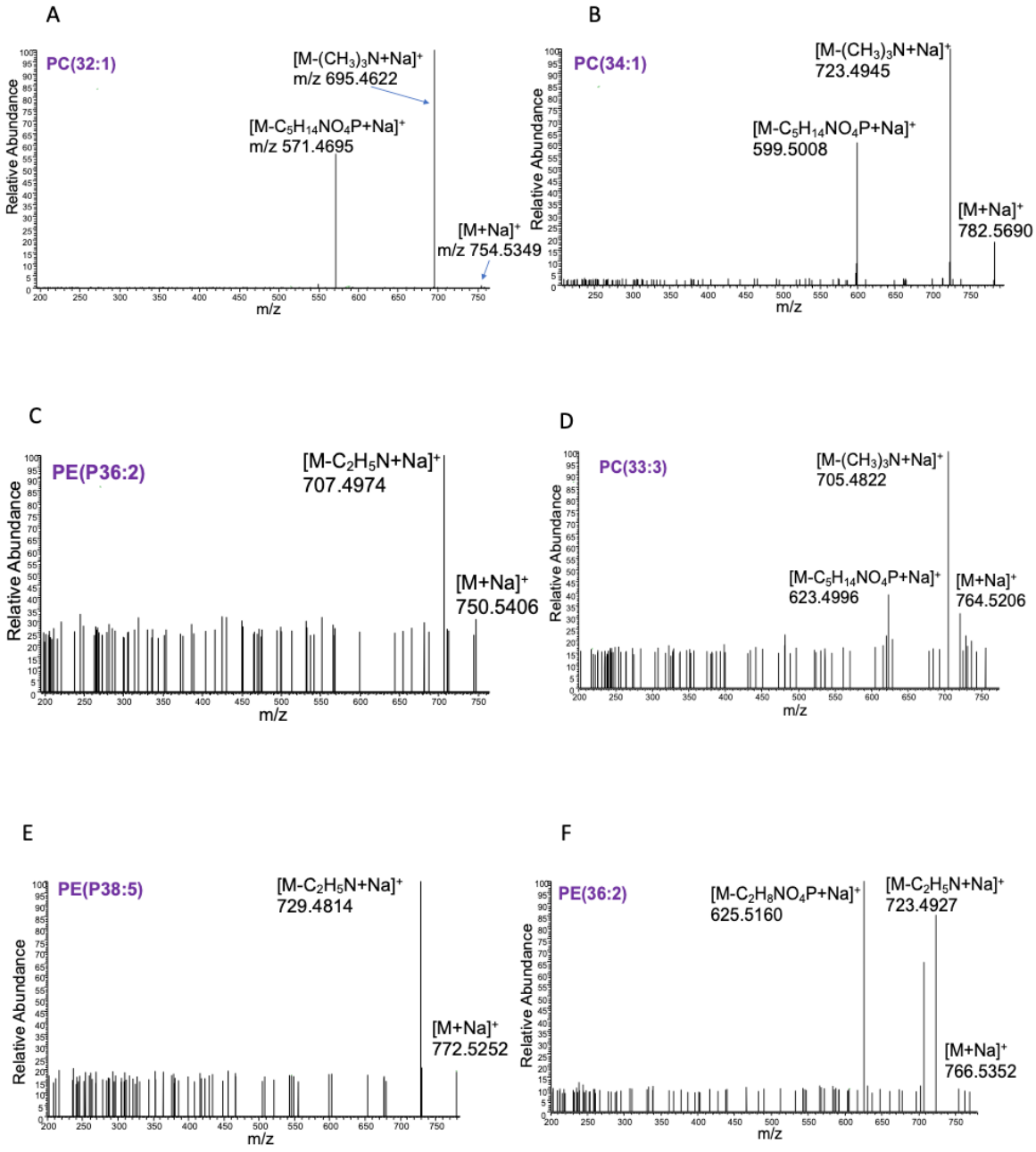

Arachidic acid
[M-H]-
m/z 311.2900
[M-CO2-H]-
m/z 267.2001
[M-H2CO3-H]-
m/z 249.1068
[M-H2O-H]-
m/z 293.2043
Relative Abundance
m/z

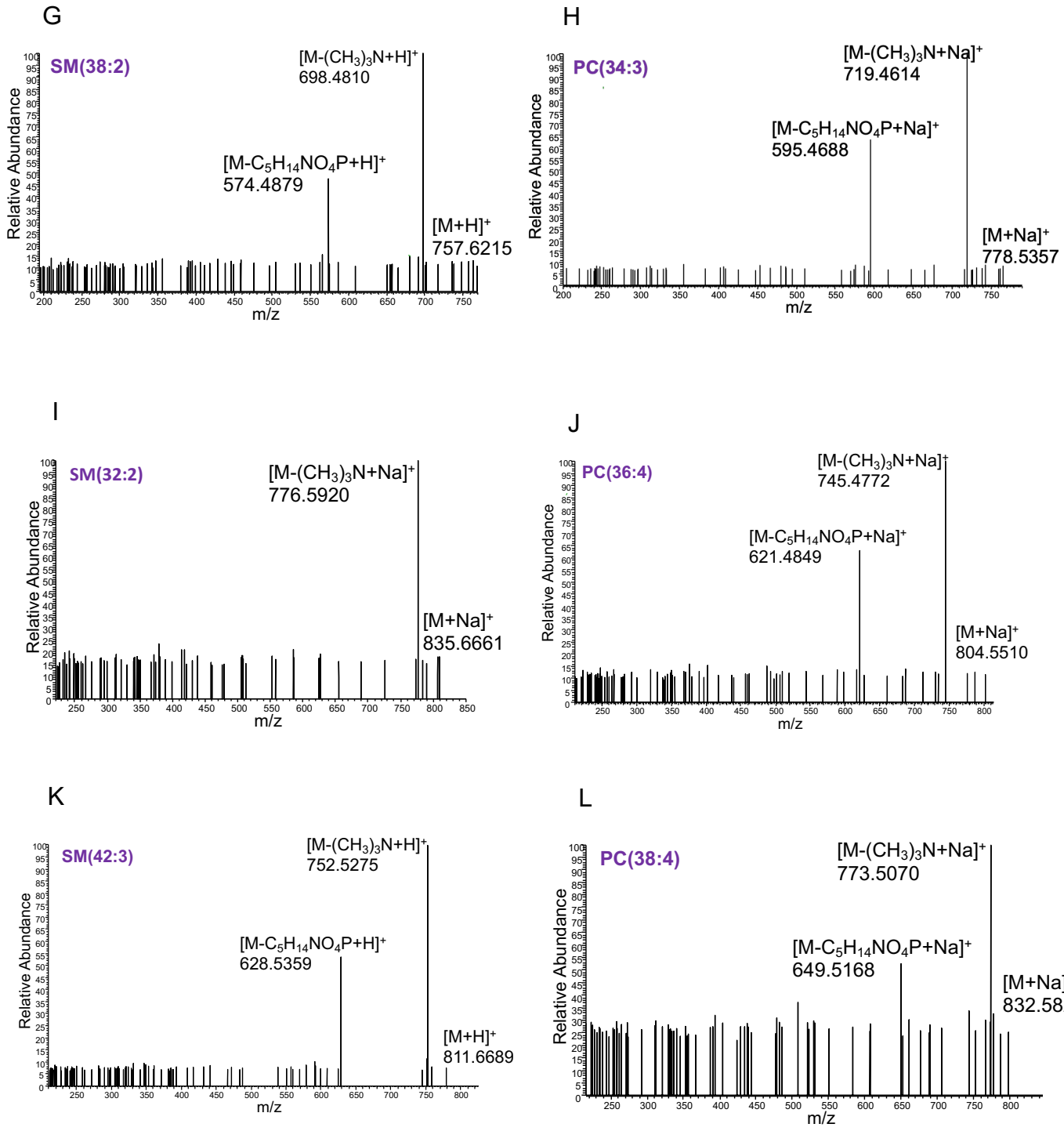
X

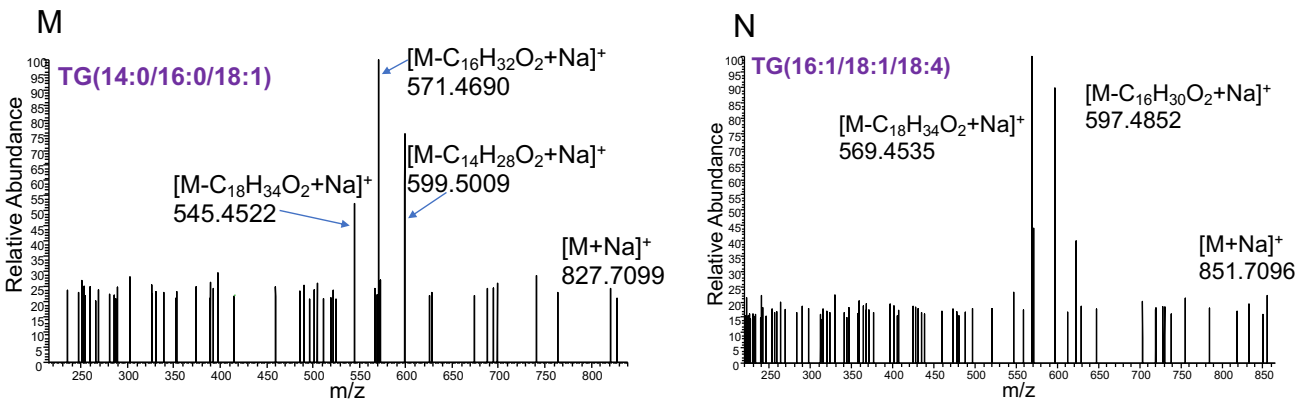

Adrenic Acid
[M-H]-
m/z 367.2470
[M-CO2-H]-
m/z 323.0559
[M-CH2O3-H]-
m/z 305.1779
[M-H2O-H]-
m/z 349.2075
Relative Abundance
m/z



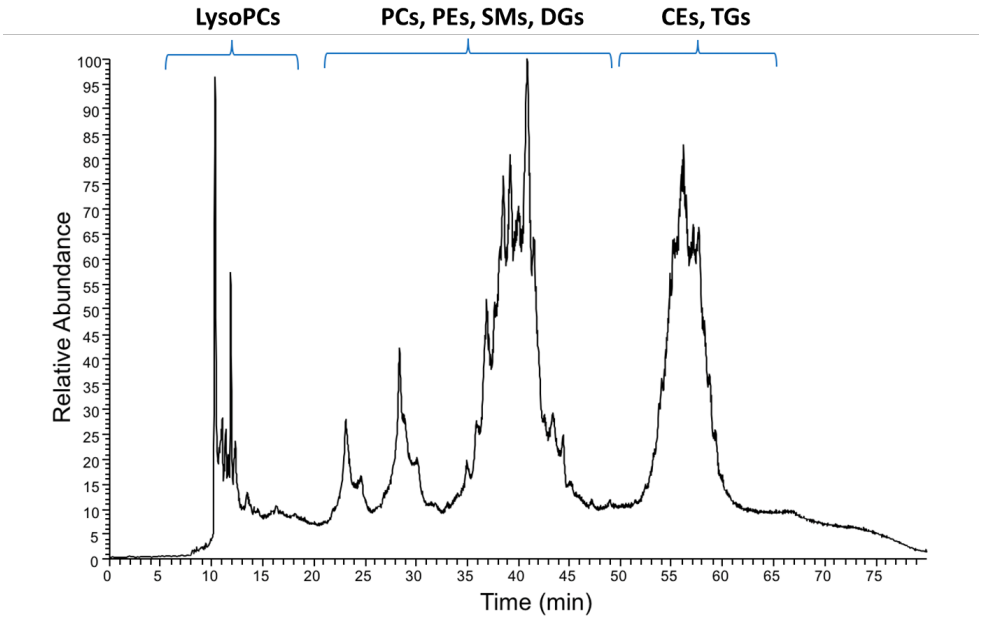
S3. Online MS^2 identification of metabolites in single IRI-resistant cells using the Single-probe SCMS technique. (A) LysoPC(P-16:0), (B) PC(31:1), (C) PC(35:4), (D) PC(33:3), (E) PC(32:0), (F) PC(34:1), (G) SM(42:0), (H) PC(36:4), (I) PC(38:4), (J) PC(40:9), (K) SM(40:2), (L) SM(40:3), (M) SM(39:1), (N) SM(40:1), (O) SM(44:2), (P) SM(41:1) (Q) SM(38:1) (R) SM(41:2) (S) SM(33:2) (T) SM(32:0) (U) TG(49:0) (V) Palmitic acid, (W) Arachidic acid, (X) Adrenic acid, (Y) Oleic acid, and (Z) Palmitoleic acid. (LysoPC: lysophosphatidylcholine; PC: phosphatidylcholine; SM: sphingomyelin; TG: triglyceride).


A
PC(32:1)
[M-(CH3)3N+Na]+
m/z 695.4622
[M-C5H14NO4P+Na]+
m/z 571.4695
[M+Na]+
m/z 754.5349
Relative Abundance
m/z
B
PC(34:1)
[M-(CH3)3N+Na]+
723.4945
[M-C5H14NO4P+Na]+
599.5008
[M+Na]+
782.5690
Relative Abundance
m/z
C
PE(P36:2)
[M-C2H5N+Na]+
707.4974
[M+Na]+
750.5406
Relative Abundance
m/z
D
PC(33:3)
[M-(CH3)3N+Na]+
705.4822
[M-C5H14NO4P+Na]+
623.4996
[M+Na]+
764.5206
Relative Abundance
m/z
E
PE(P38:5)
[M-C2H5N+Na]+
729.4814
[M+Na]+
772.5252
Relative Abundance
m/z
F
PE(36:2)
[M-C2H8NO4P+Na]+
625.5160
[M-C2H5N+Na]+
723.4927
[M+Na]+
766.5352
Relative Abundance
m/z


G
SM(38:2)
[M-(CH3)3N+H]+
698.4810
[M-C5H14NO4P+H]+
574.4879
[M+H]+
757.6215
Relative Abundance
m/z
H
PC(34:3)
[M-(CH3)3N+Na]+
719.4614
[M-C5H14NO4P+Na]+
595.4688
[M+Na]+
778.5357
Relative Abundance
m/z
I
SM(32:2)
[M-(CH3)3N+Na]+
776.5920
[M+Na]+
835.6661
Relative Abundance
m/z
J
PC(36:4)
[M-(CH3)3N+Na]+
745.4772
[M-C5H14NO4P+Na]+
621.4849
[M+Na]+
804.5510
Relative Abundance
m/z
K
SM(42:3)
[M-(CH3)3N+H]+
752.5275
[M-C5H14NO4P+H]+
628.5359
[M+H]+
811.6689
Relative Abundance
m/z
L
PC(38:4)
[M-(CH3)3N+Na]+
773.5070
[M-C5H14NO4P+Na]+
649.5168
[M+Na]+
832.5823
Relative Abundance
m/z



S4. MS^2 identification of ions of interest from cell lysate using HPLC-MS/MS. These ions include (A) PC(32:1), (B) PC(34:1), (C) PE(P36:2), (D) PC(33:3), (E) PE(P38:5), (F) PE(36:2), (G) SM(38:2), (H) PC(34:3), (I) SM(32:2), (J) PC(36:4), (K) SM(42:3), (L) PC(38:4), (M) TG(14:0/16:0/18:1), and (N) TG(16:1/18:1/18:4). (PC: phosphatidylcholine; PE: Phosphatidylethanolamine; SM: sphingomyelin; TG: triglyceride).



S5. Chromatogram of cell lysate in HPLC-MS analysis. (LysoPC: lysophosphatidylcholine; PC: phosphatidylcholine; PE: Phosphatidylethanolamine; SM: sphingomyelin; CE: cholesterol ester; DG: diglyceride; TG: triglyceride).

Reference

1. Chou, T. C., Theoretical basis, experimental design, and computerized simulation of synergism and antagonism in drug combination studies. *Pharmacol Rev* **2006,** *58* (3), 621-681.10.1124/pr.58.3.10

2. Chou, T. C., Preclinical versus clinical drug combination studies. *Leuk Lymphoma* **2008,** *49* (11), 2059-80.10.1080/10428190802353591

Appendix II: Support Information of Chapter 4

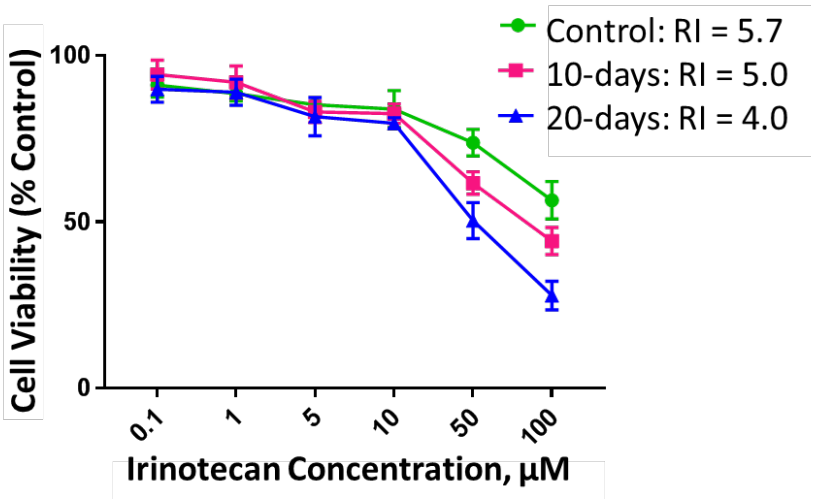


Fig. S1. Cell viability measurements of IRI-HCT116 cells (Control) and IRI-HCT116 cells cultured in drug-free medium for 10 (10-day) and 20 days (20-day). RI (resistant index) was calculated as the ratio of IC_{50} of IRI-HCT116 cells under different conditions to that of the parental HCT116 cells. Data are means ± SD, n = 5.

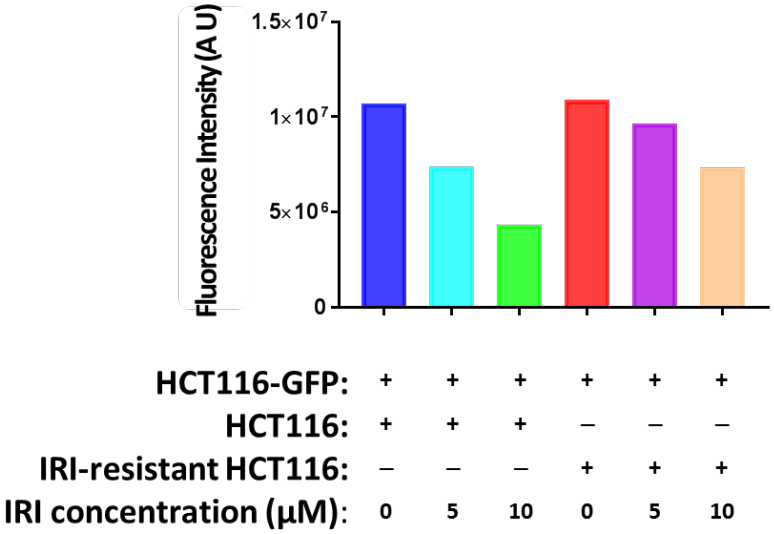


Fig. S2. Quantification of fluorescence intensity (using ImageJ) of HCT116-GFP cells in the co-culture systems (shown in Fig. 3) under different IRI treatment concentrations. HCT116-GFP cells co-cultured with the regular HCT116 cells exhibited lower fluorescence intensity (i.e., lower proliferation) compared with those co-cultured with IRI-HCT116 cells.

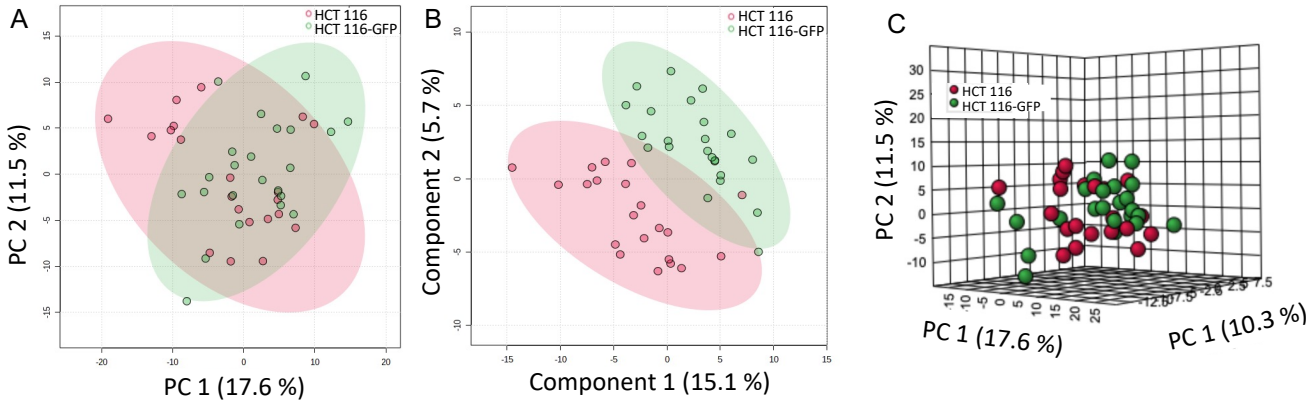


Fig. S3. (A) PCA, (B) PLS-DA of SCMS and (C) 3D PCA results from HCT116 and HCT116-GFP in the mono-culture systems (n = 20 in each group). Both PCA and PLS-DA (p = 0.698) results show that there is no significant difference of metabolic profiles between these two groups of cells.

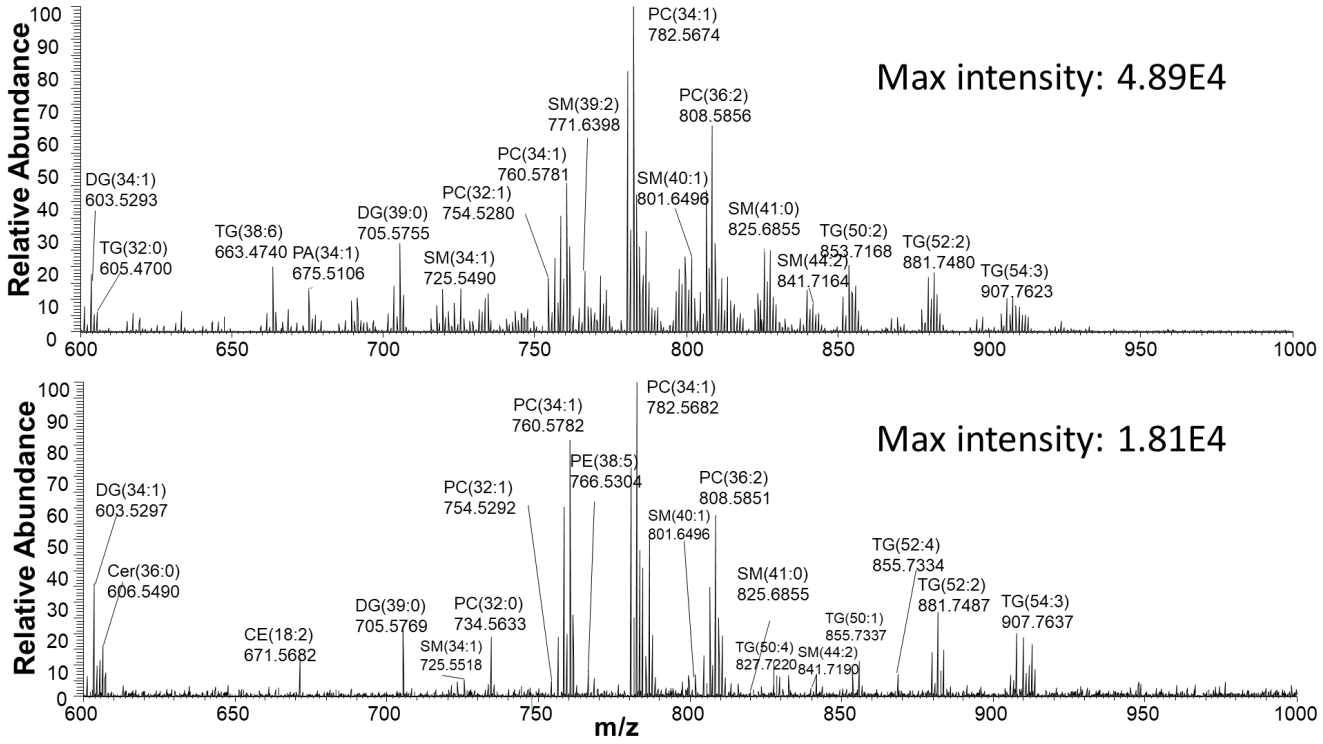


Fig. S4. Typical background-subtracted SCMS spectra of (A) a co-cultured HCT116-GFP cell and (B) a mono-cultured HCT116-GFP cell in positive ion mode. Species are tenatively labeled by searching the measured m/z values through online databases. m/z range from 600 to 1000 was highlighted to compare the SMs lipids expression.

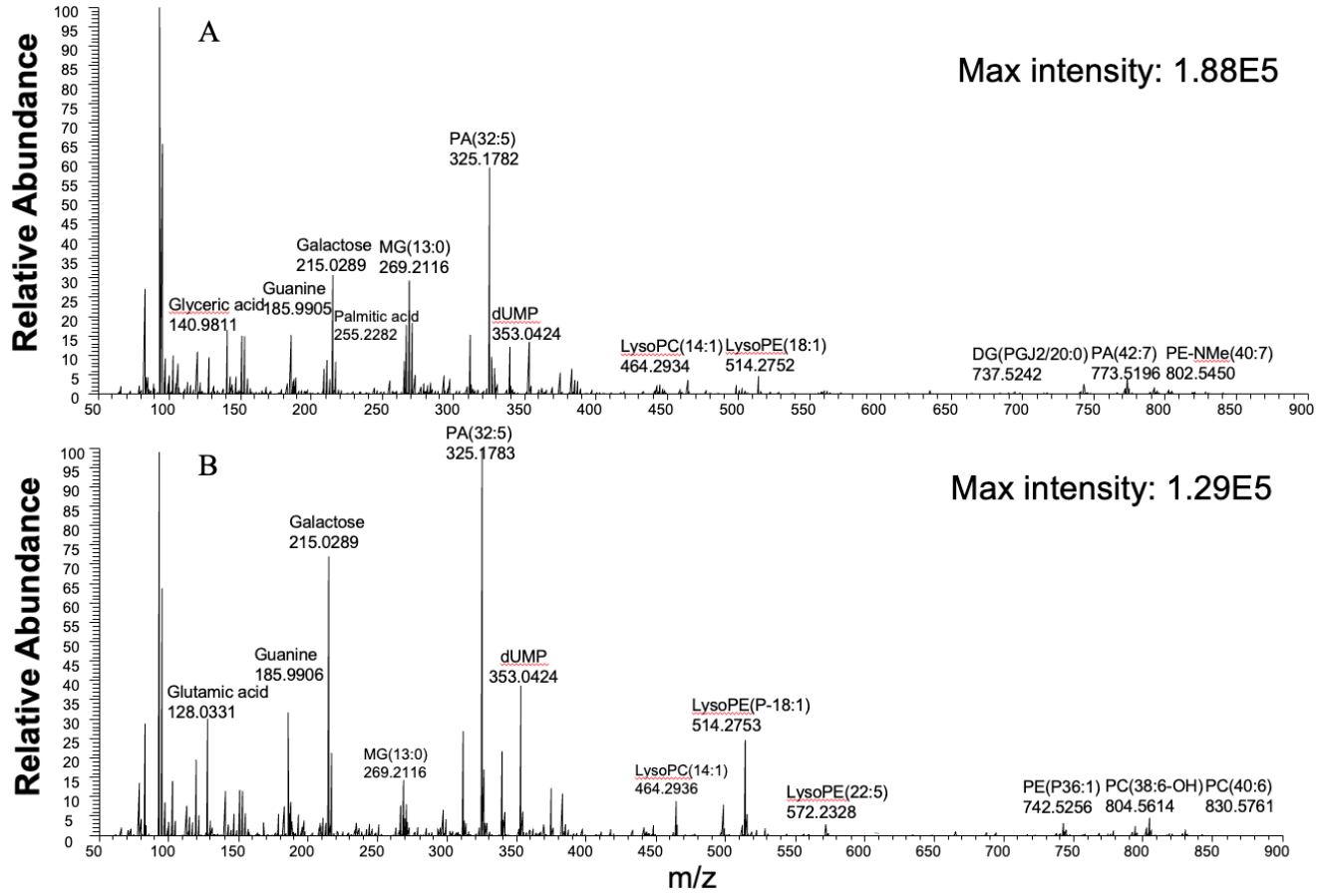


Fig. S5. Typical background-subtracted SCMS spectra of (A) a co-cultured HCT116-GFP cell and (B) a mono-cultured HCT116-GFP cell in negative ion mode. Species are tenatively labeled by searching the measured m/z values through online databases.

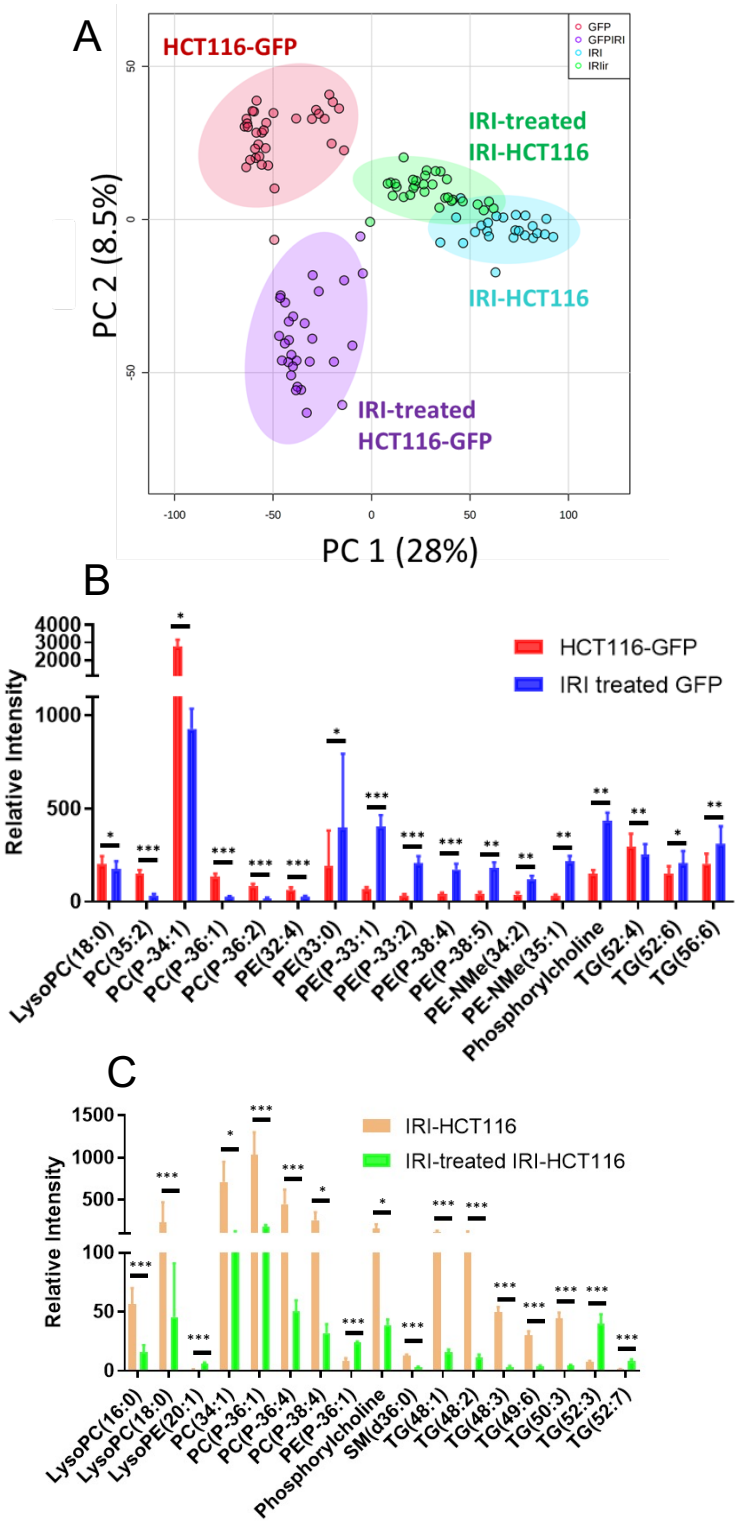
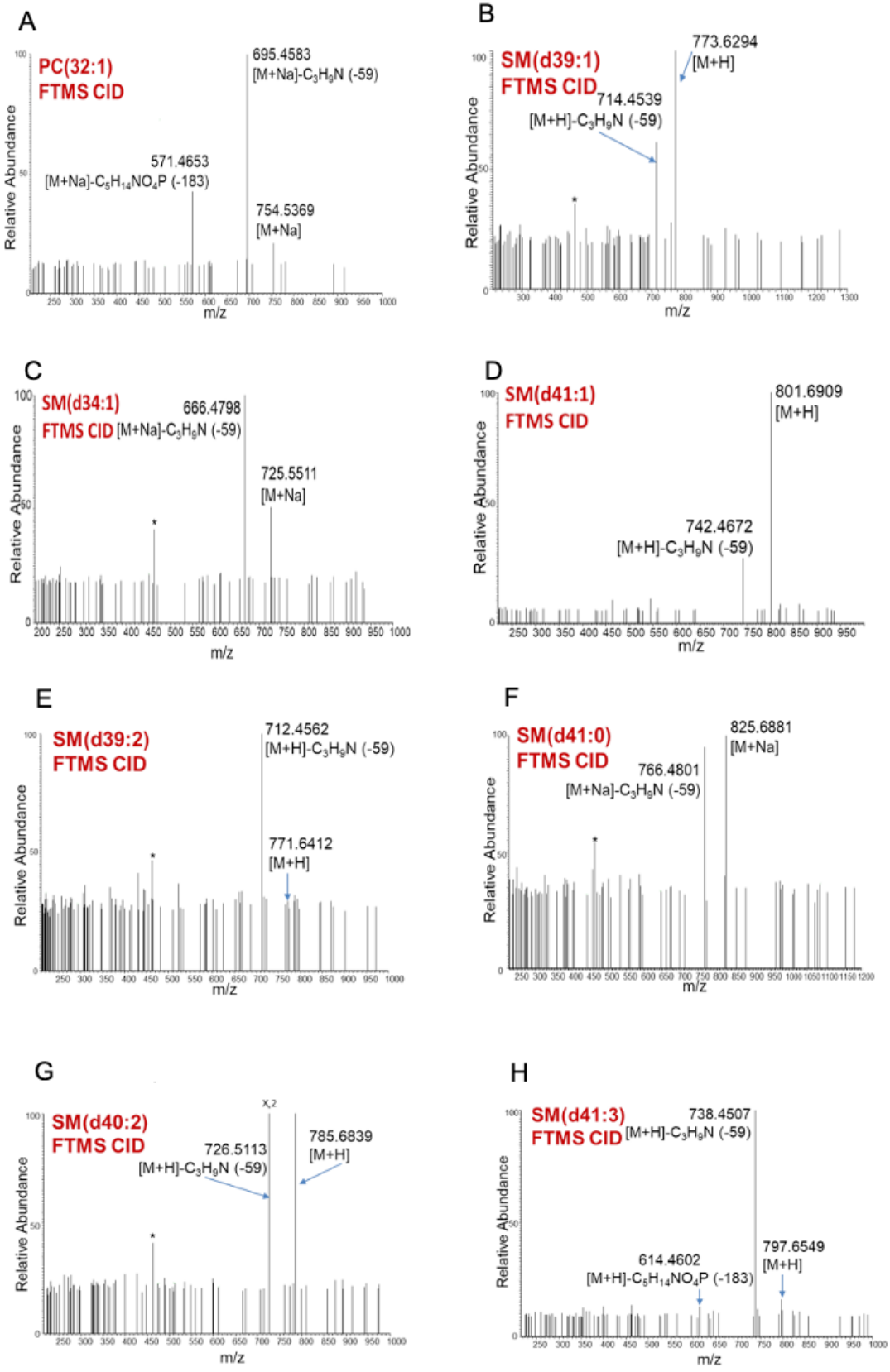


Fig. S6. Influence of IRI treatment on the metablomic profiles of HCT116-GFP (drug-sensitive) and IRI-HCT116 (drug-resistant) cells in mono-culture conditions. (A) PCA results of the SCMS data of cells with and without drug treatment. T-test results showing species with significantly altered abundances in HCT116-GFP (B) and IRI-HCT 116 (C). IRI at IC_{50} (2.9 μM and 16 μM for HCT116-GFP and IRI-resistant cells, respectively) was used for treatment. Experiments were conducted in the positive ion mode (n = 30 in each group). Species were tenatively labeled. (* p<0.05, **p<0.01, ***p<0.005.)


A
PC(32:1)
FTMS CID
695.4583
[M+Na]-C3H9N (-59)
571.4653
[M+Na]-C5H14NO4P (-183)
754.5369
[M+Na]
Relative Abundance
m/z
B
SM(d39:1)
FTMS CID
773.6294
[M+H]
714.4539
[M+H]-C3H9N (-59)
Relative Abundance
m/z
C
SM(d34:1)
FTMS CID
666.4798
[M+Na]-C3H9N (-59)
725.5511
[M+Na]
Relative Abundance
m/z
D
SM(d41:1)
FTMS CID
801.6909
[M+H]
742.4672
[M+H]-C3H9N (-59)
Relative Abundance
m/z
E
SM(d39:2)
FTMS CID
712.4562
[M+H]-C3H9N (-59)
771.6412
[M+H]
Relative Abundance
m/z
F
SM(d41:0)
FTMS CID
825.6881
[M+Na]
766.4801
[M+Na]-C3H9N (-59)
Relative Abundance
m/z
G
SM(d40:2)
FTMS CID
X,2
785.6839
[M+H]
726.5113
[M+H]-C3H9N (-59)
Relative Abundance
m/z
H
SM(d41:3)
FTMS CID
738.4507
[M+H]-C3H9N (-59)
797.6549
[M+H]
614.4602
[M+H]-C5H14NO4P (-183)
Relative Abundance
m/z

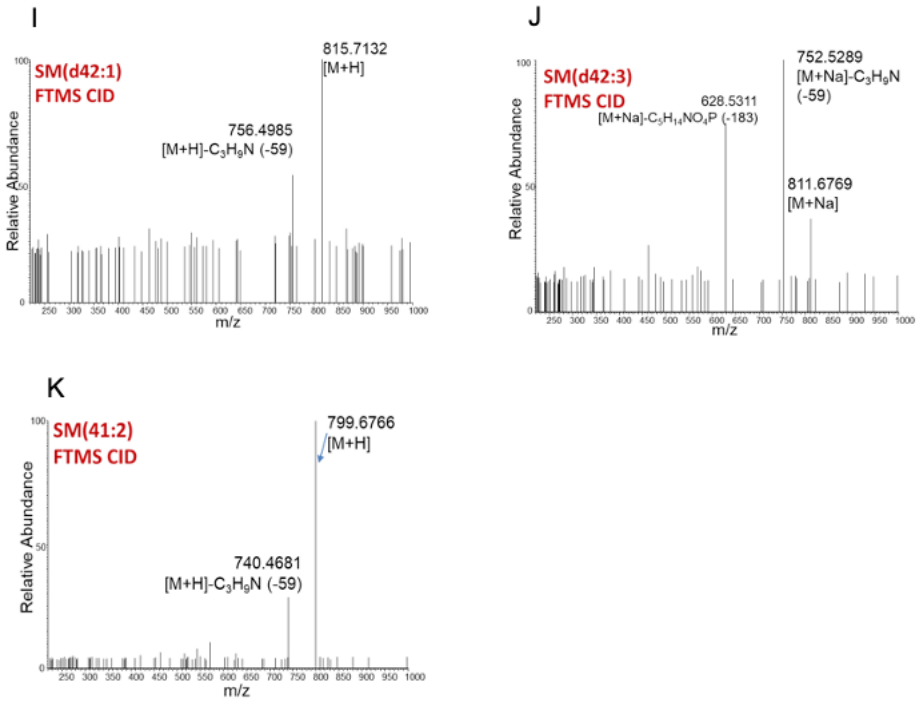
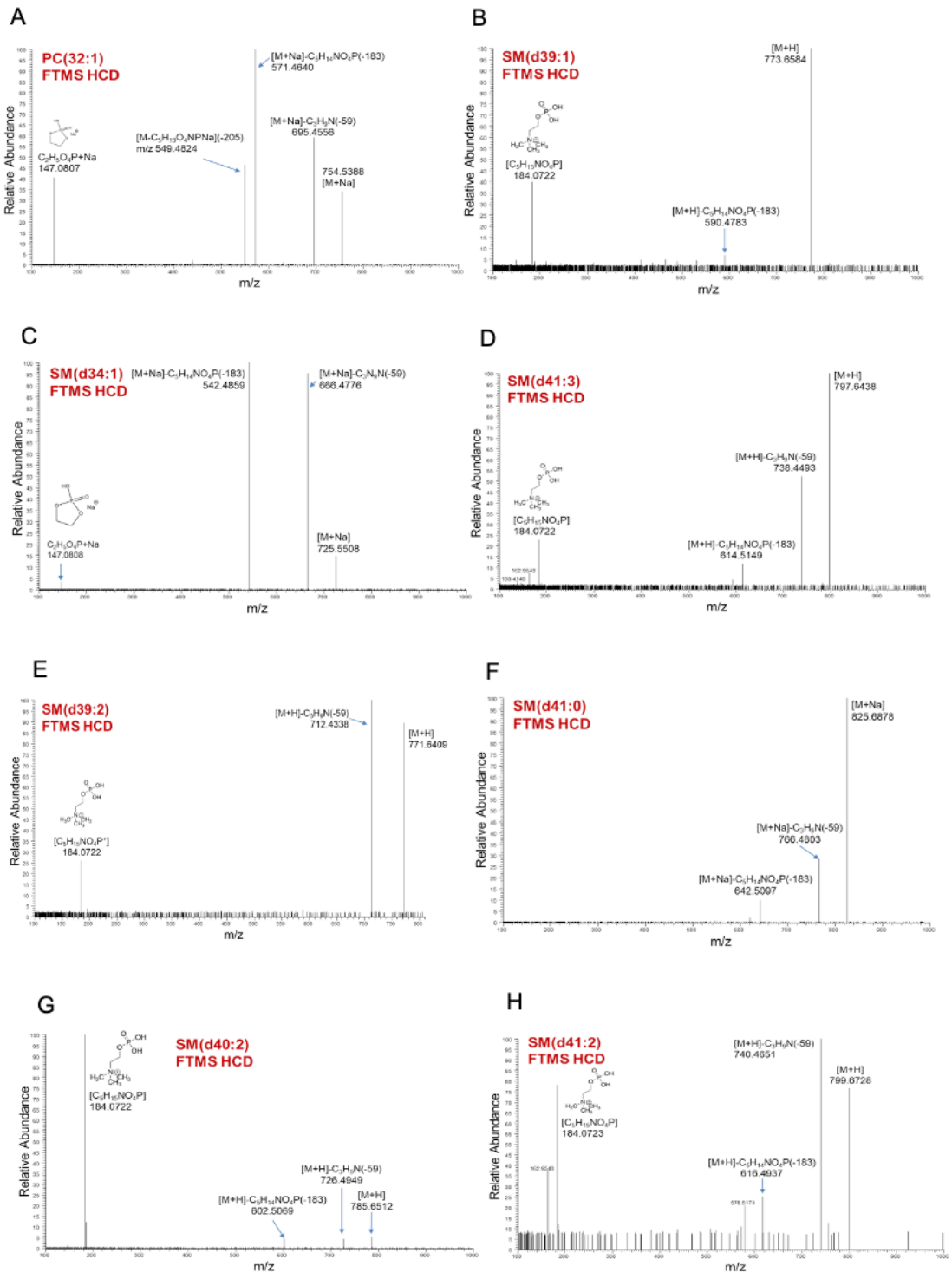


Fig. S7A. MS^2 identification of ions of interest at the single-cell level. The collision-induced dissociation (CID) with orbitrap mass analyzer (FTMS) was used for the MS^2 data collection. (A) PC(32:1), (B) SM(d39:1), (C) SM(d34:1), (D) SM(d41:1), (E) SM(d39:2), (F) SM(d41:0), (G) SM(d40:2), (H) SM(d41:3), (I) SM(d42:1), (J) SM(d42:3), (K) SM(d41:2).


A
PC(32:1)
FTMS HCD
[M+Na]-C5H14NO6P(-183)
571.4640
[M-C5H13O6NPNa](-205)
m/z 549.4824
[M+Na]-C3H9N(-59)
695.4556
754.5388
[M+Na]
C5H15O6P+Na
147.0807
Relative Abundance
m/z
B
SM(d39:1)
FTMS HCD
[M+H]
773.6584
[C5H15NO6P]
184.0722
[M+H]-C5H14NO6P(-183)
590.4783
Relative Abundance
m/z
C
SM(d34:1)
FTMS HCD
[M+Na]-C5H14NO6P(-183)
542.4859
[M+Na]-C3H9N(-59)
668.4776
[M+Na]
725.5508
C5H15O6P+Na
147.0808
Relative Abundance
m/z
D
SM(d41:3)
FTMS HCD
[M+H]
797.6438
[M+H]-C3H9N(-59)
738.4493
[C5H15NO6P]
184.0722
[M+H]-C5H14NO6P(-183)
614.5149
Relative Abundance
m/z
E
SM(d39:2)
FTMS HCD
[M+H]-C3H9N(-59)
712.4338
[M+H]
771.6408
[C5H15NO6P]
184.0722
Relative Abundance
m/z
F
SM(d41:0)
FTMS HCD
[M+Na]
825.6878
[M+Na]-C3H9N(-59)
766.4803
[M+Na]-C5H14NO6P(-183)
642.5097
Relative Abundance
m/z
G
SM(d40:2)
FTMS HCD
[C5H15NO6P]
184.0722
[M+H]-C3H9N(-59)
726.4949
[M+H]-C5H14NO6P(-183)
602.5069
[M+H]
785.6512
Relative Abundance
m/z
H
SM(d41:2)
FTMS HCD
[M+H]-C3H9N(-59)
740.4651
[M+H]
799.6728
[C5H15NO6P]
184.0723
[M+H]-C5H14NO6P(-183)
616.4937
Relative Abundance
m/z

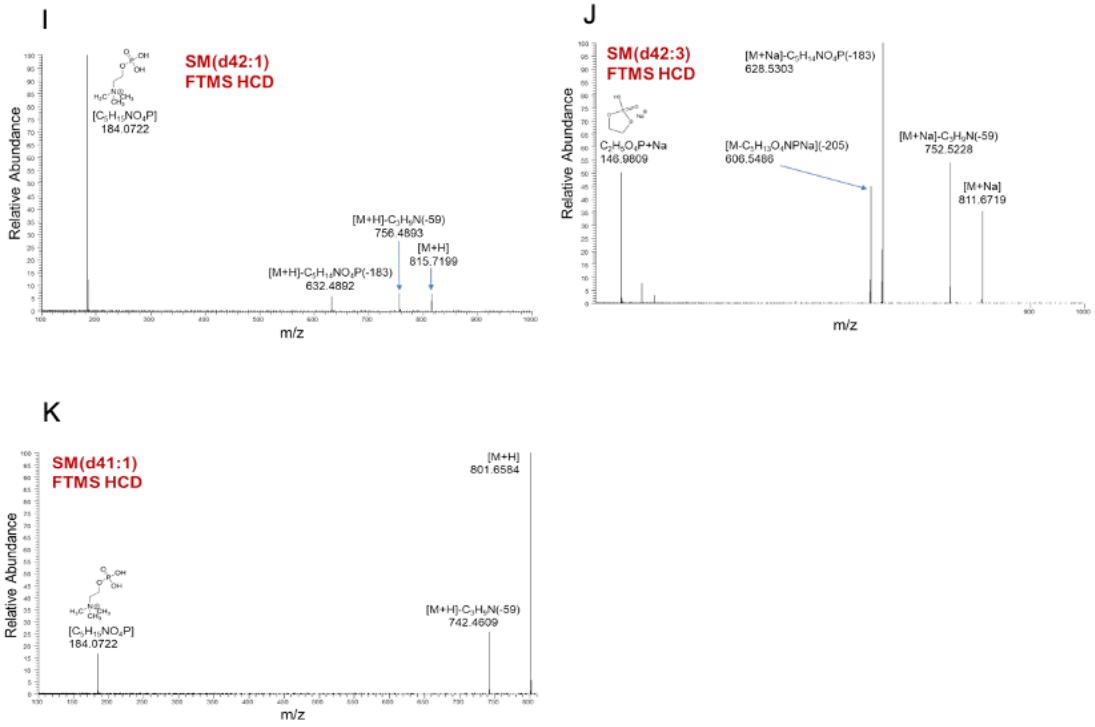


Fig. S7B. MS^2 identification of ions of interest at the single-cell level. The higher energy collision dissociation (HCD) with orbitrap mass analyzer (FTMS) was used for the MS^2 data collection. (A) PC(32:1), (B) SM(d39:1), (C) SM(d34:1), (D) SM(d41:3), (E) SM(d39:2), (F) SM(d41:0), (G) SM(d40:2), (H) SM(d41:2), (I) SM(d42:1), (J) SM(d42:3), and (K) SM(d41:1).

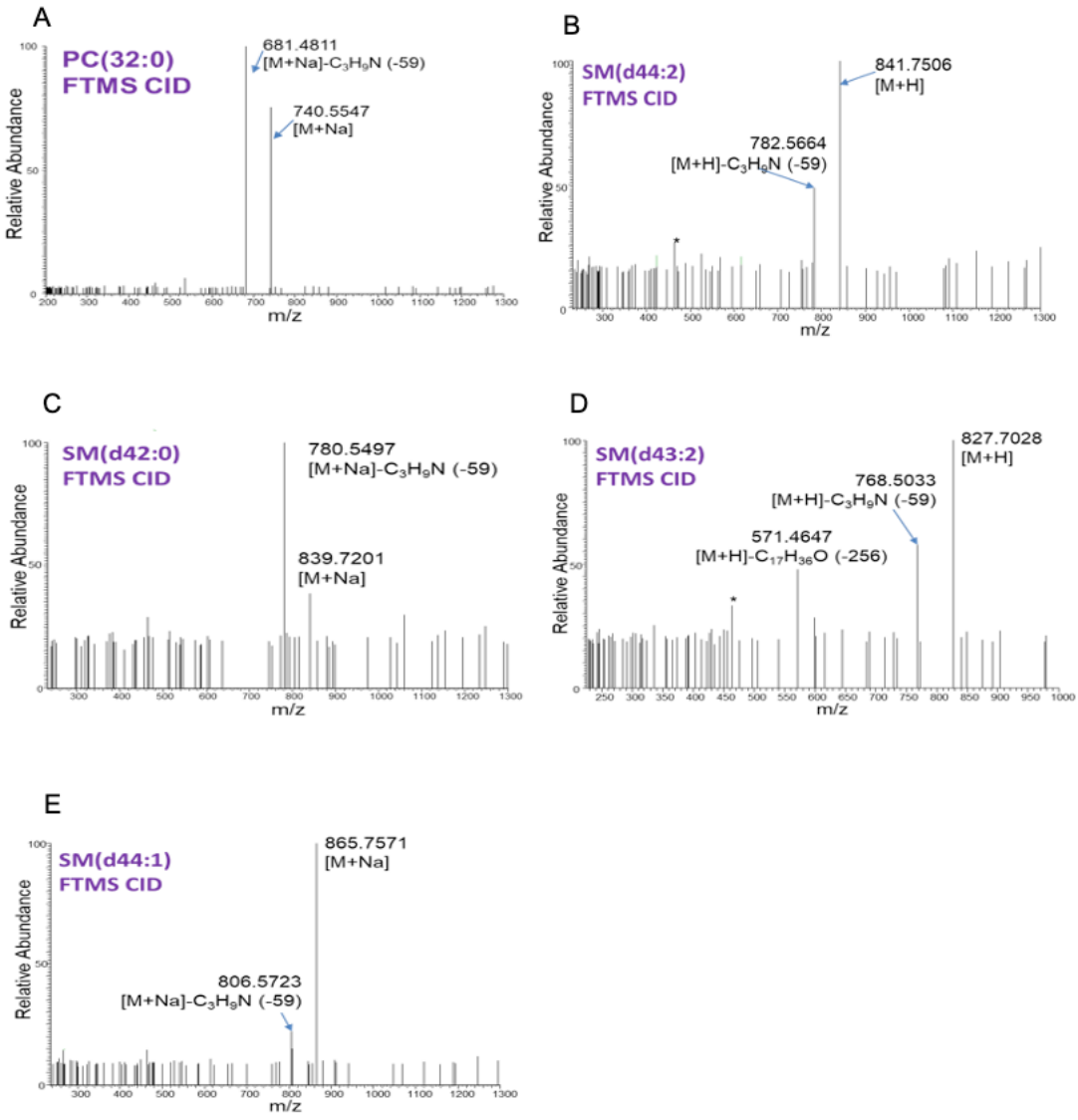


Fig. S8A. MS^2 identification of ions of interest from cell lysate using the direct injection method. The collision-induced dissociation (CID) with orbitrap mass analyzer (FTMS) was used for the MS^2 data collection. (A) PC(32:0), (B) SM(d44:2), (C) SM(d42:0), (D) SM(d43:2), and (E) SM(d44:1).

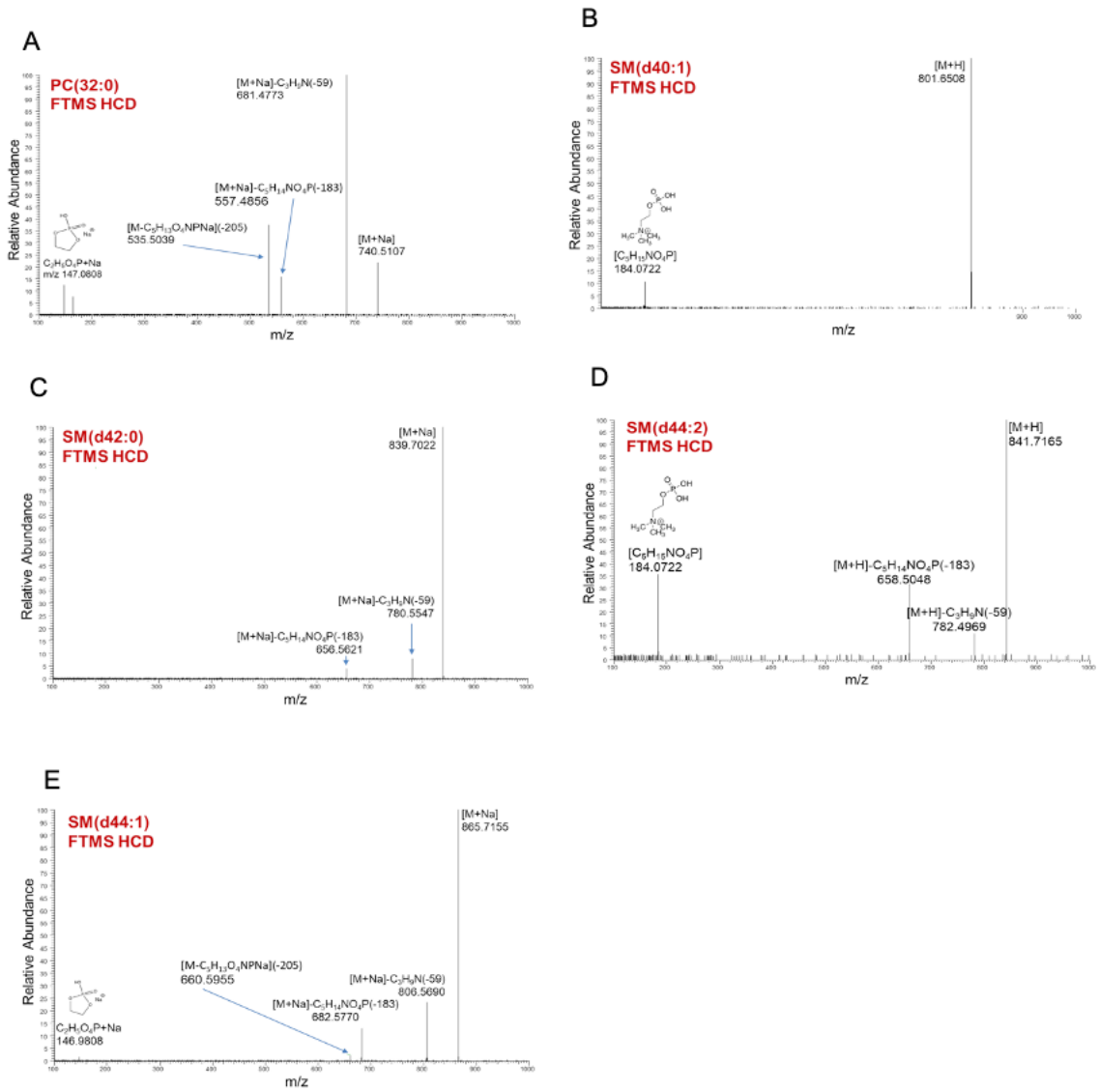
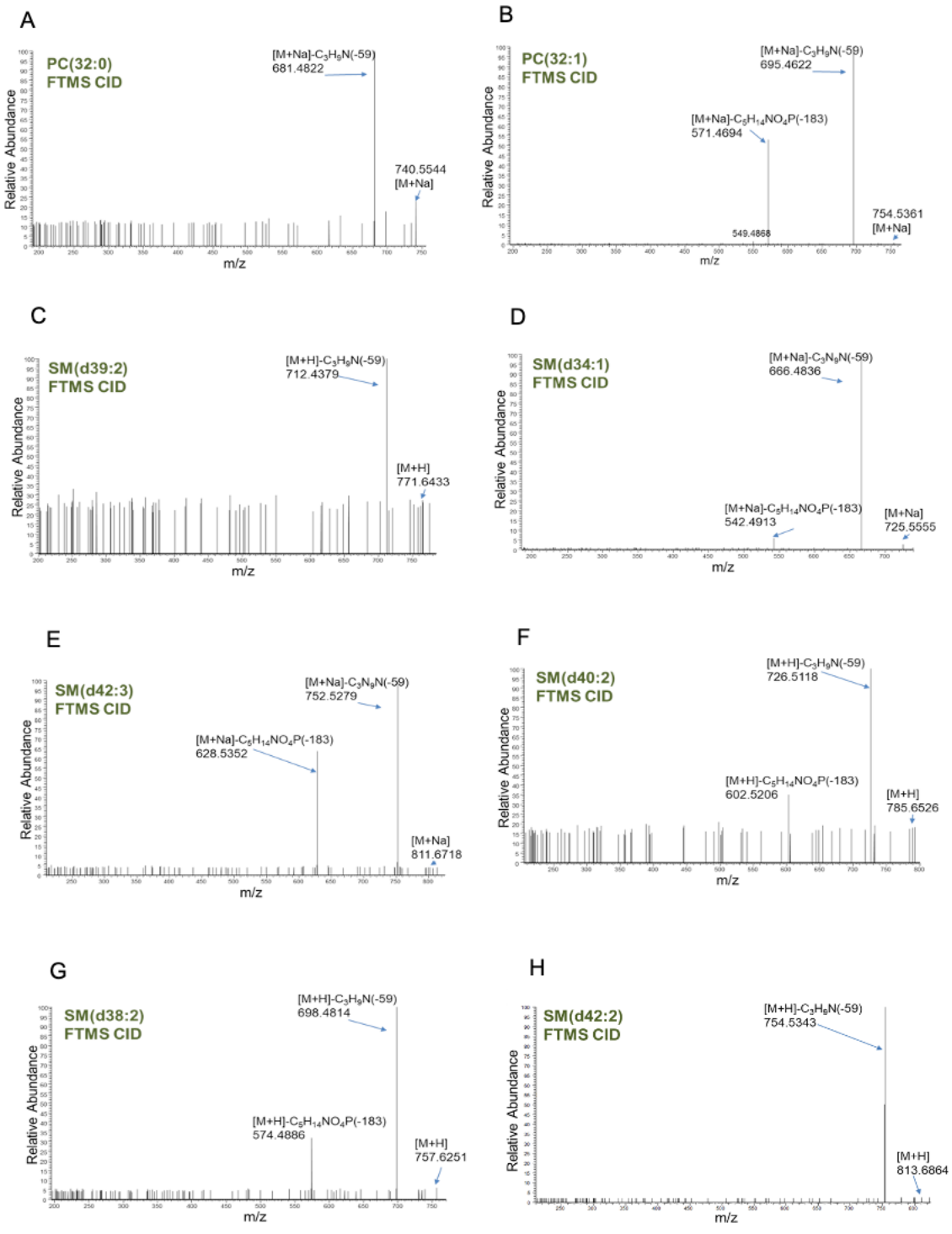


Fig. S8B. MS^2 identification of ions of interest from cell lysate using the direct injection method. The higher energy collision dissociation (HCD) with orbitrap mass analyzer (FTMS) was used for the MS^2 data collection. (A) PC(32:0), (B) SM(d40:1), (C) SM(d42:0), (D) SM(d44:2), and (E) SM(d44:1).


A
PC(32:0)
FTMS CID
[M+Na]-C3H9N(-59)
681.4822
740.5544
[M+Na]
Relative Abundance
m/z
B
PC(32:1)
FTMS CID
[M+Na]-C3H9N(-59)
695.4622
[M+Na]-C5H14NO4P(-183)
571.4694
549.4868
754.5361
[M+Na]
Relative Abundance
m/z
C
SM(d39:2)
FTMS CID
[M+H]-C3H9N(-59)
712.4379
[M+H]
771.6433
Relative Abundance
m/z
D
SM(d34:1)
FTMS CID
[M+Na]-C3H9N(-59)
666.4836
[M+Na]-C5H14NO4P(-183)
542.4913
[M+Na]
725.5555
Relative Abundance
m/z
E
SM(d42:3)
FTMS CID
[M+Na]-C3H9N(-59)
752.5279
[M+Na]-C5H14NO4P(-183)
628.5352
[M+Na]
811.6718
Relative Abundance
m/z
F
SM(d40:2)
FTMS CID
[M+H]-C3H9N(-59)
726.5118
[M+H]-C5H14NO4P(-183)
602.5206
[M+H]
785.6526
Relative Abundance
m/z
G
SM(d38:2)
FTMS CID
[M+H]-C3H9N(-59)
698.4814
[M+H]-C5H14NO4P(-183)
574.4886
[M+H]
757.6251
Relative Abundance
m/z
H
SM(d42:2)
FTMS CID
[M+H]-C3H9N(-59)
754.5343
[M+H]
813.6864
Relative Abundance
m/z

I

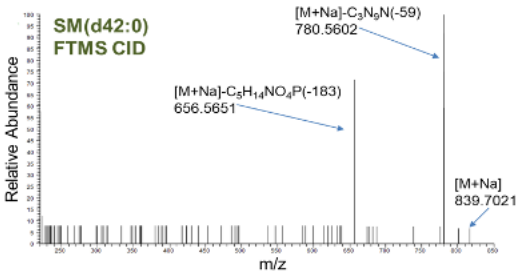


Fig. S9A. MS^2 identification of ions of interest with CID from cell lysate using HPLC-MS/MS. The collision-induced dissociation (CID) with orbitrap mass analyzer (FTMS) was used for the MS^2 data collection. (A) PC(32:0), (B) PC(32:1), (C) SM(d39:2), (D) SM(d34:1), (E) SM(d42:3), (F) SM(d40:2), (G) SM(d38:2), (H) SM(d42:2), (I) SM(d42:0).

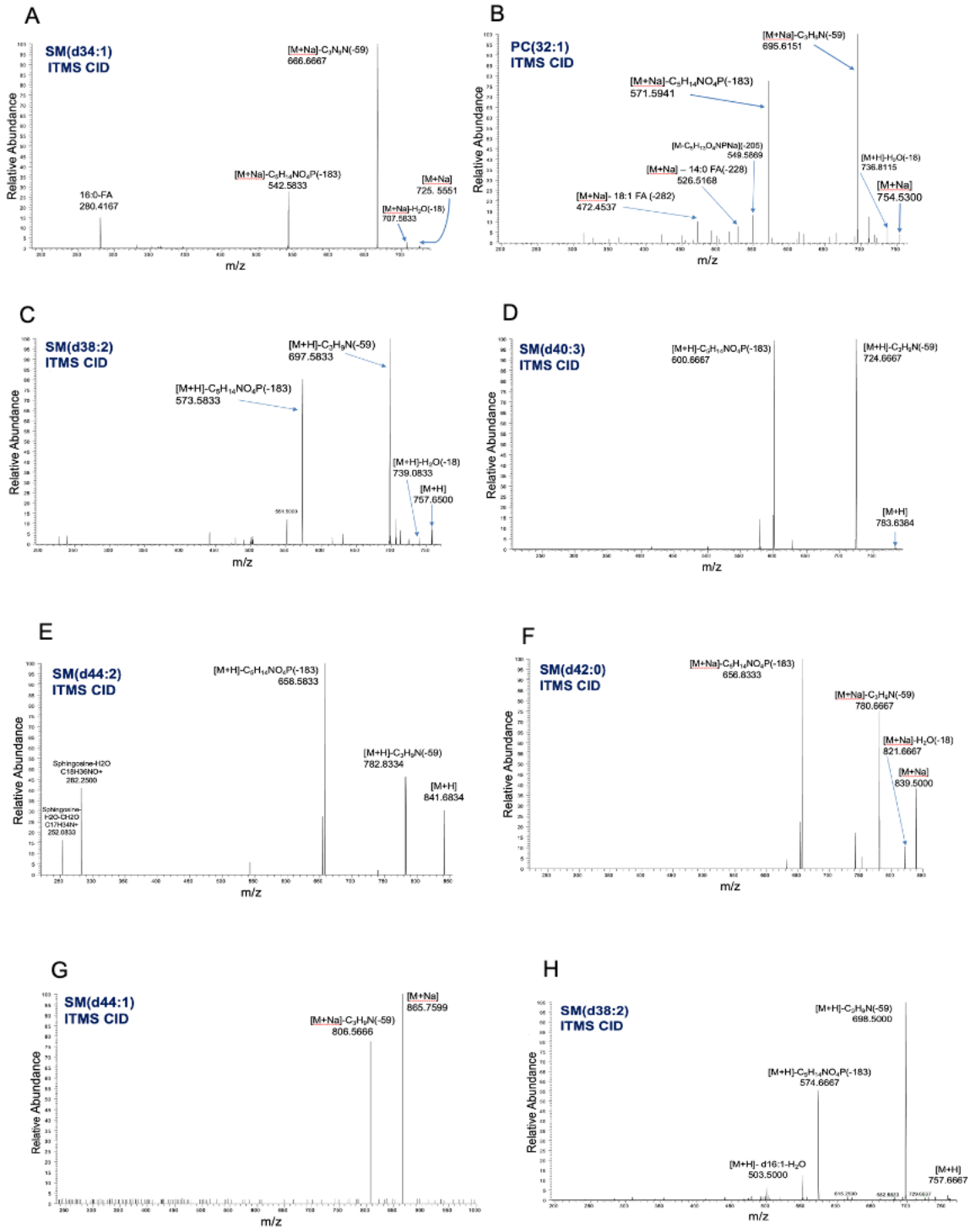


Fig. S9B. MS^2 identification of ions of interest with CID from cell lysate using HPLC-MS/MS. The ion-trap-based collision-induced dissociation (ITMS CID) was used for the MS^2 data collection. (A) SM(d34:1), (B) PC(32:1), (C) SM(d38:2), (D) SM(d40:3), (E) SM(d44:1), (F) SM(d38:2).

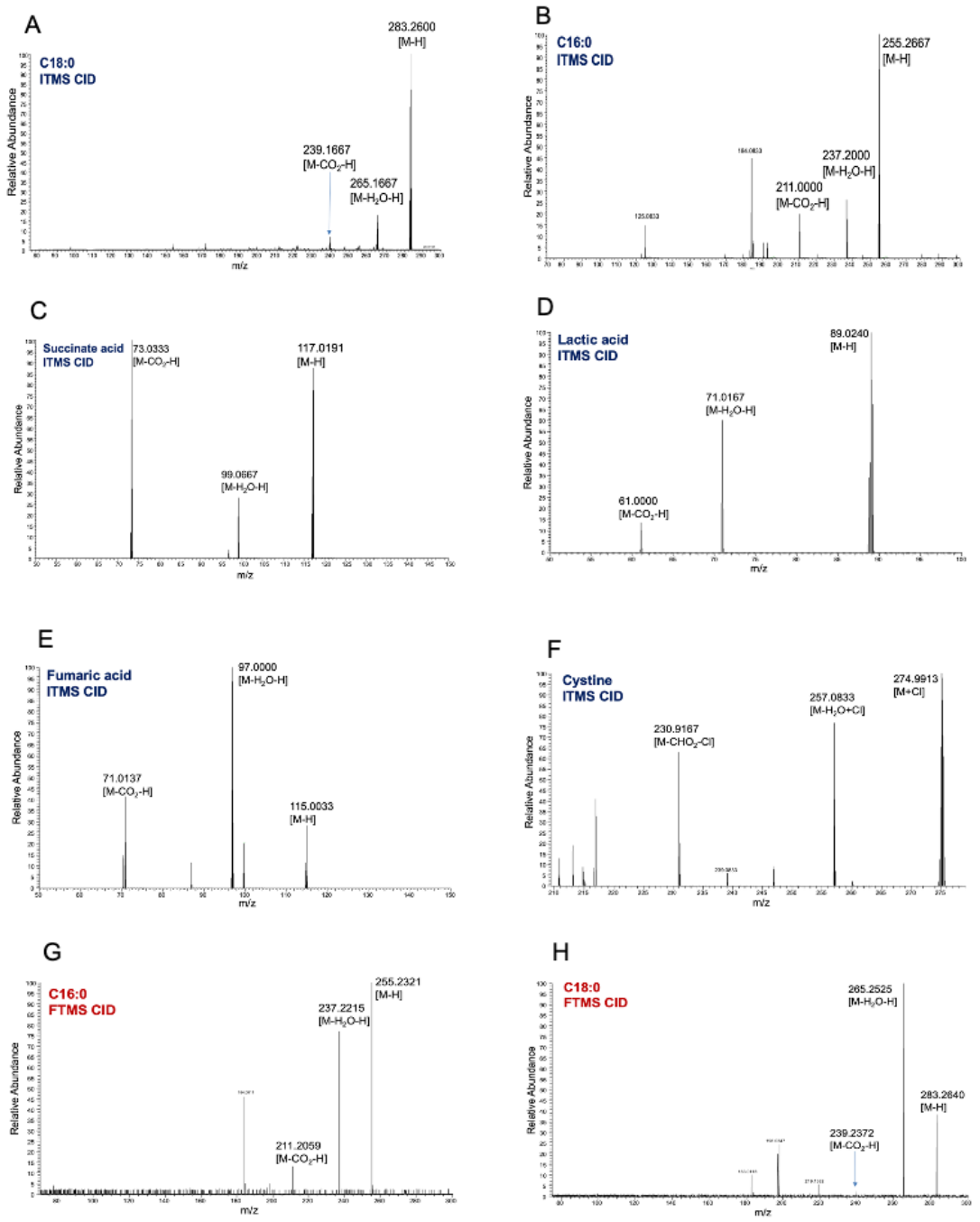


Fig. S10. MS^2 identification of ions of interest with CID from cell lysate in the negative ion mode. The ion-trap-based collision-induced dissociation (ITMS CID) was used for the MS^2 data collection for (A) C18:0, (B) C16:0, (C) Succinate acid, (D) Lactic acid, (E) Fumaric acid, (F) Cystine. The collision-induced dissociation (CID) with orbitrap mass analyzer (FTMS) was used to confirm the structures of (G) C16:0 and (H) C18:0.

Appendix III: Copyrights

Copyrights of Chapter I

ELSEVIER LICENSE
TERMS AND CONDITIONS

Apr 19, 2022

This Agreement between Ms. Xingxiu Chen ("You") and Elsevier ("Elsevier") consists of your license details and the terms and conditions provided by Elsevier and Copyright Clearance Center.

The publisher has provided special terms related to this request that can be found at the end of the Publisher's Terms and Conditions.

License Number	5277770477098
License date	Mar 28, 2022
Licensed Content Publisher	Elsevier
Licensed Content Publication	Elsevier Books
Licensed Content Title	Biosensors for Single-Cell Analysis
Licensed Content Author	Xingxiu Chen,Zhibo Yang
Licensed Content Date	Jan 1, 2022
Licensed Content Pages	34
Start Page	37
End Page	70
Type of Use	reuse in a thesis/dissertation
I am an academic or government institution with a full-text subscription to this journal and the audience of the material consists of students and/or employees of this institute?	No
Portion	full chapter
Circulation	1
Format	electronic
Are you the author of this Elsevier chapter?	Yes
How many pages did you author in this Elsevier book?	34
Will you be translating?	No
Title	Single cell mass spectrometry metabolomics study of drug-resistant cancer cells
Institution name	University of Oklahoma
Expected presentation date	Apr 2022
Requestor Location	Ms. Xingxiu Chen 101 Stephenson Parkway Norman NORMAN, OK 73019 United States Attn: Ms. Xingxiu Chen
Publisher Tax ID	98-0397604
Billing Type	Invoice
Billing Address	Ms. Xingxiu Chen 3117 Ridgecrest Ct Norman NORMAN, OK 73072 United States Attn: Ms. Xingxiu Chen
Total	**0.00 USD**
Terms and Conditions	

Copyright of Fig. 1A

ACS Publications
Most Trusted. Most Cited. Most Read.

Single Cell Profiling Using Ionic Liquid Matrix-Enhanced Secondary Ion Mass Spectrometry for Neuronal Cell Type Differentiation

Author: Thanh D. Do, Troy J. Comi, Sage J. B. Dunham, et al
Publication: Analytical Chemistry
Publisher: American Chemical Society
Date: Mar 1, 2017

Copyright © 2017, American Chemical Society

PERMISSION/LICENSE IS GRANTED FOR YOUR ORDER AT NO CHARGE

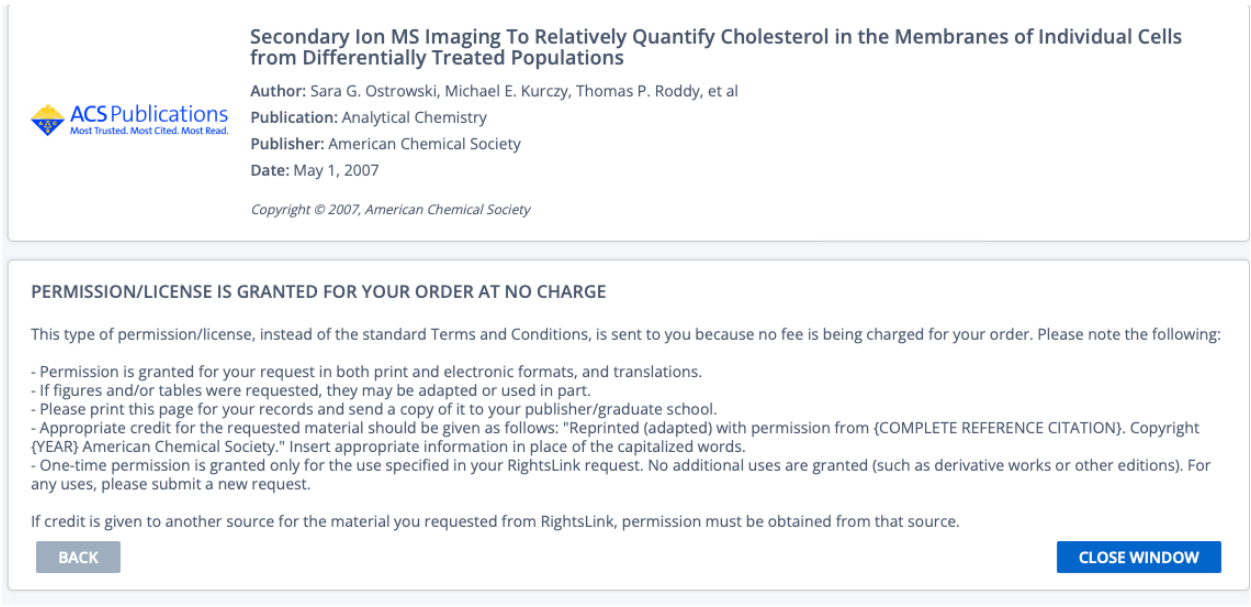
This type of permission/license, instead of the standard Terms and Conditions, is sent to you because no fee is being charged for your order. Please note the following:

- Permission is granted for your request in both print and electronic formats, and translations.
- If figures and/or tables were requested, they may be adapted or used in part.
- Please print this page for your records and send a copy of it to your publisher/graduate school.
- Appropriate credit for the requested material should be given as follows: "Reprinted (adapted) with permission from {COMPLETE REFERENCE CITATION}. Copyright {YEAR} American Chemical Society." Insert appropriate information in place of the capitalized words.
- One-time permission is granted only for the use specified in your RightsLink request. No additional uses are granted (such as derivative works or other editions). For any uses, please submit a new request.

If credit is given to another source for the material you requested from RightsLink, permission must be obtained from that source.

BACK CLOSE WINDOW

Copyright of Fig. 1B



Secondary Ion MS Imaging To Relatively Quantify Cholesterol in the Membranes of Individual Cells from Differentially Treated Populations

Author: Sara G. Ostrowski, Michael E. Kurczy, Thomas P. Roddy, et al
Publication: Analytical Chemistry
Publisher: American Chemical Society
Date: May 1, 2007

Copyright © 2007, American Chemical Society

PERMISSION/LICENSE IS GRANTED FOR YOUR ORDER AT NO CHARGE

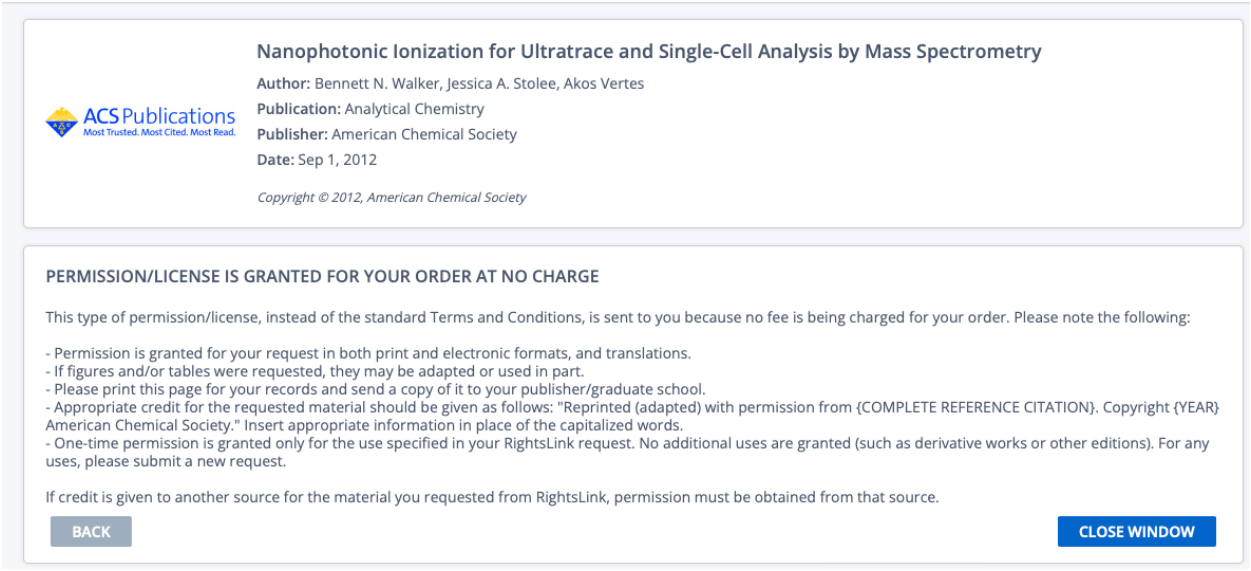
This type of permission/license, instead of the standard Terms and Conditions, is sent to you because no fee is being charged for your order. Please note the following:

- Permission is granted for your request in both print and electronic formats, and translations.
- If figures and/or tables were requested, they may be adapted or used in part.
- Please print this page for your records and send a copy of it to your publisher/graduate school.
- Appropriate credit for the requested material should be given as follows: "Reprinted (adapted) with permission from {COMPLETE REFERENCE CITATION}. Copyright {YEAR} American Chemical Society." Insert appropriate information in place of the capitalized words.
- One-time permission is granted only for the use specified in your RightsLink request. No additional uses are granted (such as derivative works or other editions). For any uses, please submit a new request.

If credit is given to another source for the material you requested from RightsLink, permission must be obtained from that source.

BACK CLOSE WINDOW

Copyright of Fig. 1D



Nanophotonic Ionization for Ultratrace and Single-Cell Analysis by Mass Spectrometry

Author: Bennett N. Walker, Jessica A. Stolee, Akos Vertes
Publication: Analytical Chemistry
Publisher: American Chemical Society
Date: Sep 1, 2012

Copyright © 2012, American Chemical Society

PERMISSION/LICENSE IS GRANTED FOR YOUR ORDER AT NO CHARGE

This type of permission/license, instead of the standard Terms and Conditions, is sent to you because no fee is being charged for your order. Please note the following:

- Permission is granted for your request in both print and electronic formats, and translations.
- If figures and/or tables were requested, they may be adapted or used in part.
- Please print this page for your records and send a copy of it to your publisher/graduate school.
- Appropriate credit for the requested material should be given as follows: "Reprinted (adapted) with permission from {COMPLETE REFERENCE CITATION}. Copyright {YEAR} American Chemical Society." Insert appropriate information in place of the capitalized words.
- One-time permission is granted only for the use specified in your RightsLink request. No additional uses are granted (such as derivative works or other editions). For any uses, please submit a new request.

If credit is given to another source for the material you requested from RightsLink, permission must be obtained from that source.

BACK CLOSE WINDOW

Copyright of Fig. 1C

CCC Marketplace™

This is a License Agreement between Xingxiu Chen ("User") and Copyright Clearance Center, Inc. ("CCC") on behalf of the Rightsholder identified in the order details below. The license consists of the order details, the CCC Terms and Conditions below, and any Rightsholder Terms and Conditions which are included below.

All payments must be made in full to CCC in accordance with the CCC Terms and Conditions below.

Order Date	19-Apr-2022	**Type of Use**	Republish in a thesis/dissertation
Order License ID	1212676-1	**Publisher**	ROYAL SOCIETY OF CHEMISTRY
ISSN	1473-0189	**Portion**	Image/photo/illustration

LICENSED CONTENT

Publication Title	Lab on a chip	**Publication Type**	e-Journal
Article Title	High-density micro-arrays for mass spectrometry.	**Start Page**	3206
		End Page	3209
Author/Editor	Royal Society of Chemistry (Great Britain)	**Issue**	23
Date	12/31/2000	**Volume**	10
Language	English	**URL**	http://www.rsc.org/loc
Country	United Kingdom of Great Britain and Northern Ireland		
Rightsholder	Royal Society of Chemistry		

REQUEST DETAILS

Portion Type	Image/photo/illustration	**Distribution**	Worldwide
Number of images / photos / illustrations	1	**Translation**	Original language of publication
Format (select all that apply)	Electronic	**Copies for the disabled?**	No
Who will republish the content?	Academic institution	**Minor editing privileges?**	No
Duration of Use	Life of current edition	**Incidental promotional use?**	No
Lifetime Unit Quantity	Up to 499	**Currency**	USD
Rights Requested	Main product		

NEW WORK DETAILS

Title	Single Cell Mass Spectrometry Metabolomics Study of Drug-resistant Cells	**Institution name**	University of Oklahoma
		Expected presentation date	2022-05-06
Instructor name	Xingxiu Chen		

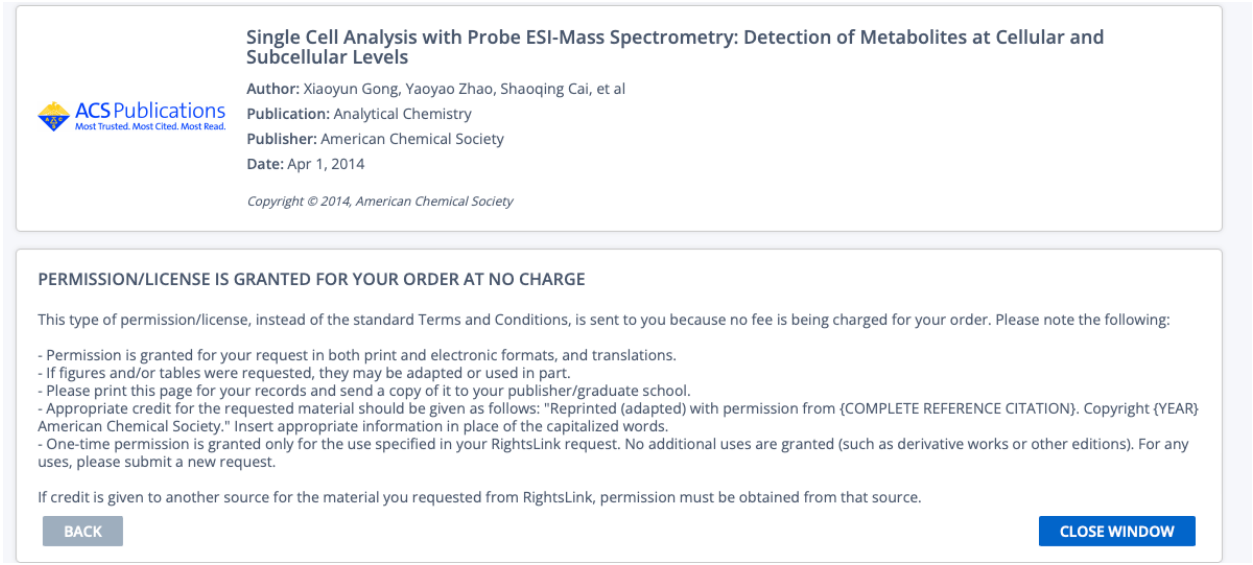
ADDITIONAL DETAILS

Order reference number	N/A	**The requesting person / organization to appear on the license**	Xingxiu Chen

REUSE CONTENT DETAILS

Title, description or numeric reference of the portion(s)	Fig. 1A	**Title of the article/chapter the portion is from**	High-density micro-arrays for mass spectrometry.
Editor of portion(s)	Urban, Pawel L.; Jefimovs, Konstantins; Amantonico, Andrea; Fagerer, Stephan R.; Schmid, Thomas; Mädler, Stefanie; Puigmarti-Luis, Josep; Goedecke, Nils; Zenobi, Renato	**Author of portion(s)**	Urban, Pawel L.; Jefimovs, Konstantins; Amantonico, Andrea; Fagerer, Stephan R.; Schmid, Thomas; Mädler, Stefanie; Puigmarti-Luis, Josep; Goedecke, Nils; Zenobi, Renato
Volume of serial or monograph	10	**Issue, if republishing an article from a serial**	23
Page or page range of portion	3206-3209	**Publication date of portion**	2010-12-06

Copyright of Fig. 2A



Single Cell Analysis with Probe ESI-Mass Spectrometry: Detection of Metabolites at Cellular and Subcellular Levels

Author: Xiaoyun Gong, Yaoyao Zhao, Shaoqing Cai, et al

Publication: Analytical Chemistry

Publisher: American Chemical Society

Date: Apr 1, 2014

Copyright © 2014, American Chemical Society

PERMISSION/LICENSE IS GRANTED FOR YOUR ORDER AT NO CHARGE

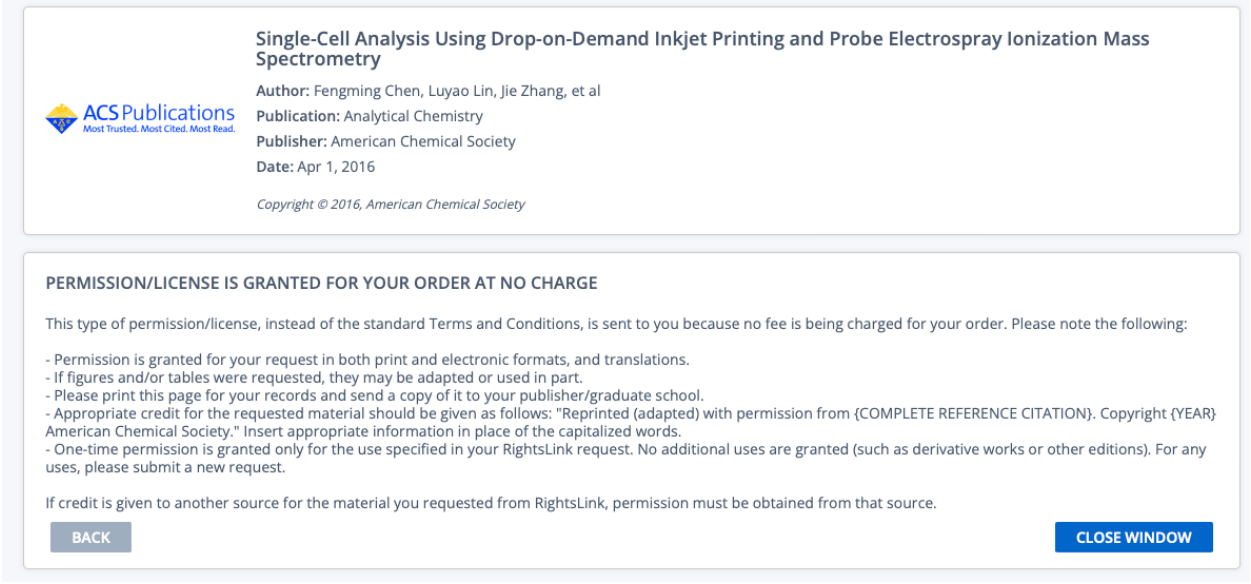
This type of permission/license, instead of the standard Terms and Conditions, is sent to you because no fee is being charged for your order. Please note the following:

- Permission is granted for your request in both print and electronic formats, and translations.
- If figures and/or tables were requested, they may be adapted or used in part.
- Please print this page for your records and send a copy of it to your publisher/graduate school.
- Appropriate credit for the requested material should be given as follows: "Reprinted (adapted) with permission from {COMPLETE REFERENCE CITATION}. Copyright {YEAR} American Chemical Society." Insert appropriate information in place of the capitalized words.
- One-time permission is granted only for the use specified in your RightsLink request. No additional uses are granted (such as derivative works or other editions). For any uses, please submit a new request.

If credit is given to another source for the material you requested from RightsLink, permission must be obtained from that source.

BACK CLOSE WINDOW

Copyright of Fig. 2C



Single-Cell Analysis Using Drop-on-Demand Inkjet Printing and Probe Electrospray Ionization Mass Spectrometry

Author: Fengming Chen, Luyao Lin, Jie Zhang, et al

Publication: Analytical Chemistry

Publisher: American Chemical Society

Date: Apr 1, 2016

Copyright © 2016, American Chemical Society

PERMISSION/LICENSE IS GRANTED FOR YOUR ORDER AT NO CHARGE

This type of permission/license, instead of the standard Terms and Conditions, is sent to you because no fee is being charged for your order. Please note the following:

- Permission is granted for your request in both print and electronic formats, and translations.
- If figures and/or tables were requested, they may be adapted or used in part.
- Please print this page for your records and send a copy of it to your publisher/graduate school.
- Appropriate credit for the requested material should be given as follows: "Reprinted (adapted) with permission from {COMPLETE REFERENCE CITATION}. Copyright {YEAR} American Chemical Society." Insert appropriate information in place of the capitalized words.
- One-time permission is granted only for the use specified in your RightsLink request. No additional uses are granted (such as derivative works or other editions). For any uses, please submit a new request.

If credit is given to another source for the material you requested from RightsLink, permission must be obtained from that source.

BACK CLOSE WINDOW

Copyright of Fig. 2B

Order Date	19-Apr-2022	Type of Use	Republish in a thesis/dissertation
Order License ID	1212678-1	Publisher	Royal Society of Chemistry
ISSN	1364-5528	Portion	Image/photo/illustration

LICENSED CONTENT

Publication Title	analyst online	Publication Type	e-Journal
Article Title	Piezoelectric inkjet assisted rapid electrospray ionization mass spectrometric analysis of metabolites in plant single cells via a direct sampling probe.	Start Page	5734
		End Page	5739
		Issue	22
Author/Editor	Society of Public Analysts (Great Britain), Chemical Society (Great Britain), Society for Analytical Chemistry, Society of Public Analysts (Great Britain), Royal Society of Chemistry (Great Britain)	Volume	139
		URL	http://www.rsc.org/is/journals/current/an...
Date	12/31/1875		
Language	English		
Country	United Kingdom of Great Britain and Northern Ireland		
Rightsholder	Royal Society of Chemistry		

REQUEST DETAILS

Portion Type	Image/photo/illustration	Distribution	Worldwide
Number of images / photos / illustrations	1	Translation	Original language of publication
Format (select all that apply)	Electronic	Copies for the disabled?	No
Who will republish the content?	Academic institution	Minor editing privileges?	No
Duration of Use	Life of current edition	Incidental promotional use?	No
Lifetime Unit Quantity	Up to 499	Currency	USD
Rights Requested	Main product		

NEW WORK DETAILS

Title	Single Cell Mass Spectrometry Metabolomics Study of Drug-resistant Cells	Institution name	University of Oklahoma
		Expected presentation date	2022-05-06
Instructor name	Xingxiu Chen		

ADDITIONAL DETAILS

Order reference number	N/A	The requesting person / organization to appear on the license	Xingxiu Chen / University of Oklahoma

REUSE CONTENT DETAILS

Title, description or numeric reference of the portion(s)	Fig. 2	Title of the article/chapter the portion is from	Piezoelectric inkjet assisted rapid electrospray ionization mass spectrometric analysis of metabolites in plant single cells via a direct sampling probe.
Editor of portion(s)	Yu, Zhan; Chen, Lee Chuin; Ninomiya, Satoshi; Mandal, Mridul Kanti; Hiraoka, Kenzo; Nonami, Hiroshi	Author of portion(s)	Yu, Zhan; Chen, Lee Chuin; Ninomiya, Satoshi; Mandal, Mridul Kanti; Hiraoka, Kenzo; Nonami, Hiroshi
Volume of serial or monograph	139		
Page or page range of portion	5734-5739	Issue, if republishing an article from a serial	22
		Publication date of portion	2014-11-20

Copyright of Fig. 3A

This Agreement between Ms. Xingxiu Chen ("You") and John Wiley and Sons ("John Wiley and Sons") consists of your license details and the terms and conditions provided by John Wiley and Sons and Copyright Clearance Center.

Your confirmation email will contain your order number for future reference.

Printable Details

License Number	5292691095409
License date	Apr 19, 2022

Licensed Content

Licensed Content Publisher	John Wiley and Sons
Licensed Content Publication	Cancer Science
Licensed Content Title	Live single cell mass spectrometry reveals cancer-specific metabolic profiles of circulating tumor cells
Licensed Content Author	Kazufumi Honda, Yoshihiro Shimizu, Tsutomu Masujima, et al
Licensed Content Date	Jan 5, 2019
Licensed Content Volume	110
Licensed Content Issue	2
Licensed Content Pages	10

Order Details

Type of use	Dissertation/Thesis
Requestor type	University/Academic
Format	Electronic
Portion	Figure/table
Number of figures/tables	1
Will you be translating?	No

About Your Work

Title	Single cell mass spectrometry metabolomics study of drug-resistant cancer cells
Institution name	University of Oklahoma
Expected presentation date	Apr 2022

Additional Data

Portions	Fig.1

Requestor Location

Requestor Location	Ms. Xingxiu Chen 3117 Ridgecrest Ct Norman NORMAN, OK 73072 United States Attn: Ms. Xingxiu Chen

Tax Details

Publisher Tax ID	EU826007151

Price

Total	0.00 USD

Copyright of Fig. 3B

Your confirmation email will contain your order number for future reference.

Printable Details

License Number	5292691335117
License date	Apr 19, 2022

Licensed Content

Licensed Content Publisher	Elsevier
Licensed Content Publication	Analytical Biochemistry
Licensed Content Title	Living cell manipulation, manageable sampling, and shotgun picoliter electrospray mass spectrometry for profiling metabolites
Licensed Content Author	Yousef Gholipour,Rosa Erra-Balsells,Kenzo Hiraoka,Hiroshi Nonami
Licensed Content Date	Feb 1, 2013
Licensed Content Volume	433
Licensed Content Issue	1
Licensed Content Pages	9

Order Details

Type of Use	reuse in a thesis/dissertation
Portion	figures/tables/illustrations
Number of figures/tables/illustrations	1
Format	electronic
Are you the author of this Elsevier article?	No
Will you be translating?	No

About Your Work

Title	Single cell mass spectrometry metabolomics study of drug-resistant cancer cells
Institution name	University of Oklahoma
Expected presentation date	Apr 2022

Additional Data

Portions	Fig. 1C

Requestor Location

Requestor Location	Ms. Xingxiu Chen 3117 Ridgecrest Ct Norman NORMAN, OK 73072 United States Attn: Ms. Xingxiu Chen

Tax Details

Publisher Tax ID	98-0397604

Price

Total	0.00 USD

Copyright of Fig. 3C

ACS Publications
Most Trusted. Most Cited. Most Read.

Quantitative Extraction and Mass Spectrometry Analysis at a Single-Cell Level

Author: Ruichuan Yin, Venkateshkumar Prabhakaran, Julia Laskin
Publication: Analytical Chemistry
Publisher: American Chemical Society
Date: Jul 1, 2018

Copyright © 2018, American Chemical Society

PERMISSION/LICENSE IS GRANTED FOR YOUR ORDER AT NO CHARGE

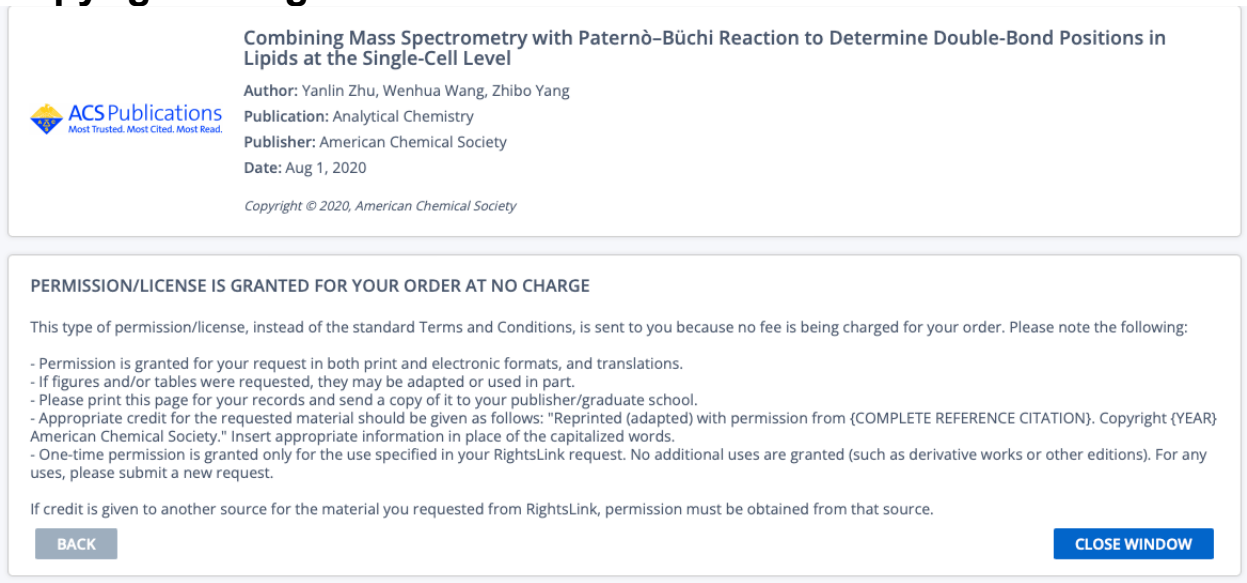
This type of permission/license, instead of the standard Terms and Conditions, is sent to you because no fee is being charged for your order. Please note the following:

- Permission is granted for your request in both print and electronic formats, and translations.
- If figures and/or tables were requested, they may be adapted or used in part.
- Please print this page for your records and send a copy of it to your publisher/graduate school.
- Appropriate credit for the requested material should be given as follows: "Reprinted (adapted) with permission from {COMPLETE REFERENCE CITATION}. Copyright {YEAR} American Chemical Society." Insert appropriate information in place of the capitalized words.
- One-time permission is granted only for the use specified in your RightsLink request. No additional uses are granted (such as derivative works or other editions). For any uses, please submit a new request.

If credit is given to another source for the material you requested from RightsLink, permission must be obtained from that source.

BACK CLOSE WINDOW

Copyright of Fig. 3D



Combining Mass Spectrometry with Paternò–Büchi Reaction to Determine Double-Bond Positions in Lipids at the Single-Cell Level

Author: Yanlin Zhu, Wenhua Wang, Zhibo Yang
Publication: Analytical Chemistry
Publisher: American Chemical Society
Date: Aug 1, 2020

Copyright © 2020, American Chemical Society

PERMISSION/LICENSE IS GRANTED FOR YOUR ORDER AT NO CHARGE

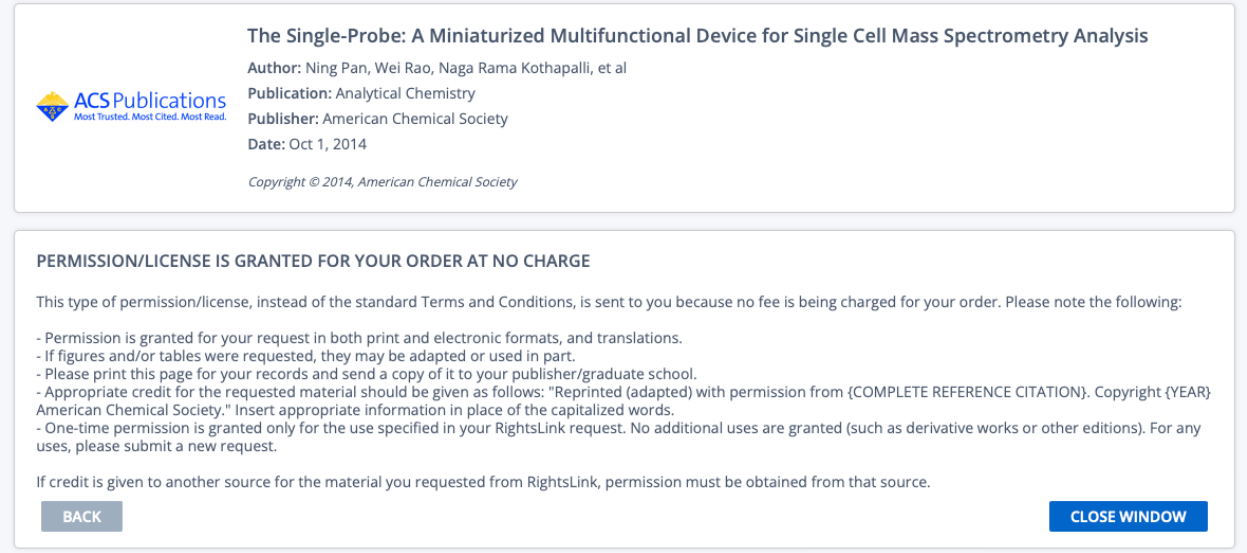
This type of permission/license, instead of the standard Terms and Conditions, is sent to you because no fee is being charged for your order. Please note the following:

- Permission is granted for your request in both print and electronic formats, and translations.
- If figures and/or tables were requested, they may be adapted or used in part.
- Please print this page for your records and send a copy of it to your publisher/graduate school.
- Appropriate credit for the requested material should be given as follows: "Reprinted (adapted) with permission from {COMPLETE REFERENCE CITATION}. Copyright {YEAR} American Chemical Society." Insert appropriate information in place of the capitalized words.
- One-time permission is granted only for the use specified in your RightsLink request. No additional uses are granted (such as derivative works or other editions). For any uses, please submit a new request.

If credit is given to another source for the material you requested from RightsLink, permission must be obtained from that source.

BACK CLOSE WINDOW

Copyright of Fig. 4A



The Single-Probe: A Miniaturized Multifunctional Device for Single Cell Mass Spectrometry Analysis

Author: Ning Pan, Wei Rao, Naga Rama Kothapalli, et al
Publication: Analytical Chemistry
Publisher: American Chemical Society
Date: Oct 1, 2014

Copyright © 2014, American Chemical Society

PERMISSION/LICENSE IS GRANTED FOR YOUR ORDER AT NO CHARGE

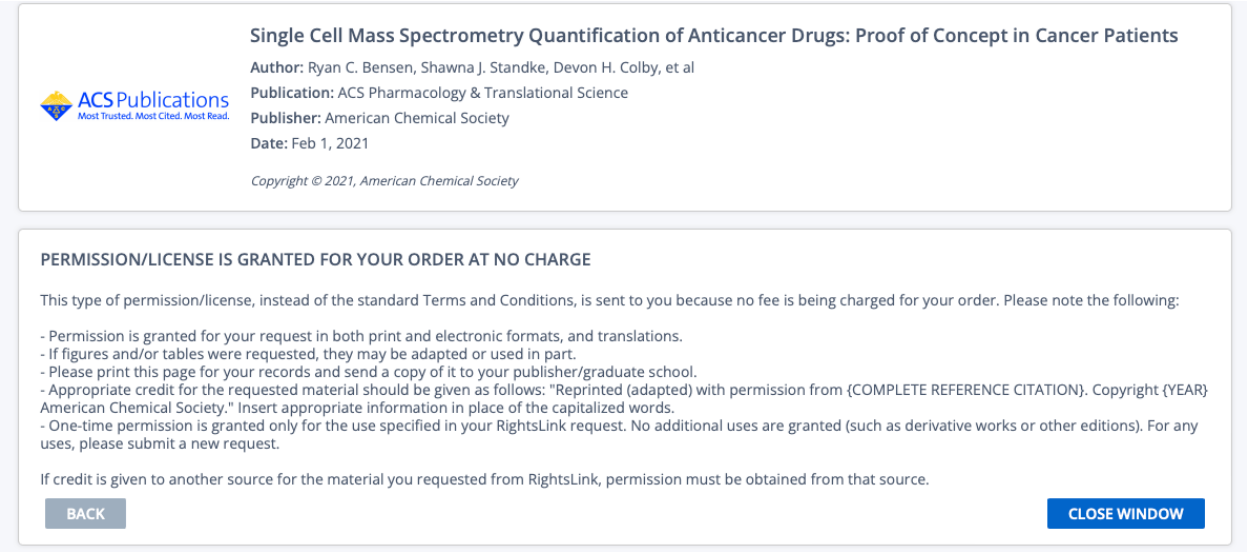
This type of permission/license, instead of the standard Terms and Conditions, is sent to you because no fee is being charged for your order. Please note the following:

- Permission is granted for your request in both print and electronic formats, and translations.
- If figures and/or tables were requested, they may be adapted or used in part.
- Please print this page for your records and send a copy of it to your publisher/graduate school.
- Appropriate credit for the requested material should be given as follows: "Reprinted (adapted) with permission from {COMPLETE REFERENCE CITATION}. Copyright {YEAR} American Chemical Society." Insert appropriate information in place of the capitalized words.
- One-time permission is granted only for the use specified in your RightsLink request. No additional uses are granted (such as derivative works or other editions). For any uses, please submit a new request.

If credit is given to another source for the material you requested from RightsLink, permission must be obtained from that source.

BACK CLOSE WINDOW

Copyright of Fig. 4B



Single Cell Mass Spectrometry Quantification of Anticancer Drugs: Proof of Concept in Cancer Patients

Author: Ryan C. Bensen, Shawna J. Standke, Devon H. Colby, et al
Publication: ACS Pharmacology & Translational Science
Publisher: American Chemical Society
Date: Feb 1, 2021

Copyright © 2021, American Chemical Society

PERMISSION/LICENSE IS GRANTED FOR YOUR ORDER AT NO CHARGE

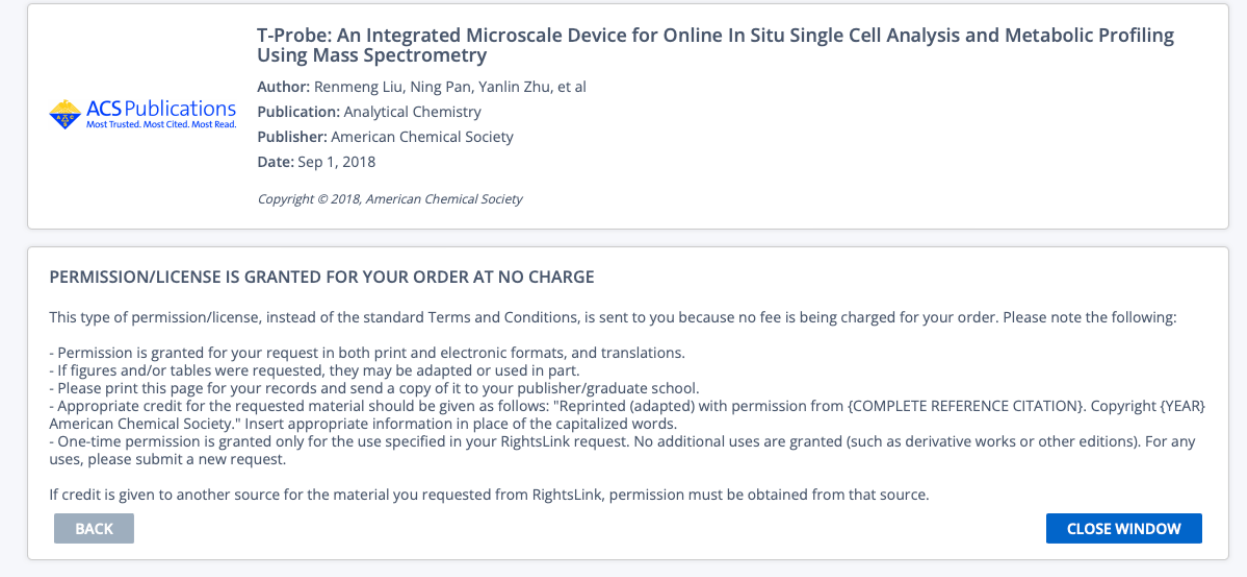
This type of permission/license, instead of the standard Terms and Conditions, is sent to you because no fee is being charged for your order. Please note the following:

- Permission is granted for your request in both print and electronic formats, and translations.
- If figures and/or tables were requested, they may be adapted or used in part.
- Please print this page for your records and send a copy of it to your publisher/graduate school.
- Appropriate credit for the requested material should be given as follows: "Reprinted (adapted) with permission from {COMPLETE REFERENCE CITATION}. Copyright {YEAR} American Chemical Society." Insert appropriate information in place of the capitalized words.
- One-time permission is granted only for the use specified in your RightsLink request. No additional uses are granted (such as derivative works or other editions). For any uses, please submit a new request.

If credit is given to another source for the material you requested from RightsLink, permission must be obtained from that source.

BACK CLOSE WINDOW

Copyright of Fig. 4C



T-Probe: An Integrated Microscale Device for Online In Situ Single Cell Analysis and Metabolic Profiling Using Mass Spectrometry

Author: Renmeng Liu, Ning Pan, Yanlin Zhu, et al
Publication: Analytical Chemistry
Publisher: American Chemical Society
Date: Sep 1, 2018

Copyright © 2018, American Chemical Society

PERMISSION/LICENSE IS GRANTED FOR YOUR ORDER AT NO CHARGE

This type of permission/license, instead of the standard Terms and Conditions, is sent to you because no fee is being charged for your order. Please note the following:

- Permission is granted for your request in both print and electronic formats, and translations.
- If figures and/or tables were requested, they may be adapted or used in part.
- Please print this page for your records and send a copy of it to your publisher/graduate school.
- Appropriate credit for the requested material should be given as follows: "Reprinted (adapted) with permission from {COMPLETE REFERENCE CITATION}. Copyright {YEAR} American Chemical Society." Insert appropriate information in place of the capitalized words.
- One-time permission is granted only for the use specified in your RightsLink request. No additional uses are granted (such as derivative works or other editions). For any uses, please submit a new request.

If credit is given to another source for the material you requested from RightsLink, permission must be obtained from that source.

BACK CLOSE WINDOW

Copyright of Fig. 4D

Thank you for your order.

This Agreement between Ms. Xingxiu Chen ("You") and Elsevier ("Elsevier") consists of your license details and the terms and conditions provided by Elsevier and Copyright Clearance Center.

Your confirmation email will contain your order number for future reference.

Printable Details

License Number	5292700439855
License date	Apr 19, 2022

Licensed Content

Licensed Content Publisher	Elsevier
Licensed Content Publication	Analytica Chimica Acta
Licensed Content Title	Redesigning the T-probe for mass spectrometry analysis of online lysis of non-adherent single cells
Licensed Content Author	Yanlin Zhu,Renmeng Liu,Zhibo Yang
Licensed Content Date	Nov 25, 2019
Licensed Content Volume	1084
Licensed Content Issue	n/a
Licensed Content Pages	7

Order Details

Type of Use	reuse in a thesis/dissertation
Portion	figures/tables/illustrations
Number of figures/tables/illustrations	1
Format	electronic
Are you the author of this Elsevier article?	No
Will you be translating?	No

About Your Work

Title	Single cell mass spectrometry metabolomics study of drug-resistant cancer cells
Institution name	University of Oklahoma
Expected presentation date	May 2022

Additional Data

Portions	Fig. 2

Requestor Location

Requestor Location	Ms. Xingxiu Chen 3117 Ridgecrest Ct Norman NORMAN, OK 73072 United States Attn: Ms. Xingxiu Chen

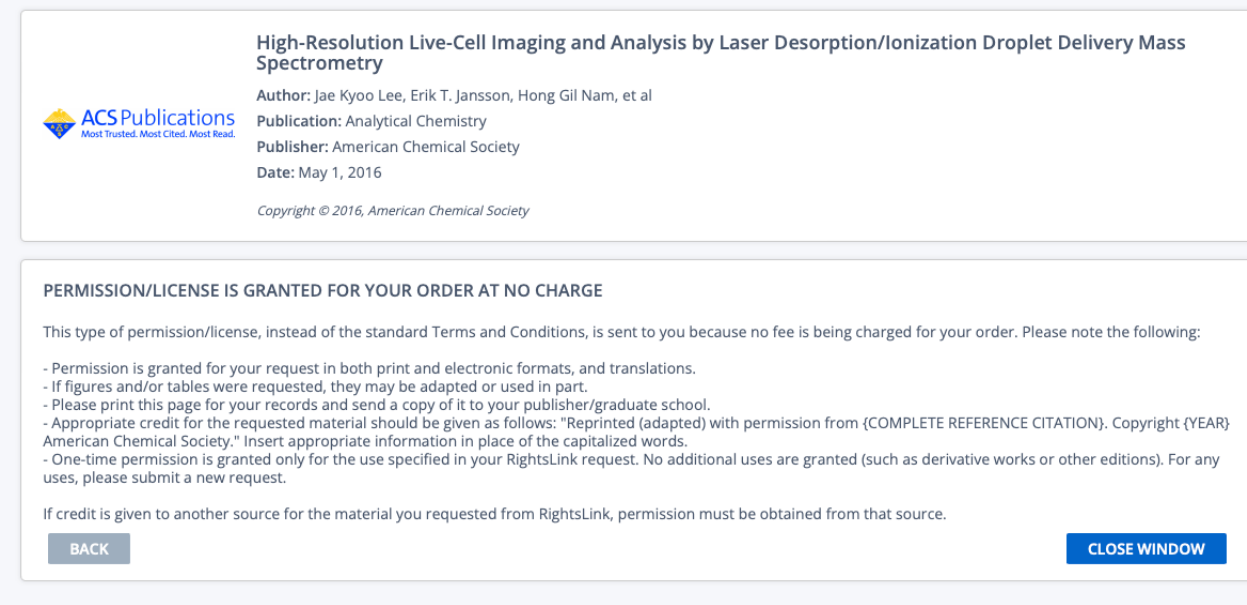
Tax Details

Publisher Tax ID	98-0397604

Price

Total	0.00 USD

Copyright of Fig. 5A



High-Resolution Live-Cell Imaging and Analysis by Laser Desorption/Ionization Droplet Delivery Mass Spectrometry

Author: Jae Kyoo Lee, Erik T. Jansson, Hong Gil Nam, et al
Publication: Analytical Chemistry
Publisher: American Chemical Society
Date: May 1, 2016

Copyright © 2016, American Chemical Society

PERMISSION/LICENSE IS GRANTED FOR YOUR ORDER AT NO CHARGE

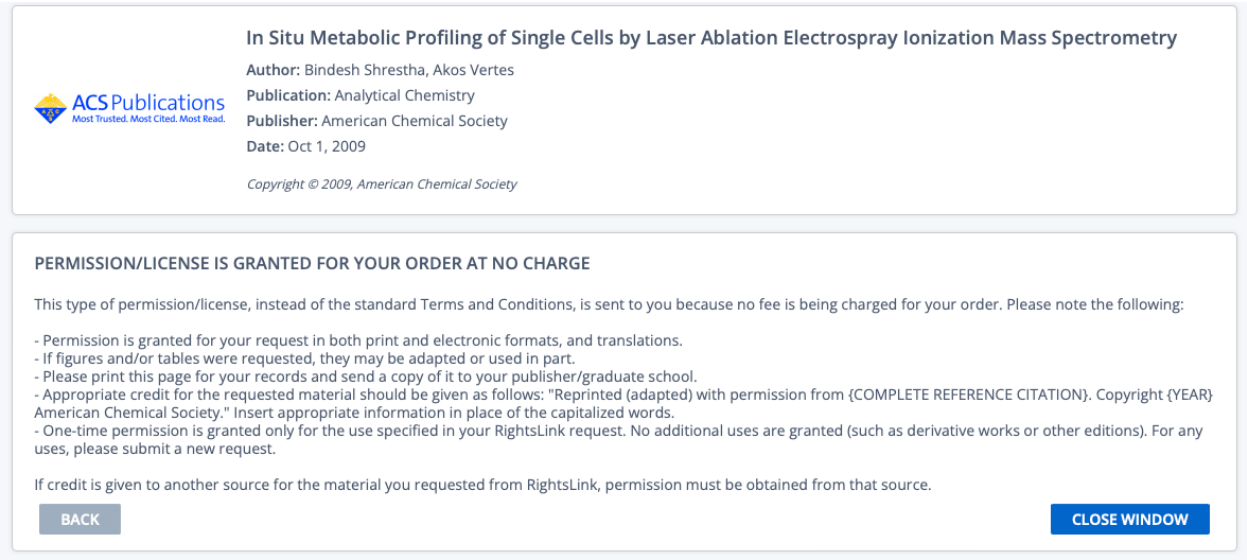
This type of permission/license, instead of the standard Terms and Conditions, is sent to you because no fee is being charged for your order. Please note the following:

- Permission is granted for your request in both print and electronic formats, and translations.
- If figures and/or tables were requested, they may be adapted or used in part.
- Please print this page for your records and send a copy of it to your publisher/graduate school.
- Appropriate credit for the requested material should be given as follows: "Reprinted (adapted) with permission from {COMPLETE REFERENCE CITATION}. Copyright {YEAR} American Chemical Society." Insert appropriate information in place of the capitalized words.
- One-time permission is granted only for the use specified in your RightsLink request. No additional uses are granted (such as derivative works or other editions). For any uses, please submit a new request.

If credit is given to another source for the material you requested from RightsLink, permission must be obtained from that source.

BACK CLOSE WINDOW

Copyright of Fig. 5B



In Situ Metabolic Profiling of Single Cells by Laser Ablation Electrospray Ionization Mass Spectrometry

Author: Bindesh Shrestha, Akos Vertes
Publication: Analytical Chemistry
Publisher: American Chemical Society
Date: Oct 1, 2009

Copyright © 2009, American Chemical Society

PERMISSION/LICENSE IS GRANTED FOR YOUR ORDER AT NO CHARGE

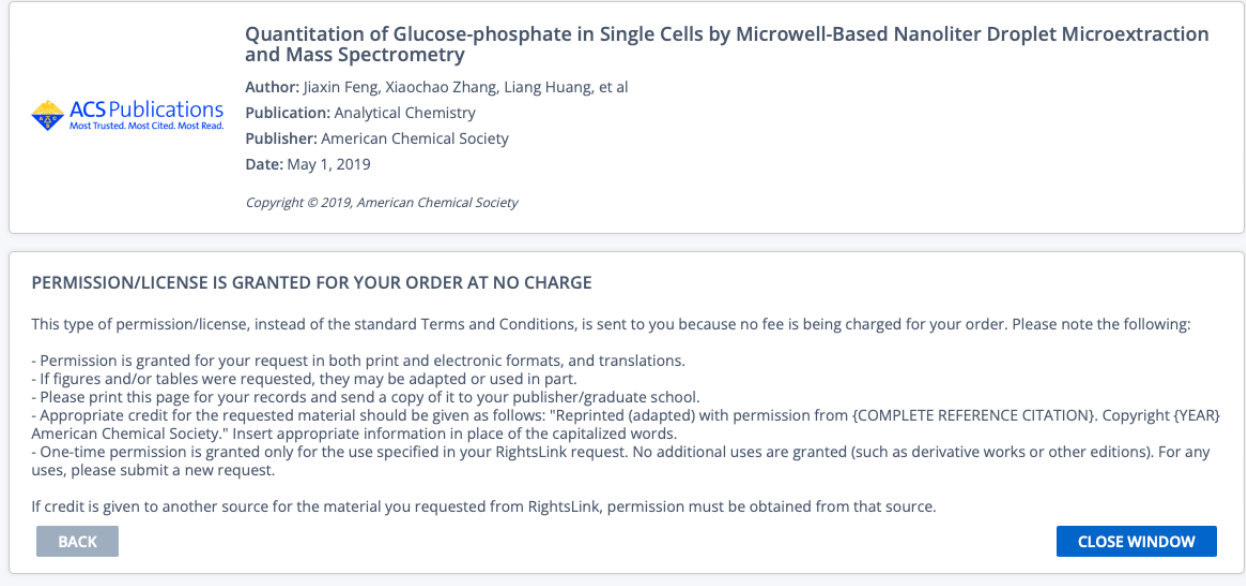
This type of permission/license, instead of the standard Terms and Conditions, is sent to you because no fee is being charged for your order. Please note the following:

- Permission is granted for your request in both print and electronic formats, and translations.
- If figures and/or tables were requested, they may be adapted or used in part.
- Please print this page for your records and send a copy of it to your publisher/graduate school.
- Appropriate credit for the requested material should be given as follows: "Reprinted (adapted) with permission from {COMPLETE REFERENCE CITATION}. Copyright {YEAR} American Chemical Society." Insert appropriate information in place of the capitalized words.
- One-time permission is granted only for the use specified in your RightsLink request. No additional uses are granted (such as derivative works or other editions). For any uses, please submit a new request.

If credit is given to another source for the material you requested from RightsLink, permission must be obtained from that source.

BACK CLOSE WINDOW

Copyright of Fig. 6A



Quantitation of Glucose-phosphate in Single Cells by Microwell-Based Nanoliter Droplet Microextraction and Mass Spectrometry

Author: Jiaxin Feng, Xiaochao Zhang, Liang Huang, et al
Publication: Analytical Chemistry
Publisher: American Chemical Society
Date: May 1, 2019

Copyright © 2019, American Chemical Society

PERMISSION/LICENSE IS GRANTED FOR YOUR ORDER AT NO CHARGE

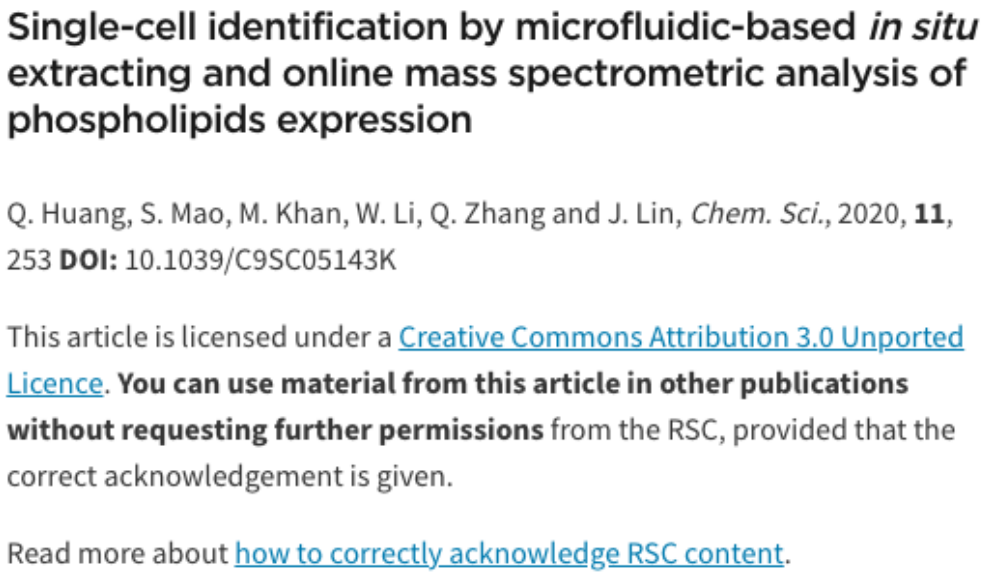
This type of permission/license, instead of the standard Terms and Conditions, is sent to you because no fee is being charged for your order. Please note the following:

- Permission is granted for your request in both print and electronic formats, and translations.
- If figures and/or tables were requested, they may be adapted or used in part.
- Please print this page for your records and send a copy of it to your publisher/graduate school.
- Appropriate credit for the requested material should be given as follows: "Reprinted (adapted) with permission from {COMPLETE REFERENCE CITATION}. Copyright {YEAR} American Chemical Society." Insert appropriate information in place of the capitalized words.
- One-time permission is granted only for the use specified in your RightsLink request. No additional uses are granted (such as derivative works or other editions). For any uses, please submit a new request.

If credit is given to another source for the material you requested from RightsLink, permission must be obtained from that source.

BACK CLOSE WINDOW

Copyright of Fig. 6B



Single-cell identification by microfluidic-based *in situ* extracting and online mass spectrometric analysis of phospholipids expression

Q. Huang, S. Mao, M. Khan, W. Li, Q. Zhang and J. Lin, *Chem. Sci.*, 2020, **11**, 253 **DOI:** 10.1039/C9SC05143K

This article is licensed under a Creative Commons Attribution 3.0 Unported Licence. **You can use material from this article in other publications without requesting further permissions** from the RSC, provided that the correct acknowledgement is given.

Read more about how to correctly acknowledge RSC content.

Copyright of Fig. 6C

ACS Publications
Most Trusted. Most Cited. Most Read.

Metabolic Differentiation of Neuronal Phenotypes by Single-cell Capillary Electrophoresis–Electrospray Ionization-Mass Spectrometry

Author: Peter Nemes, Ann M. Knolhoff, Stanislav S. Rubakhin, et al
Publication: Analytical Chemistry
Publisher: American Chemical Society
Date: Sep 1, 2011

Copyright © 2011, American Chemical Society

PERMISSION/LICENSE IS GRANTED FOR YOUR ORDER AT NO CHARGE

This type of permission/license, instead of the standard Terms and Conditions, is sent to you because no fee is being charged for your order. Please note the following:

- Permission is granted for your request in both print and electronic formats, and translations.
- If figures and/or tables were requested, they may be adapted or used in part.
- Please print this page for your records and send a copy of it to your publisher/graduate school.
- Appropriate credit for the requested material should be given as follows: "Reprinted (adapted) with permission from {COMPLETE REFERENCE CITATION}. Copyright {YEAR} American Chemical Society." Insert appropriate information in place of the capitalized words.
- One-time permission is granted only for the use specified in your RightsLink request. No additional uses are granted (such as derivative works or other editions). For any uses, please submit a new request.

If credit is given to another source for the material you requested from RightsLink, permission must be obtained from that source.

BACK CLOSE WINDOW

Copyright of Fig. 6D

CUSTOMER INFORMATION

Payment by invoice: You can cancel your order until the invoice is generated by contacting customer service.

Billing Address

Ms. Xingxiu Chen
3117 Ridgecrest Ct
Norman
Norman, OK 73072
United States

+1 (917) 379-6490
xingxiuchen@ou.edu

Customer Location

Ms. Xingxiu Chen
3117 Ridgecrest Ct
Norman
Norman, OK 73072
United States

PO Number (optional)

N/A

Payment options

Invoice

PENDING ORDER CONFIRMATION

Confirmation Number: Pending
Order Date: 19-Apr-2022

Print Friendly Format
Includes Publisher Terms and Conditions

1. analyst online 0.00 USD

Article: In situ metabolic analysis of single plant cells by capillary microsampling and electrospray ionization mass spectrometry with ion mobility separation.

Order License ID	Pending	**Publisher**	Royal Society of Chemistry
ISSN	1364-5528	**Portion**	Image/photo/illustration
Type of Use	Republish in a thesis/dissertation		

View Details Print License

Total Items: 1 **Total Due: 0.00 USD**

Copyright of Chapter III

